Chapter I

Introduction

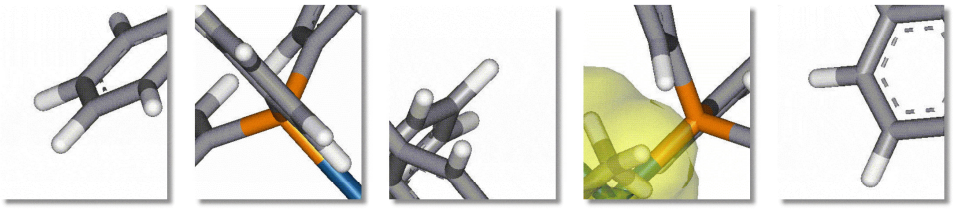

1.1 Cancer

Cancer is not a single disease but a broad group characterised by malignant cells that are clearly distinguished from normal cells by uncontrolled growth (Workman, 2001). They are caused by abnormalities in the sequence and expression of critical genes, most notably oncogenes and tumour suppressor genes. The language of cancer is to be found in the resulting deregulation of crucial biochemical pathways that control proliferation, the cell cycle, survival/apoptosis, angiogenesis, invasion and metastasis. Aberrant cellular growth is a primary cause in the development of malignant tumours (Suyama *et al.,* 2002). However, additional events take place, which enable tumour cells to invade tissue barriers and metastasise to distant sites. These events include detachment of cells from the primary tumour, the crossing of tissue boundaries, entrance and exit from the circulatory system, the infiltration of distant organs, and the formation of metastatic implants.

1.2 Cancer incidences

Cancer has troubled humans throughout recorded history. This disease remains a major public health issue at the beginning of the 21st century (Grella *et al.,* 2003). It is the leading cause of death worldwide (www.who.int, 2005). From a total of 58 million deaths worldwide in 2005, it accounts for 7.6 million (or 13%) of all deaths. That is more than the percentage of deaths caused by HIV/AIDS, tuberculosis and malaria put together (McIntyre, 2007). There are currently 25 million people living with cancer.

The main types of cancer leading to overall cancer mortality are: (www.who.int, 2005).

- Lung (1.3 million deaths/year);
- Stomach (almost 1 million deaths/year);
- Liver (662,000 deaths/year);
- Colon (655, 000 deaths/year) and

- Breast (502, 000 deaths/year).

More than 70% of all cancer deaths in 2005 occurred in low and middle income countries. Deaths from cancer in the world are projected to continue rising, with an estimated 9 million people dying from cancer in 2015 and 11.4 million dying in 2030. According to World Cancer Report (World Health Organisation, 2003), this predicted sharp increase will mainly be due to steadily ageing populations in both developed and developing countries. Other factors include current trends in smoking prevalence and the growing adoption of unhealthy lifestyles. However, the report also provides clear evidence that healthy lifestyles and public health action by governments and health practitioners could stem this trend, and prevent as many as one third of cancers worldwide. The report also reveals that cancer has emerged as a major public health problem in developing countries, matching its effect in industrialised nations.

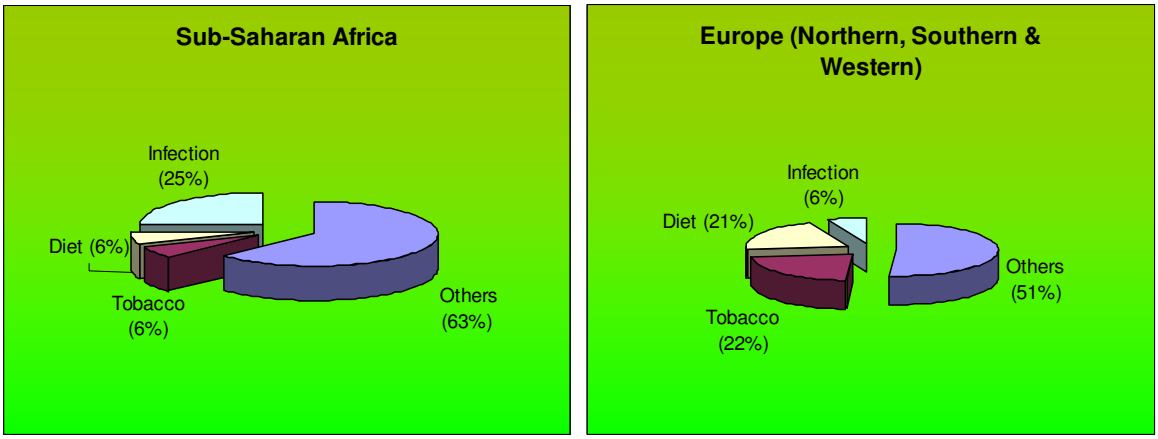

Fig. 1.1: The three main cancer-causing factors in Sub-Saharan Africa and parts of Europe

Tobacco causes cancer at many sites including; lung, throat, mouth, pancreas, bladder, stomach, liver and kidney (Selikoff, 2005). Overweight and obesity are associated with colon, breast, uterus, oesophagus and kidney cancers. One-fifth of cancers worldwide are due to infections (*Fig. 1.1*), mainly from hepatitis viruses (liver), papillomaviruses (cervix), *Helicobacter pylori* (stomach), Schistosomes (bladder), the liver fluke (bile duct) and human immunodeficiency virus (Kaposi's sarcoma and lymphoma).

In South Africa, a total of 29 208 new cancer cases in females and 29 499 new cases in males were reported (The National Cancer Registry, 2003). One in four males and one in five females (adjusted for under-reporting), aged 0-74 years, were at risk of developing cancer. The most common cancers in South Africa are shown in Table 1.1 below.

Table 1.1: The most common cancers in South Africa, in descending order of occurrence

Males	**Females**	**Children (males and females, 0-14 years)**
Prostate	Cervix	Leukaemia
Lung	Breast	Kidney
Oesophagus	Colorectal	Brain
Bladder	Oesophagus	Non-Hodgkin's lymphoma
Colorectal	Lung	Bone

1.3 Cancer treatment

Clinically, weapons to fight cancer are surgery, radiotherapy and chemotherapy (Grella *et al.,* 2003).

1.3.1 Surgery

For centuries, surgery alone could offer a cure for cancer (Shiu, 2003). It remains the principal modality of treatment for many of the common cancers seen today. For example, treatment for hepatic colorectal metastases has greatly evolved over the last two decades, such that this rapidly fatal stage IV disease has become treatable by surgery and potentially curable (Morris *et al.,* 2006). In recent years, there have been improvements in clinical and radiologic staging resulting in more rational planning of surgical and adjuvant treatments.

1.3.2 Radiotherapy

Approximately 50% of all cancer patients are treated with radiotherapy, either as primary treatment with curative intent or for palliation of cancer related symptoms (Vink *et al.,* 2007). Likelihood of tumour response after radiotherapy is determined by the total radiation dose required for tumour cell kill and varies between tumour types, ranging from very radiosensitive low grade lymphomas (90% tumour control at 4 Gy) to notoriously radioresistant malignant gliomas (not responsive at clinically achievable doses). For patients treated with radiotherapy, fibrosis, necrosis and severe organ dysfunction may appear months to years after treatment accomplishment (Koukourakis and Danielidis, 2005).

The therapeutic index (TI) defines the ratio of the percentage of tumour control and the percentage of complications associated with a certain therapeutic regimen (Koukourakis and Danielidis, 2005). In radiotherapy, radio-sensitizing agents aim to improve the TI by increasing the tumour control rate, while cytoprotective policies do the same by reducing the complication rate. Cisplatin and carboplatin have a substantial activity in sensitising tumour cells to radiotherapy in head and neck, lung, oesophagus, cervix, bladder and rectum cancer (Desoize and Madoulet, 2002).

1.3.3 Anti-cancer agents

Classical anti-cancer drugs (*Table 1.2*) were grouped as chemotherapy, hormonal therapy and immunotherapy (Espinosa *et al.,* 2003).

Table 1.2: Classical classification of anti-cancer drugs

Chemotherapy	Alkylators
	Antibiotics
	Antimetabolites
	Topoisomerases inhibitors
	Mitosis inhibitors
	Others
Hormonal therapy	Steroids
	Anti-oestrogens
	Anti-androgens
	LH-RH analogs
	Anti-aromatase agents
Immunotherapy	Interferon
	Interleukin 2
	Vaccines

The group "others" has expanded so much and it has been proposed that classification is based on the target (Espinosa *et al.,* 2003). The target may be located in the tumour cell or in other elements that interact with the tumour cells (endothelium, extracellular matrix, immune system, host cells).

The treatment of cancer has traditionally used agents that interfere with the cell division process (Don and Hogg, 2004). More recently, research and novel therapies have targeted the growth signals that drive the proliferation and survival of cancer cells (for example, Herceptin, for the treatment of breast cancer) and the tumour vasculature (for example, antibodies against vascular endothelial growth factor). DNA-interactive drugs in clinical use represent one of the most important drug classes in cancer therapy (Grella *et al.,* 2003). In general, there are three major types of the above mentioned clinically important drugs:

- The intercalators, which insert between the base pairs of the double helix and determine a significant change of DNA conformation being accompanied by unwinding and elongation of the duplex;

- The alkylators, which react covalently with DNA bases and;
- The DNA strand breakers, which generate reactive radicals that produce cleavage of the polynucleotide strands.

Increased cure rates have been achieved in childhood cancer, testicular cancer, leukaemia and lymphoma; and survival improvements have been obtained with adjuvant drug treatment of breast and ovarian cancer (Workman, 2001). However, the goal of routine care or long term management of cancer as a chronic disease remains frustratingly elusive and the development of preventative agents is even more embryonic and challenging.

1.4 Limitations of current cancer treatment

1.4.1 Lack of selectivity

The majority of current cancer drugs are cytotoxic agents that exert their effects on all proliferating cells, both normal and cancerous (Workman, 2001). This is the case even for recently successful drugs such as irinotecan in colorectal cancer, taxanes in breast, ovarian and lung cancer; and carboplatin in ovarian cancer. Since cytotoxic agents have a selectively 'anti-proliferative' action rather than selective 'anti-cancer' properties, the therapeutic window for tumour versus normal tissue is modest at best and toxic side effects are the norm. Exposure of normal tissues that have a high rate of cellular proliferation (such as bone marrow, gastrointestinal epithelial cells and cells of the hair follicles) to these anti-proliferative drugs leads to major toxicities (Mollinedo and Gajate, 2006). Renal and gastrointestinal toxicity has been reduced considerably in the clinic by intravenous hydration and anti-emetics that antagonise the 5-hydroxytryptamine type 3 receptor (Screnci and McKeage, 1999).

1.4.2 Resistance to drugs

Most tumour types are resistant to current chemotherapy or become resistant during treatment (Broxterman *et al.,* 2003). During the past decades, drug resistance research has identified a myriad of ways by which cancer cells can

elude chemotherapy (Nygren and Larsson, 2003). Resistance in the clinic manifests itself as initial lack of meaningful response (refractoriness) to treatment or regrowth of tumour after an initial response (Broxterman *et al.,* 2003). In the latter case, the recurrent tumour is almost invariably more resistant to treatment than it was at first presentation and treatment. Another manifestation of clinical drug resistance is the frequent occurrence of partial responses. Different subpopulations of tumour cells will be invariably present in tumours, where the predominant cell type will determine anti-tumour response, but the most resistant cells may determine the probability of cure.

The other type of resistance is multidrug resistance (MDR) which is usually caused by the presence of membrane-bound glycoprotein pumps in humans, animals and other organisms (Wang *et al.,* 2003). These pumps keep some foreign substances, such as xenobiotics, toxic agents and drugs from being absorbed, and they are usually called multidrug efflux pumps. The pumps are expressed and distributed in various organs and normal tissues, ranging from lung, liver, kidney, gastrointestinal tract to adrenal, gravid uterus and capillary endothelium in the brain. Based on impressive pre-clinical data, most attention in the clinic has been put on strategies for circumvention of Pgp-mediated MDR using, e.g verapamil and cyclosporin A (Nygren and Larsson, 2003).

1.5 The need for new anti-cancer drugs

The clinical application of new anti-neoplastic drugs has been hindered by their low therapeutic index and lack of efficacy in humans (Sanchez *et al.,* 2001). Thus, an approach to improve old and new anti-cancer drugs has been to manipulate their pharmacokinetic properties. Four interrelated factors determine pharmacokinetic behaviour of a drug: absorption, distribution, metabolism and excretion. Problems such as drug-drug interactions, poor efficacy and high toxicity in humans in contrast to action in laboratory animals, or to variation in these problems among subjects within a population, frequently have their origin in drug metabolism issues.

At one time, the treatment of cancer focused on systemic, non-specific, high-dose chemotherapy, whereas now the goal is to find a drug that balances minimal adverse events (AEs) with maximal anti-tumour activity (Abou-Jawde *et al.,* 2003). Initial steps in the development of such cancer treatments have led to the creation of several new anti-cancer agents. Improved systemic drug therapy is particularly important for the treatment of patients with advanced metastatic cancer, for whom surgery and radiation therapy can no longer be curative (Workman, 2001). Advanced technology and an understanding of the genetic changes that transform a normal cell into a cell uncontrolled by the normal feedback mechanism have facilitated the creation of a new generation of targeted treatments and cancer vaccines (Abou-Jawde *et al.,* 2003).

1.6 Drug design and targets

It is important to note that advances in potential anti-cancer therapies have increasingly involved combinations of current cytotoxic agents with new, molecularly targeted agents (Landis-Piwowar *et al.,* 2006). The literature emphasis on combinational chemistry and the screening of millions of compounds tends to obscure the fact that the world of drug-like properties is quite limited, and that most of the information content related to desirable drug-like properties is contained in a relatively small number of compounds (Lipinski, 2000). When evaluating molecular targets for potential combinational therapies, significant drug-development challenges arise, for example, whether to use a single molecularly targeted agent, a molecularly targeted agent combined with a standard chemotherapeutic drug, or a combination of various molecularly targeted agents.

New agents discovered for possible use as anti-cancer therapy include genes, proteins, growth factors and receptors, and those involved in specific pathways, for example, angiogenesis, signal transduction, cell cycle, cell apoptosis, invasion, metastasis, drug resistance and blood flow (Gupta *et al.,* 2002). Many current drugs were discovered by trial and error (Landis-Piwowar *et al.,* 2006). Therefore, the brute force methods such as high–throughput synthesis and screening can be an effective approach when the target information is not known. If the structure of

the target is unknown, a process called ligand-based drug design can be applied in which analysis of known, active ligands is used to find similarity among other, novel ligands that could alter the activity of a target protein.

1.7 Metal based drugs

When one discusses “drugs”, one often thinks only of organic molecules (Tiekink, 2003). This belies the fact that metal complexes too, play an important role in chemotherapy. Against the background that approximately one third of proteins and enzymes require at least one metal ion to function properly, perhaps it is not surprising that metal complexes have a role to play in medicine as well. The interactions of heavy metals such as platinum, gold with N, S-donor atoms have been recognised for their anti-carcinogenic properties with the potential to develop metal-based drugs (Lobana *et al.,* 2000). Metal ions and metal coordination compounds are known to affect cellular processes in a dramatic way (Reedijk, 2003). This metal effect influences not only natural processes, such as cell division and gene expression, but also non-natural processes, such as toxicity, carcinogenicity, and anti-tumour chemistry. However, the mechanisms of action of metal-based drugs are often not well understood (Jakupec *et al.,* 2003).

Medicinal inorganic chemistry is a discipline of growing significance in both therapeutic and diagnostic medicine (Ronconi and Sadler, 2007). Inorganic compounds have been used in medicine for many centuries, but often only in an empirical way with little attempt to design the compounds to be used, and with little or no understanding of the molecular basis of their mechanism of action. Progress in the design of metal-based inorganic drugs has been slow due to problems relating to substitution and hydrolytic equilibria, redox and polymerisation reactions (Berners-Price and Sadler, 1987a).

The interactions of heavy metals such as platinum and gold with N,S donor atoms have been recognised for their anti-cancer properties with the potential to develop metal-based drugs (Amin *et al.,* 2004). The successful use of metal complexes as therapeutic and diagnostic agents depends on the control of their kinetic and

thermodynamic properties through appropriate choice of oxidation state, types and numbers of bound ligands, and coordination geometry (Sadler, 1997). In this way, it is possible to achieve specificity of biological activity and most importantly, to minimise toxic side-effects. However, before rational drug design can be pursued, a detailed knowledge of the mechanism of action is required (Hambley, 1997). Equally, if one is to "design out" toxic side effects, it is important to know what drug/target interactions are responsible for the toxicity.

Broad interest in the pharmacological properties of metal compounds first arose with the pioneering work of Barnett Rosenberg, who in the late 1960s by chance discovered the cytostatic effects of cisplatin and related compounds (Jakupec *et al.,* 2003). It seemed that biological activity (anti-tumour activity) had to be unique among heavy metal compounds (Kuduk-Jaworska *et al.,* 2004). This was seen as a result of the specific kinetic and structural properties of Pt^{2+} centre making possible the specific impact on genomic DNA. It was shown later that in addition to platinum(II) complexes, numerous planar and octahedral platinum complexes as well as compounds of other platinum-group metals exhibited anti-tumour properties. Anti-tumour activity has been reported for a variety of compounds involving metals such as titanium, vanadium, iron, gold, silver, copper, palladium, ruthenium, germanium and tin (Schurig *et al.,* 1989).

1.7.1 Palladium based drugs

The low anti-tumour activity of palladium complexes has been attributed to rapid hydrolysis leading to easy dissociation (in solution) of leaving groups and to the formation of very reactive species unable to reach their pharmacological targets (Akdi *et al.,* 2002). Based on the structural analogy between Pt(II) and Pd(II) complexes, some studies on Pd(II) compounds as suitable drugs have been carried out. However, advances in this area have been scarce probably due to kinetic reasons; it is well known that comparable Pt(II) compounds always react more slowly by a factor of 10^5 than corresponding Pd(II) complexes.

Relatively few palladium (II) and palladium (IV) complexes have been investigated for their cytotoxic anti-tumour activity (Kuduk-Jaworska *et al.,* 2004). Among them

were complexes with neutral amine ligands such as ethylenediamine, diaminocyclohexane, ammonia, pyridine and pyrimidine derivatives, alkylaminophosphine oxides, mercapto-imidazoles and pyrimidines. The promising anti-proliferative activity was found in Pd-complexes with chelating ligands or alkyl- or aryl-thiosemicarbazones.

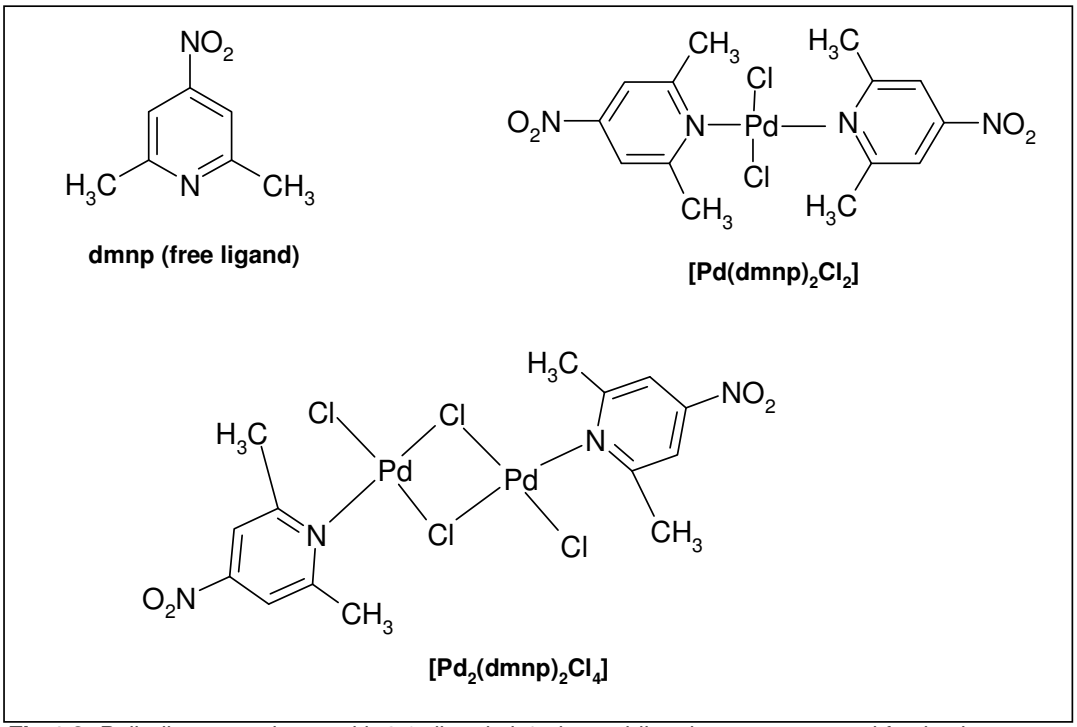

Fig 1.2: Palladium complexes with 2,6-dimethyl-4-nitropyridine that were assayed for *in vitro* cytotoxicity against four human cancer cell lines.

Two kinds of palladium complexes with 2, 6-dimethyl-4-nitropyridine (dmnp) (*Fig. 1.2*) were prepared and tested for *in vitro* cytotoxicity against four human cancer cell lines: SW707 (adenocarcinoma of the rectum), T47D (breast cancer), HCV (bladder cancer) and A549 (non-small cell lung carcinoma). Free ligand and $[Pd_2(dmnp)_2Cl_4]$ showed moderate activity while $[Pd(dmnp)_2Cl_2]$ was strongly active against all four cell lines (Kuduk-Jaworska *et al.,* 2004). The highest activity was observed against T47D, which is a cell line known to be poorly responsive (rather resistant) to platinum-based drugs. The IC_{50} (concentration of the compound required to kill 50% of tumour cells) values for the most potent compound ranged from 0.46-8.4 µg/ml.

1.7.2 Platinum based anti-tumour drugs

An important property of platinum coordination compounds is the fact that the Pt-ligand bond has a thermodynamic strength of a typical coordination bond (say 100 KJ/mol or below) which is much weaker than (covalent) C-C and C-N or C-O single and double bonds (which are between 250 and 500 KJ/mol) (Reedijk, 2003). However, the ligand-exchange behaviour of Pt compounds is quite slow, which gives them high kinetic stability and results in ligand exchange reactions of minutes to days, rather than milliseconds to seconds for many other coordination compounds.

Knowledge of the relationship between the ligand structure and cytotoxicity of Pt-based complexes is still limited, even if several rules may be apparent (Alverdi *et al.,* 2004). A number of platinum coordination compounds exhibit anti-viral and anti-tumour activities (Balcarová *et al.,* 1998). Most of the well known anti-cancer complexes have the general formula cis-$[PtX_2(NHR_2)_2]$, in which R = organic fragment and X = leaving group, such as chloride or (chelating bis)carboxylate (Reedijk, 2003). Platinum drugs play an important role in the treatment of testis, ovarian and cervical cancer (Screnci and McKeage, 1999). Toxicity to the peripheral nervous system is now the major dose-limiting toxicity for at least some of the platinum drugs currently of clinical interest.

A few platinum drugs currently in clinical use are described below:

a) Cisplatin

The recent history of metal-containing anti-tumour agents began with the unexpected detection of anti-tumour properties of inorganic compound *cis*-diamminedichloroplatinum (II) in 1969 (Kuduk-Jaworska *et al.,* 2004). It was first synthesised in 1844 and named at that time as Peyrone's chloride (Desoize and Madoulet, 2002). Rosenberg, 120 years later, reported its inhibitory activity on *Escherichia coli* division. Its efficacy in human cancer patients was established in 1970's.

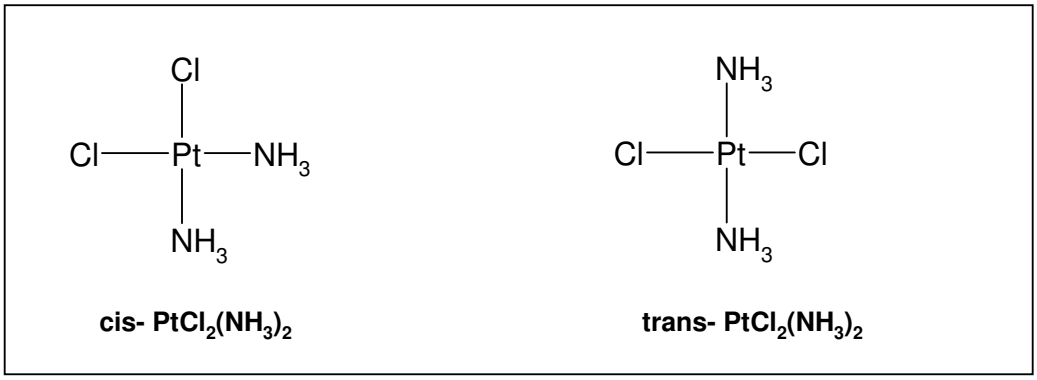

Fig 1.3: Structures of the classical compounds of *cis*-Platin and *trans*-Platin.

The efficacy of platinum agents against cancer could be related to inhibition of DNA synthesis or to saturation of the cellular capacity to repair platinum adducts of DNA (Desoize and Madoulet, 2002). t*rans*-Adducts are more easily repaired than *cis*-adducts, for this reason, the *cis* configuration of the diaquo intermediate is 30 times more toxic than the *trans* configuration. Cisplatin is a widely used anti-cancer drug that is highly effective against testicular and ovarian cancers. It is also used alone or in combination with other drugs such as bleomycin, doxorubicin for treatment of tumours of the head and neck, lung, ovarian, cervix and bladder (Daghriri *et al.,* 2004). Its clinical utility has been limited due to the frequent development of drug resistance and severe side effects such as neurotoxicity, nephrotoxicity, ototoxicity, myelosuppression, nausea and vomiting.

Driven by the impressive impact of cisplatin on cancer chemotherapy, great efforts have been made to develop new derivatives with improved pharmacological properties (Jakupec *et al.,* 2003). It has become the prototype of a unique class of anti-neoplastic agents now comprising of numerous derivatives, many of which have been abandoned in pre-clinical or early clinical stages of their development, while a few others have succeeded in becoming established in routine clinical practice. Structure-activity relationships for a class of related compounds confirmed that only those compounds having *cis*-geometry block cell growth.

b) Carboplatin

Carboplatin [$(H_3N)_2Pt(CBDC)$], (CBDC, 1,1'-cyclobutyldicarboxylato group), a second generation analogue of cisplatin has reduced toxic side effects for the

same efficiency (Abu-Surrah *et al.,* 2003). Briston-Myers Squibb developed this drug, with collaboration of a number of oncologists and academic institutes (Desoize and Madoulet, 2002). After excessive pre-clinical screening, involving a large number of platinum derivatives, carboplatin was selected mainly because of its lower non-haematological toxicity compared with cisplatin. Unfortunately, it exhibits cross-resistance with its parent compound. The dose limiting toxicity is myelosuppression, chiefly thrombocytopenia.

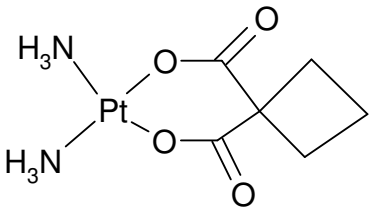

Fig 1.4: Carboplatin

The combination of carboplatin with paclitaxel is of great interest, since toxicity is reduced (Desoize and Madoulet, 2002). This combination is used notably in cancers of the ovary, head and neck, bladder and in non-small-cell lung cancer (NSCLC).

c) Oxaliplatin

Oxaliplatin (*trans-l*-1,2-diaminocyclohexane platinum(II) oxalate) is a third generation analogue of cisplatin (Abu-Surrah *et al.,* 2003). Oxaliplatin (Eloxatin®, Sanofi-Synthelabo) was first approved in 1998 in France and subsequently in the rest of Europe and more recently (2002) by the Food and Drug Administration in the United States (Galanski *et al.,* 2005).

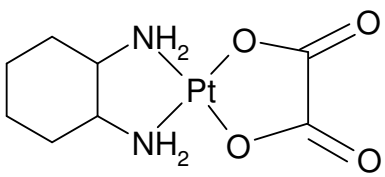

Fig 1.5: Oxaliplatin

This drug gave interesting results in ovarian, breast, head and neck cancer and in non-Hodgkin's lymphoma, malignant melanoma, glioblastoma and NSCLC (Desoize and Madoulet, 2002). It is active against certain tumours which are primarily resistant to cisplatin and carboplatin (Galanski *et al.,* 2005). It is used in clinics in combination with 5-fluorouracil and Leukovorin for the treatment of patients with colorectal cancer, which is the second leading cause of cancer death in developed countries. The toxicity profile of oxaliplatin is favourable, with frequencies for ototoxicity of <1% and for renal toxicity <3%, except for unusual toxicity with regard to peripheral sensory nerves (Kweekel *et al.,* 2005). Sensory neuropathy usually arises during infusion, affects hands, feet and perioral area and is enhanced by cold. These effects appear to be cumulative and generally reverse within 4-6 months after treatment discontinuation.

1.8 Metal phosphines as anti-tumour agents

Currently, platinum complexes with structures different from that of cisplatin are being considered with the idea that they would have a different spectrum of activity and hence not develop cross-resistance to cisplatin (Huq *et al.,* 2004). Somewhat disappointingly, the thousands of compounds estimated to have been prepared and tested have led to few new drugs or fundamental advances (Hambley, 1997). An additional motivation has been the desire to find compounds that do not have the many toxic side effects that cisplatin exhibits.

Progress in the design of metal-phosphine complexes as anti-tumour drugs depends on an understanding of the mechanism of action (Berners-Price and Sadler, 1987a). Phosphorus is an important biological element, but only P(V) compounds are found in biological systems. The relative cytotoxic potencies of phosphines depend on a number of factors, including lipophilicity, redox potential and pK_a. However, there is a paucity of relevant chemical data due to the fact that phosphines are rarely studied under biologically relevant conditions, *i.e.*, in the presence of H_2O and O_2.

1.8.1 Gold phosphines in medicine

Chemotherapeutic applications of gold(I) complexes for the treatment of rheumatoid arthritis have been studied extensively for more than 60 years (Song *et al.,* 1999). The metal may play an important role in protecting the ligand from oxidation and it has been shown that gold phosphine complexes are much more cytotoxic than the free ligands. Auranofin (*Fig. 1.6*), for instance, has anti-tumour activity, although $P(C_2H_5)_3$ is inactive. This thioglucose derivative of triethylphosphine Au(I) was selected for extensive clinical trials and approved for clinical use in 1985 under the trade name Ridaura.

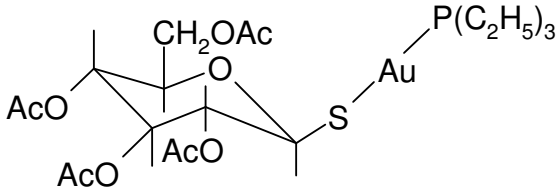

Fig 1.6: Auranofin

This and other linear Au(I) phosphine complexes are potentially cytotoxic to tumour cells in culture (Berners-Price and Sadler, 1996). However, *in vivo*, auranofin exhibits modest anti-tumour activity against only P388 leukaemia in mice, and only when administered intraperitoneally (i.e, the drug comes into direct contact with the tumour cells). Several thiolate-supported gold drugs are commercially used in modern medicine. However, unlike thiols and other sulphur compounds, phosphines are not natural products and are generally difficult to prepare (Song *et al.,* 1999). Therefore, previous clinical tests of anti-cancer gold phosphine complexes have been limited to some simple phosphines that are commercially available. Nevertheless, this pioneering work has shown that the anti-cancer activity of Au(I)-phosphine complexes is critically dependent on the molecular architecture of the phosphine ligands.

1.8.2 Cationic metal complexes as potential anti-tumour agents

The biochemistry of a metal in a certain oxidation state is very much determined by its affinity for various ligands (Ahrland, 1983). Not only are the absolute strengths of the metal-ligand interactions important, but also the relative affinities between ligands of various properties and types. The *bis*-chelated 1:2 Au(I) diphosphine complex $[Au(dppe)_2]Cl$ (*Fig. 1.7*) (where dppe is $Ph_2PCH_2CH_2PPh_2$) has been shown to exhibit anti-tumour activity against a range of tumour models in mice (Berners-Price *et al.,* 1999b). Structure-activity relationships have been evaluated for a wide range of diphosphine ligands and their metal complexes.

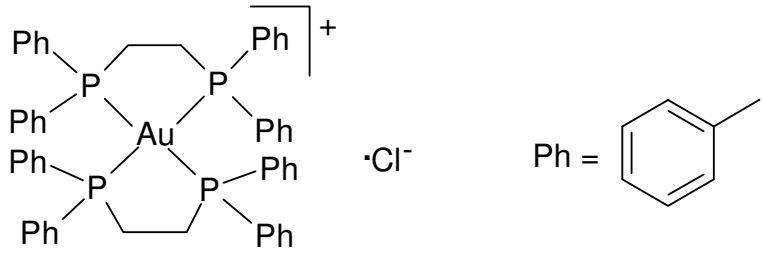

Fig 1.7: $[Au(dppe)_2]Cl$

The highest activity for complexes of the type $[Au(R_2P(CH_2)_nPR'_2)_2]^+$, is found where R = R'= Ph and n = 2, 3 or *cis*-CH=CH (Berners-Price *et al.,* 1999b). Phosphorus 31 NMR studies show that in the presence of thiols and blood plasma, these compounds readily undergo ring-closure reactions to form a four-coordinate cation $[Au(dppe)_2]^+$ (Berners-Price *et al.,* 1992). Salts of this cation exhibit a broad spectrum of anti-tumour activity as do analogous silver(I) and copper(I) diphosphine complexes. Replacement of the phenyl substituents on the phosphine with other groups led to a decrease or loss of anti-tumour activity. Pre-clinical development of $[Au(dppe)_2]^+$ was abandoned after the identification of severe hepatotoxicity in dogs, attributed to alterations in mitochondrial function (Berners-Price *et al.,* 1999a). $[Au(dppe)_2]^+$ was extremely lipophilic (containing eight hydrophobic phenyl substituents) and consequently non-selectively targeted mitochondria in all cells.

In recent work, the adopted approach was to modify the diphosphine ligands of metal complexes related to $[Au(dppe)_2]^+$ in order to vary the hydrophilic character

of the complexes and achieve greater selectivity for tumour cells versus normal cells (Berners-Price *et al.,* 1999a). In order to retain aromatic substituents which seem to be important for anti-tumour activity, Berners-Price and co-workers replaced some or all of them with more hydrophilic pyridyl groups. Their work was stimulated by the observation that the *bis*-chelated Au(I) complex $[Au(d2pyrpe)_2]Cl$, [d2pyrpe is 1,2-bis-(di-2-pyridylphosphino)ethane] was found to exhibit activity in mice bearing P388 leukaemia, whereas the corresponding 4-pyridyl complex $[Au(d4pyrpe)_2]Cl$ was inactive. They demonstrated that the position of the N-atom in the pyridyl ring finely modulated the lipophilic balance by influencing the structural types that existed for Au(I) and Ag(I) complexes.

Pd analogues of $[Au(dppe)_2]Cl$ have previously being prepared and tested for anti-tumour activity (Schurig *et al.,* 1989). These complexes, $[Pd(dppe)_2]Cl_2$ and $[Pd(dppen)_2]Cl_2$, were tested for cytotoxicity against a tumour cell line composed of murine and human tumour cell lines. The results showed low potency. They were also tested for anti-tumour activity on ip-implanted tumours and both of them showed inactivity and were not well tolerated.

1.9 Hypothesis

Varying the metal and lipophilicity can modify the selectivity and cytotoxic properties of anti-neoplastic drugs containing Platinum Group Metals.

1.10 Aim of study

The aim of the project was to synthesise Pd and Pt analogues of $[Au(dppe)_2]^+$ that varied in lipophilicity and consequently possessed the ability to exhibit high selectivity and anti-neoplastic activity.

1.11 Objectives of the study

The first objective of this project involved the synthesis of Pd and Pt analogues of $[Au(dppe)_2]^+$ that varied in alkyl backbones and/or substituents on the phosphorus atom (*Fig. 1.8*). This was perceived as essential in altering lipophilicity of the complexes. The phenyl complexes contained either an ethane or ethene backbone while the pyridyl ones possessed only the ethane bridge.

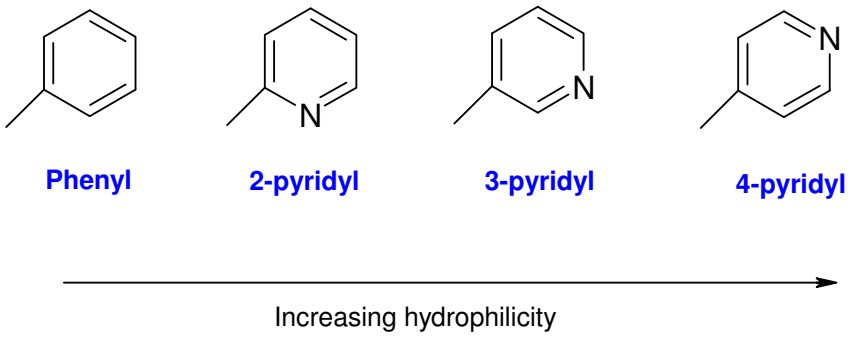

Fig 1.8: Substituents on phosphorus atoms

The complexes synthesised in this project have the general formula shown below (Fig 1.9).

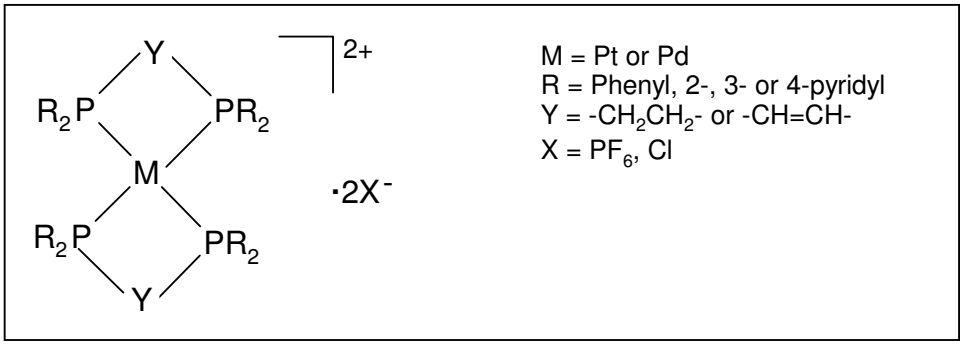

Fig 1.9: General structure of the complexes discussed in this study.

The second aspect of this study dealt with synthesising compounds that were stable enough to reach the target (tumour cells) in the presence of biological fluids. Kinetic lability in the metal-phosphine bonds is of importance so that the phosphine itself is reactive at the target site, as in Au(I), Ag(I) and Cu(I) diphosphine complexes (Berners-Price and Sadler, 1987a). On the other hand, one approach to solving the problem of rapid hydrolysis of palladium complexes is

the identification of novel substances that can be used as binding blocks for palladium anti-tumour drugs (Akdi *et al.,* 2002).

The third objective was to correlate properties of the compounds, i.e. lipophilicity, stability to *in vitro* cytotoxicity and selectivity in both cancerous and normal cells. This was in an attempt to understand the structure-activity relationship that may exist across the range of both Pd and Pt complexes. It has been shown that the different solubility profiles of Au(I) and Ag(I) pyridylphosphine complexes influences their cellular uptake and hence results in differences in anti-tumour selectivity and potency (Berners-Price *et al.,* 1999a).

The anti-neoplastic potency of these complexes against selected cancer cell lines was compared to $[Au(dppe)_2]Cl$. No inconsistency was expected in the comparison of compounds with different counterions (PF_6^- vs Cl^-) because studies have shown that activity was found to be independent of the nature of the counterion, I^- or PF_6^- (Tiekink, 2002). The most promising candidate (based on *in vitro* assays) was selected for further investigations with special focus on its anti-mitochondrial activity. This focus was necessary as the study was based on $[Au(dppe)_2]Cl$ which has been reported to have an anti-mitochondrial mode of action in tumour cells (Berners-Price *et al.,* 1999a).

Besides anti-mitochondrial action, the modes of cell death (apoptosis vs necrosis) as well as cell cycle effects were investigated. The final objective was to determine the bio-distribution of the radiolabelled lead candidate as well as its maximum tolerated dose *in vivo* (Wistar rats and Balb/c mice, respectively).

Chapter II

Phosphines and metal phosphine complexes

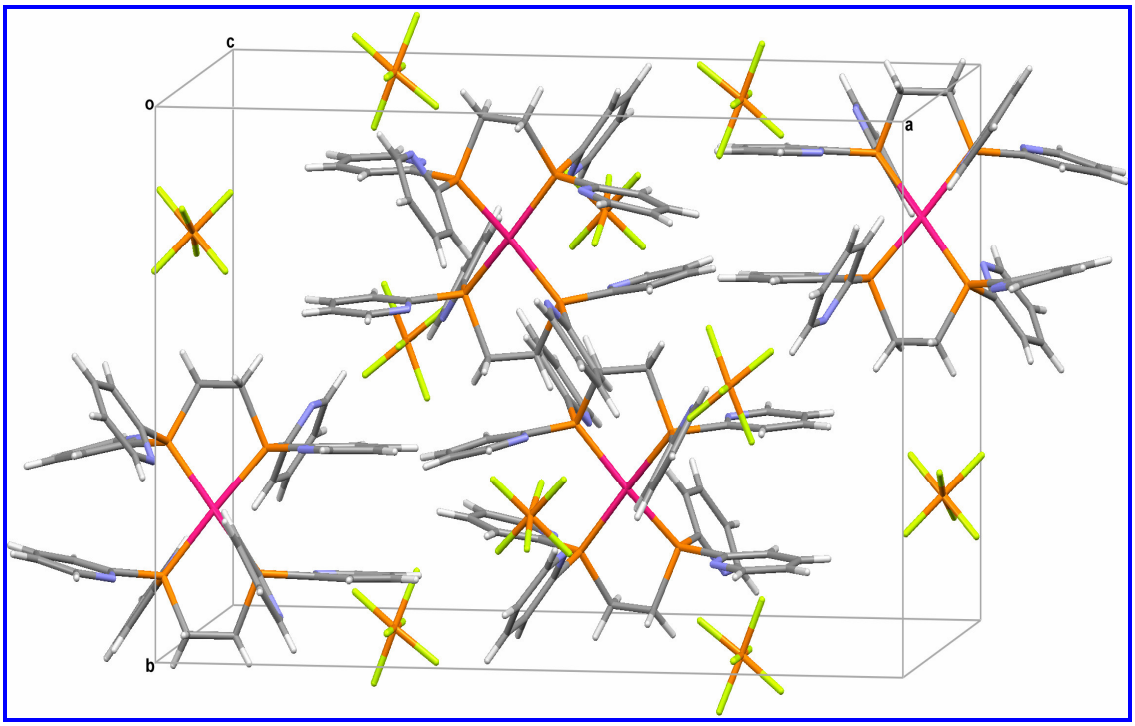

2.1 Phosphine ligands

Organic phosphines (or phosphanes) PR_3 play an important role as ligands in coordination chemistry in general and organometallic chemistry in particular (Vogler and Kunkely, 2002). Phosphines are well known to stabilise transition metals in low oxidation states but their versatility as ligands is also documented by their ability to coordinate to transition metals in higher oxidation states including metals with a d^0 electronic configuration. These ligands provide a lone pair at the phosphorus atom which is used for the formation of an M-PR_3 σ-bond. In the case of d^0 complexes, only this σ-bond exists. However, for the electron-rich d^n metals in low oxidation state, π back bonding becomes important.

2.1.1 Electronic vs Steric effects

The chemical characteristics of phosphines have continued to be the subject of many theoretical and experimental studies since the pioneering work by Tolman (Tolman, 1977) to define and quantify the steric and electronic properties of these widely used molecules (Fredericks *et al.,* 1994). These two main aspects are involved in the coordination of tertiary phosphine ligands to transition metal atoms (Roodt *et al.,* 2003). The electronic character of the M-P bond is a combined effect of the σ bond formed by donation of the lone pair electron from the P to the M atom and secondly by the ability of the P ligand to accept electron density from the metal by back-donation into a combination of the empty 3d-orbitals and σ*-orbitals of the P-atom. A second factor influencing the coordination of a ligand is the spatial demand, or steric size, associated with the specific ligand.

Organic substituents on phosphine ligands not only change the electronic properties of the ligands but may also influence their steric requirements (Mingos, 1998). Attempts have been made to quantify these effects for phosphines by measuring the pK_a values of the corresponding values of the subsequent conjugate acids $[HPR_3]^+$, which provide an estimate of the donor properties of the ligands, and the Tolman cone angle which estimates the steric requirements of the ligands. For example, the dissociation of phosphine ligands in $[Pd(PR_3)_4]$ appears to be dominated by steric effects and the dissociation constant *K* defined below:

$$[Pd(PR_3)_4] \overset{K}{\rightleftharpoons} Pd(PR_3)_3 + PR_3$$

It increases in the order $PPh(Bu^t)_2$ > PCy_3 > $P(Pr^i_3)$ > PPh_3 ~ PEt_3 > $PMePh_2$ ~ PMe_2Ph ~PMe_3.

In phosphines and cyclopentadienyls, a change of substituent causes a change not only in the steric, but also in the electronic effect of the ligand, because the R group that is varied is directly attached to the donor atom (Crabtree, 2005). For example, going from PPh_3 to PCy_3 causes a change in both factors, and each factor cannot be varied independently. They are both typically cone-shaped, so rotation about the M-L bond should not have major consequences for either steric or electronic effects. More electronegative substituents on P are expected to give a shorter M-P bond because they put more phosphorus *s* character into the bond (Tolman, 1977). For example, the substituents on the phosphorus atoms of 2.1 are similar in size but very different electronically.

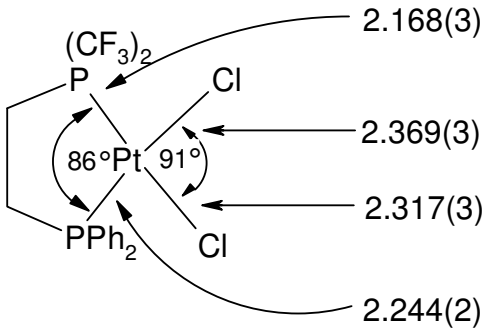

2.1

The Pt-$P(CF_3)_2$ bond is shorter by 0.07 Å compared to the Pt-PPh_2 bond and the corresponding *trans* Pt-Cl bonds differ by 0.05 Å. These effects must be largely electronic. A very similar structure was found for the Pd analogue. In summary, increasing the angles between substituents will decrease the percentage of *s* character in the phosphorus lone pair (Tolman, 1977). Changing the electronegativity of atoms can also affect bond distances and angles. Thus, electronic and steric effects are intimately related and difficult to separate in any pure way.

2.1.2 Heteroatomic substituents on phosphine ligands

The majority of phosphine ligands PR_3, carry alkyl and aryl substituents at the phosphorus atom (Vogler and Kunkely, 2002). In a more general sense, R may also be a halogen atom (phosphorus halides, PX_3) or, for example, an OR group [phosphites, $P(OR)_3$]. It has long been recognised that changing substituents on phosphorus ligands can cause marked changes in the behaviour of the free ligands and of their transition metal complexes (Tolman, 1977). The diversity of tertiary phosphines in terms of their Lewis basicity and bulkiness renders them excellent candidates to tune the reactivity of square-planar complexes towards a variety of chemical processes, such as oxidative addition and substitution reactions (Roodt *et al.,* 2003). In general, substituents with better electron-donating capabilities will increase the Lewis basicity of the phosphine, while electron-withdrawing substituents increase the π acceptor ability. The 2-pyridyl group is electron-withdrawing relative to a phenyl substituent, and the weaker σ-basicity of the phosphorus of the $PPh_{3-n}pyr_n$ ligands (versus PPh_3) likely accounts for the relative stabilities (Baird *et al.,* 1995).

2.1.3 Bridging and chelating phosphine ligands

The chelate effect is one of the oldest concepts in coordination chemistry and has been successfully explained largely in terms of the entropy change involved in the chelation process (Minahan *et al.,* 1984). In general terms, the factors that appear to be important include: the nature of the central metal atom, the nature of the ligand donor atoms, the chelate chain length, the rigidity of the chelate backbone, the steric effects of the atoms or groups attached to the donor atoms and the nature of the coordinated anions.

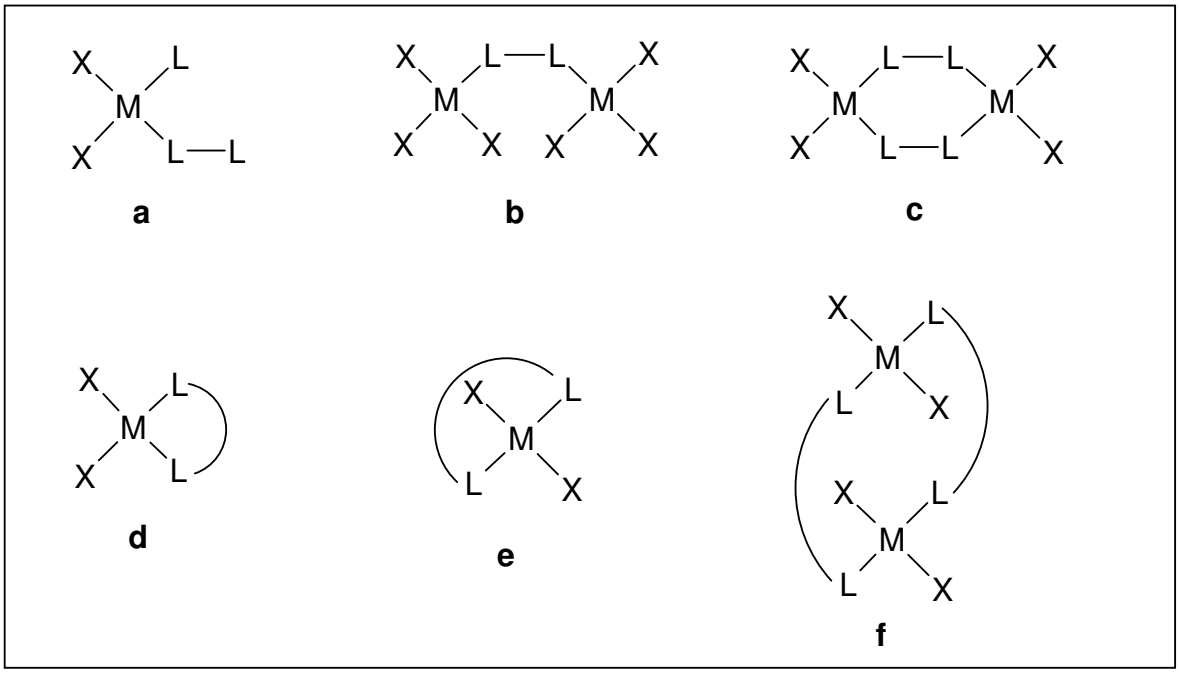

Fig 2.2: Bidentate ligand bonding modes in a square planar complex (Minahan *et al.,* 1984).

The three basic classes of potential phosphine chelate ligands are diphosphines, alkenylphosphines, and ligands with the potential to be cyclometallated (Garrou, 1981). Derivatives of diphosphine itself, H_2PPH_2, contain two donor atoms linked by a single bond and cannot, on geometrical grounds, undergo chelation (Bell, 1977). As in the case of organic diamines, chelation first appears to be possible when the donor atoms are separated by an ethylene bridge. This is so for the substituted diphosphines, $R_2PCH_2CH_2PR_2$, for example, in diphenylphosphino-ethane, where R = C_6H_5.

The versatile diphosphine ligands are particularly appropriate for the synthesis of low-valent metal complexes (Effendy *et al.,* 2004). Bis(diphenylphosphino) methane (dppm) and 1,2-bis-(diphenylphosphino)ethane (dppe) are widely used in inorganic chemistry, the former affording binuclear metal complexes in the μ–dppm form, while the latter predominately affords chelating and bridging complexes. Phosphine substitution reactions between $[Ru(\eta^5\text{-}C_5H_5)(PPh_3)_2Cl]$ and dppe have shown the latter to act as both bridging and as a chelating ligand with the formation of [RuCp(dppe)Cl] and $[\{RuCp(Cl)\}_2(\mu_2\text{-dppe})_2]$ (Moura *et al.,* 1999).

One approach to the synthesis of bimetallic complexes is the use of binucleating ligands that will rather bridge than chelate (Budzelaar *et al.,* 1990). Two of the more popular classes are diphosphinomethanes and 2-pyridylphosphine ligands (*2.3*).

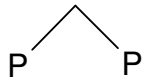

diphosphinomethane

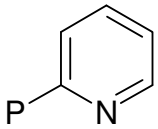

pyridylphosphine

2.3

Both of these ligands tend to form complexes in which two metal atoms are surrounded by two ligand molecules in a "*trans*" fashion (Budzelaar *et al.,* 1990). Because of the asymmetry of the 2-pyridylphosphine ligand, two types of M_2L_2 complexes may be formed, "head-to-tail" and "head-to-head" (*2.4*).

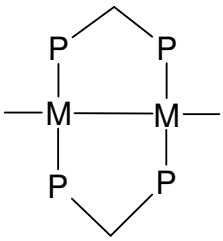

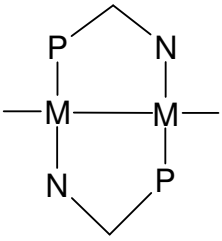

head -to - tail

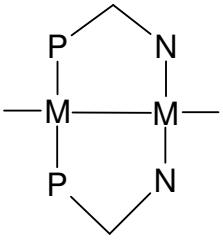

head - to - head

2.4

2.2 Pyridylphosphines

The chemistry of heterodifunctional ligands incorporating both "soft" (e.g. P) and "hard" (e.g. N or O) donor atoms continues to attract interest (Jones *et al.,* 1999). Some years ago, Rauchfuss (Jeffrey and Rauchfuss, 1979) introduced the concept of *hemilability* for ligands possessing a combination of soft and hard donor ligands (Espinet and Soulantica, 1999). This term was originally used for phosphine-amine and phosphine ether ligands that 'would bind well enough to platinum group metals to permit isolation but would readily dissociate the hard end

component, thus generating a vacant coordination site for substrate binding'. A distinguished family of hemilabile ligands is that combining phosphorus and nitrogen atoms. These ligands can display quite different coordination modes compared to P-P or N-N ligands.

Pyridylphosphines are an important class of functionalised phosphines containing both P- and N-donor centres (Durran *et al.,* 2006). Many studies have focused on simple pyridylphosphines most notably Ph_2Ppyr, $PhPpyr_2$ and $Ppyr_3$ (pyr = 2-pyridyl). These phosphines have been shown to display various coordination modes, serve as useful building blocks for di- and polynuclear compounds and have catalytic applications. The solubility of these ligands in water increases with increasing number of pyridyl substituents, for example, $Ppyr_3$ readily dissolves at pH ~3, because the first protonation equilibrium corresponds to a pK_a value of 4.2 at 20℃ (Baird *et al.,* 1995).

Interest in pyridine containing natural products and pharmaceuticals, as well as pyridine building blocks for various applications such as material science and supramolecular chemistry, has resulted in extensive efforts on synthesis methodologies (Trécourt *et al.,* 2000). Lithiation reactions allow many functionalisations either by direct reaction with electrophiles or transmetallation to allow cross-coupling reactions. The first reported preparation of a pyridylphosphine was presented (Davies and Mann, 1944) as part of a study on the optical resolution of tertiary phosphines (Newkome, 1993). Pyridylmagnesium bromide, initially generated via the entrainment process, was treated with phenyl(4-bromophenyl)chlorophosphine to afford (5%) the first pyridylphosphine **a** (*Fig. 2.5*).

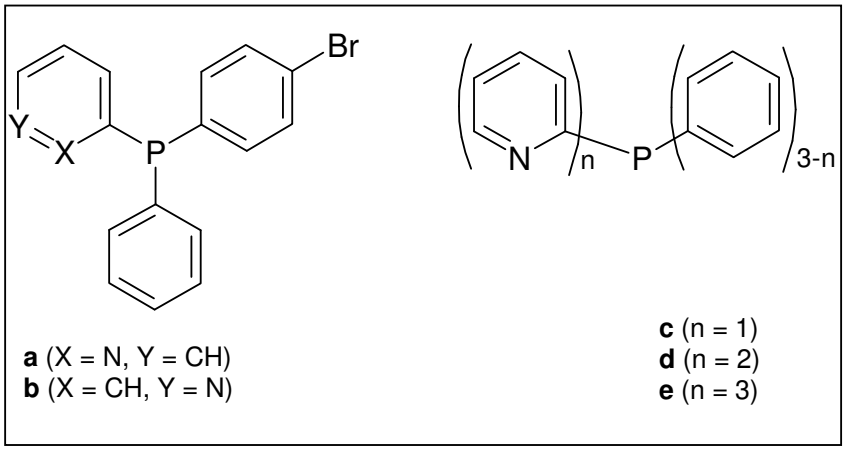

Fig. 2.5: Examples of the first pyridylphosphines

When 3-pyridylmagnesium bromide was reacted similarly, the only known, 3-pyridylphosphine **b** was prepared in poor yield (7%). Tris-2 pyridylphosphine **e** was prepared (13%) from 2-pyridylmagnesium bromide with PCl_3, whereas in 1948, this procedure was extended to the synthesis of **c** and **d**. Synthetic routes have been improved over the years and compounds **c**, **d** and **e** have been prepared in good yield by straightforward modification of the standard butyllithium metal halogen exchange method (Bowen *et al.,* 1998).

Recent work, using classical synthetic procedures in phosphorus chemistry, has shown that numerous other new pyridylphosphines can be synthesised (Durran *et al.,* 2006). These include PN-bidentate, mixed OPN-, PNP-, CNP-terdentate, chiral, phosphine oxide, and sulphide based pyridyl modified ligands. Additionally, there are typical *P*-derivatives of pyridylphosphines, which include oxides, sulphides, selenides, methides and methylphosphonium salts (Newkome, 1993).

2.3 Metal pyridylphosphines

Two researchers (Uhlig and Maaser, 1966) initially reported the preparation of Ni(II), Co(II), Zn(II) and Cu(II) complexes of $Ph_2PCH_2CH_2$(2-pyr) (Newkome, 1993). Throughout the 1970s, a few research groups utilised other simple pyridylphosphines to prepare various uncomplicated metal ion complexes, which were characterised by the application of the traditional techniques, such as infra-red, conductivity, molecular weight, magnetic susceptibility, electronic spectra, X-

ray powder diffraction, elemental analyses, as well as studies of their electrochemical properties.

The coordination chemistry of the pyridylphosphines $PPh_{3-n}pyr_n$, where n = 1-3, has developed noticeably and there have been reports on catalysis using pyridylphosphine complexes (Xie and James, 1991). A few examples are hydroformylation of olefins and water-gas-shift reaction catalysed by Rh species, conversion of methanol to ethanol using Ru species, and conversion of propyne to methylmethacrylate using Pd species. This is due to decades of work on phosphine coordination chemistry that has provided relatively easy synthetic routes to a dazzling array of different complexes (Crabtree, 2005).

One important property of potentially multidentate ligands is that they can stabilise metal ions in a variety of oxidation states and geometries (Espinet and Soulantica, 1999). The π-acceptor character of the phosphorus ligand can stabilise a metal center in a low oxidation state, while the nitrogen σ-donor ability makes the metal more susceptible to oxidative addition reactions. A widely used pyridylphosphine is (diphenyl)(2-pyridyl)phosphine, PPh_2pyr **f** (*Fig. 2.6*), which as a ligand can adopt three different coordination modes: *P*-monodentate, *P,N*-chelate and *P,N*-bridge (Jones *et al.,* 1999; Zhang and Cheng, 1996).

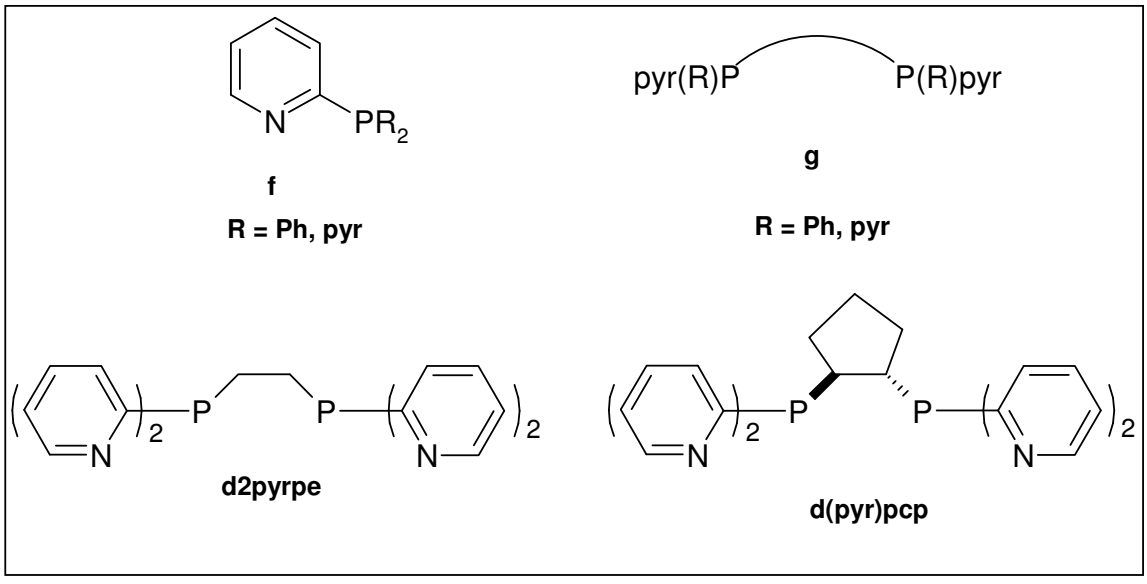

Fig 2.6: Some examples of 2-pyridylphosphine ligands

The formation of complexes where the P-N ligand acts as a chelate depends very much on the stability of the chelate ring formed (Espinet and Soulantica, 1999). In general, four membered rings are strained, whereas seven- or longer membered rings are not often geometrically favoured. Five- and six-membered chelates are expected to have the best and most stable conformation.

Interest in type **g** ligands stems from the idea that protonation of non-coordinated pyridine N atoms on the ligand would be a convenient route to water solubilisation of the corresponding metal complexes, with the ultimate objective being the homogenous catalytic hydrogenation of olefins in aqueous media (Jones *et al.,* 1999). Synthetic and characterisation details of the coordination chemistry of the ligands d(pyr)pcp and d2pyrpe towards a range of Ru(II) and Pt(II) fragments has also been described. [d(pyr)pcp = 1,5-bis-(di-2-pyridylphosphino)-cyclopentane and d2pyrpe = 1,2-bis-(di-2-pyridylphosphino)ethane].

1:2 adducts of Ag(I) and Au(I) with 1,2-bis-(di-n-pyridylphosphino)ethane (dnpyrpe) for n = 2, 3 and 4 have also been synthesised and solution properties determined by multinuclear NMR spectroscopy (Berners-Price *et al.,* 1999b; Berners-Price *et al.,* 1999a). The complexes of d3pyrpe and d4pyrpe are simple monomeric $[M(d3pyrpe)_2]^+$ and $[M(d4pyrpe)_2]^+$ species which have a much higher water solubility than the 2-pyridyl complexes (which crystallise in the solid state as dimeric, $[\{M(d2pyrpe)_2\}_2]^{2+}$, complexes). The 2-pyridylphosphine complexes of Ni(0), Ni(II), monomeric Pt(0), monomeric Pd(II), and dinuclear $Pd_2(I)$ and $Pt_2(I)$ have also been reported (Baird *et al.,* 1995). The d2pyrpe ligand has been shown to exhibit *P*,*P* bonding at Pt(II) (Jones *et al.,* 1999). Several of its complexes have some solubility in water and are completely soluble in dilute aqueous solution. A comprehensive review on the extensive studies that have been carried out on pyridylphosphines, related ligands, and their metal complexes is available (Espinet and Soulantica, 1999).

2.4 Metal complexes of diphenylphosphine ligands

The ligand bis-(diphenylphosphino)ethane (dppe) is the archetypal bidentate phosphine ligand which has probably been the most extensively used of all bidentate phosphine ligands in organometallic chemistry (Butler *et al.,* 2000). The *bis*-coordinated bis(diphenylphosphino)alkane and –alkene group 8 metal complexes have been synthesised via reaction of suitable group 8 metal precursors with two equivalents of bis-(diphenylphosphino)ethane, -ethene or –propane (Schurig *et al.,* 1989). A range of metal complexes of iron, cobalt, rhodium, iridium, nickel and palladium has been prepared. Complexes of Ag(I), Cu(I) and Au(I) diphenylphosphine have also been reported in the literature (Berners-Price *et al.,* 1988).

Diphosphine bridged-digold complexes $[\{AuCl\}_2(\mu\text{-}Ph_2P(CH_2)_2PPh_2)]$ are readily converted into the *bis*-chelated species in the presence of added diphosphine ligand (Berners-Price *et al.,* 1987b). Chelated complexes of the type $[Au(R_2P(CH_2)_nPR'_2)_2]Cl$ (n = 2 or 3) form readily when R and R' are phenyl and also with the more rigid ligand *cis*-$Ph_2PCH{=}CHPPh_2$. The interaction between bidentate diphosphines $R_2P(Y)_nPR_2$ (Y= CH_2, n= 1, 2 or 3) and silver salts has also attracted a great deal of interest because the resultant complexes have found applications in homogenous catalysis and also as anti-tumour agents (Effendy *et al.,* 2004).

2.4.1 Palladium and Platinum diphenylphosphines

Cationic palladium phosphine complexes have been actively studied due to their role in an enormous number of important synthetic transformations and for the polymerisation of polar and non-polar olefins (Thirupathi *et al.,* 2005). Palladium (II) salts form very stable complexes with tertiary phosphines and arsines (Chow *et al.,* 1974). Among the bidentate group VB chelates coordinated to palladium(II) are: 1,2-bis-(diphenylphosphino)ethane (dppe) and 1,2-bis-(diphenylarsino)ethane, *cis*- and *trans*-1,2-bis-(dimethylarsino)ethylene, *o*-phenylenebis-(dimethylarsine), 1,8-bis-(dimethylarsino)naphthalene, (*o*-diphenylphosphinophenylene)diphenyl-arsine and *o*-phenylenebis-(diphenylarsine).

The synthesis and characterisation of palladium and platinum complexes of 1,2-bis-(diphenylphosphino)ethane (dppe) and 1,2-bis-(diphenylphosphino)ethene (*cis*-dppen) have previously been described (*Fig. 2.7*) (Westland, 1965; Chow *et al.,* 1974; Oberhauser *et al.,* 1995; Oberhauser *et al.,* 1998,).

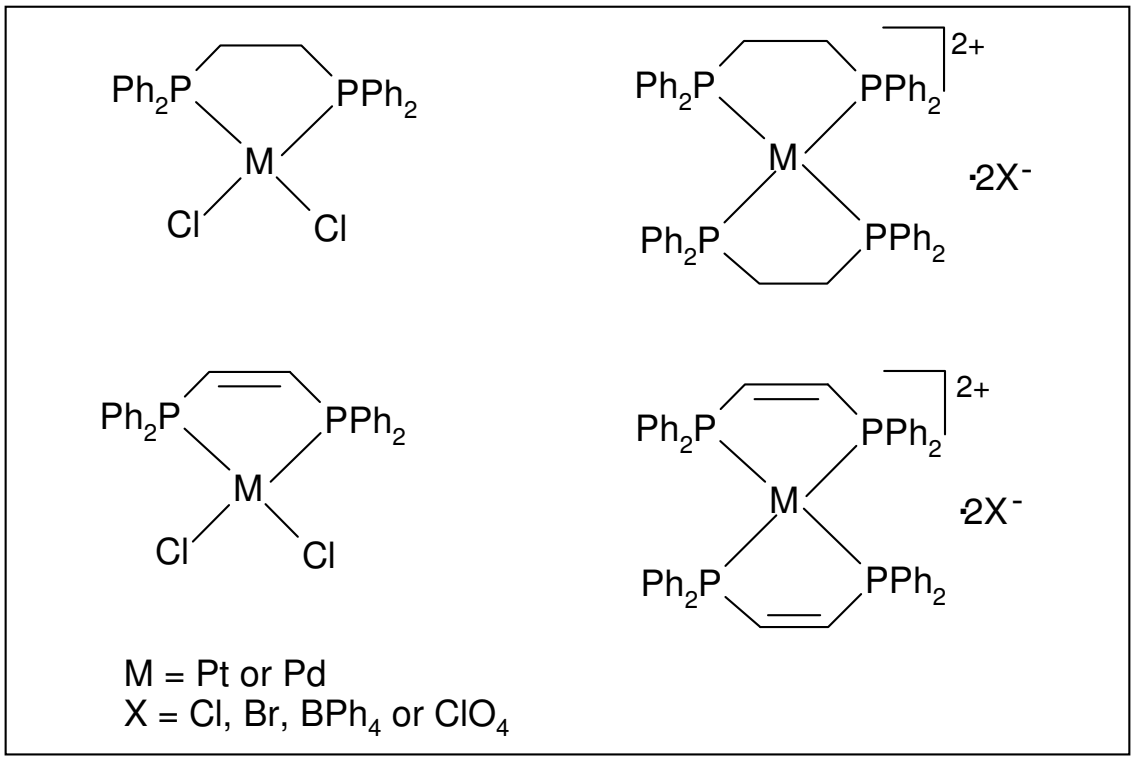

Fig 2.7: Examples of Pd and Pt phenylphosphine complexes

Recent studies have shown that in complexes of diphosphines with unsaturated backbones such as *cis*-dppen or 1, 2-bis-(diphenylphosphino)acetylene (dppa), *π* bonding, interactions between aliphatic double or triple bonds and the metal-ligand bonds are present (Oberhauser *et al.,* 1998). The unsaturated nature of the chelating diphosphine leads to the enhancement of Pt-to-P *π*-bonding (Oberhauser *et al.,* 1995). As a consequence, some degree of rehybridisation takes place at the phosphorus and aliphatic carbon atoms. In the case of *cis*-dppen this leads to completely planar structures in [$PtCl_2$(*cis*-dppen)] and [Pt(*cis*-dppen)$_2$][BPh_4]$_2$. Although the influence of *π*-bonding is less important on the reactivity of most metal phosphine complexes than *σ*-bonding and steric effects, in the case of dppa, several *π*- and *σ*-bonding possibilities occur (Oberhauser *et al.,* 1997a). The metal-phosphorus d*π*-d*π* back bonding results in unique bridging properties of dppa.

Chapter III

Preparation and characterisation of Pt and Pd phosphine complexes

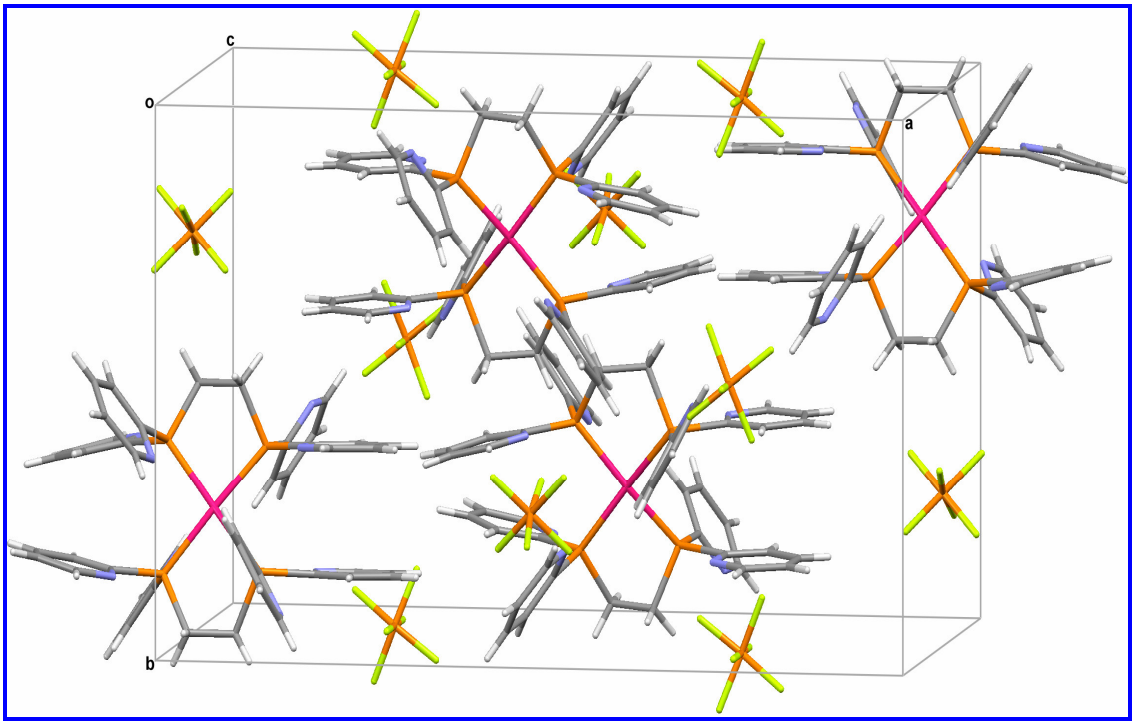

The synthesis of Pt and Pd analogues of $[Au(dppe)_2]Cl$ produced compounds that were difficult to purify and manipulate/handle. Due to the fact that stability and purity are essential properties in drug development, the chloride counterion was changed to PF_6^-. The coordination chemistry of cationic Pt and Pd complexes with bis-(diphenylphosphino)ethane or bis-(diphenylphosphino)ethene and bis-(2-, 3- and 4-bipyridylphosphino)ethane ligands were investigated and the results are discussed in this chapter.

3.1 Synthesis of metal phenylphosphine complexes

3.1.1 Preparation of 1,2-bis-(diphenylphosphino)ethane complexes of Platinum and Palladium

Synthesis of the above compounds is summarised below (Scheme 3.1).

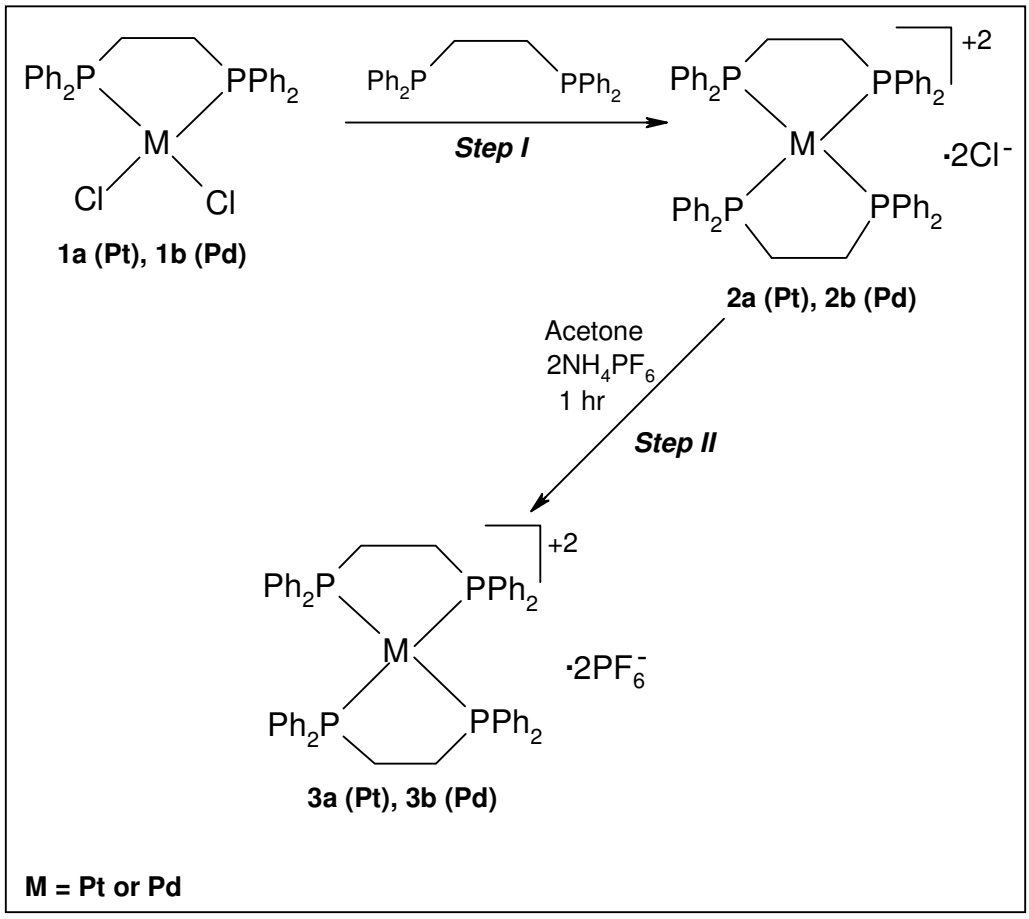

Scheme 3.1: Synthetic procedure for the preparation of Pd and Pt complexes with bis(diphenylphosphine)ethane ligands.

The known complexes **1a**, **2a**, **1b** and **2b** were synthesised according to a literature procedure (Westland, 1965) while the substitution of Cl^- with PF_6^- (*step II*) was carried out by modification of another procedure (Jones *et al.,* 1999). The latter procedure was initially used in the synthesis of a platinum pyridylphosphine complex. The compounds $[Pt(dppe)_2][PF_6]_2$ (**3a**) and $[Pd(dppe)_2][PF_6]_2$ (**3b**) were obtained in moderate yields (58 and 48 %, respectively). These complexes were far easier to purify than the corresponding complexes that contained Cl^- and stable enough to handle in the solid state as well as in solution. Both complexes were purified from DMF (boiling DMF in the case of the palladium complex) and ether vapour at room temperature. White needle-like crystals were obtained in both cases.

1,2-bis-(diphenylphosphino)ethane- and ethene complexes were insoluble in most NMR solvents and their ^1H NMR spectra showed multiplets in the expected regions (δ 7.2-7.8) due to aromatic protons. Analysis of chelating phosphine complexes is usually accomplished by IR spectroscopy, if dealing with carbonyl complexes, or ^{31}P NMR spectroscopy where one observes a deshielding effect upon bonding and thus can easily tell whether a bisphosphine is functioning in a monodentate or bidentate fashion (Garrou, 1981).

Table 3.1: $^{31}P\{^1H\}$ NMR data of Pt, Pd and Au complexes with 1,2-bis-(diphenylphosphino)ethane

	[a] $^{31}P\{^1H\}$ NMR	
	δ,ppm	**^1J (^{195}Pt-^{31}P), Hz**
dppe	-13.7 (s)	-
$PtCl_2$(dppe)	43.4 (s), [b]43.8 (s)	3547, [b]3600
$[Pt(dppe)_2]Cl_2$	49.2 (s)	2333
$[Pt(dppe)_2][PF_6]_2$ (3a)	49.3 (s)	2321
	-143.2 (spt)	712 (PF_6)
$PdCl_2$(dppe)	67.5 (s)	-
$[Pd(dppe)_2]Cl_2$	57.4 (s)	-
$[Pd(dppe)_2][PF_6]_2$ (6a)	58.1 (s)	-
	-143.3 (spt)	711 (PF_6)
$[Au(dppe)_2]Cl$	21.6, [c]21.9, [d]18.7	-

[a]Measured in DMSO (δ, ppm). Spectra were run at 298 K.

[b]Literature values in DMSO (Hope *et al.,* 1986)

[c]Literature values in D_2O (Berners-Price and Sadler, 1987b)

[d]Literature values in $CDCl_3$ (Berners-Price *et al.,* 1987b)

s = singlet, spt = septet

The ^{31}P NMR data presented above (*Table 3.1*) indicates that the free ligand (dppe) is more shielded (-13.7 ppm) than the complexes in both metals. This shift is treated quantitatively as the coordination chemical shift; Δ, defined as δ{P(coordinated)} – δ{P(free ligand)} (Gambaro *et al.,* 1989). However, the phosphorus resonances of the complexes behave differently in the formation of *bis*-chelated complexes from *mono*-chelated species. The ^{31}P chemical shift of $[PtCl_2(dppe)]$ appears upfield, 43.4 ppm; lit. 43.8 ppm (Hope *et al.,* 1986) with respect to $[Pt(dppe)_2]Cl_2$ (48.9 ppm) and $[Pt(dppe)_2][PF_6]_2$ (49.3 ppm). In contrast, ^{31}P chemical shift of $[PdCl_2(dppe)]$ (67.5 ppm) appears downfield with respect to $[Pd(dppe)_2]Cl_2$ (57.4 ppm) and $[Pd(dppe)_2][PF_6]_2$ (58.1 ppm).

The influence of the non-coordinating anion, PF_6^- compared with Cl^-, is insignificant as demonstrated in the chemical shifts for both platinum and palladium complexes. The observed values of $^1J(^{195}Pt\text{-}^{31}P)$, 2321-3547 Hz, rule out the presence of a system containing a platinum-carbon bond (Banditelli *et al.,* 1982). Ligands with short chelate backbones such as $Ph_2P(CH_2)_nPPh_2$ (n = 2, 3, 4) form *cis* chelated complexes with both palladium(II) and platinum(II) of general formula $[M(L\sim L)_2]MX_4$ or $[M(L\sim L)X_2]$ (Minahan *et al.,* 1984). In these cases, the length of the chelate backbone prevents the formation of the *trans* chelate since it is not sufficient to span the *trans* positions in a square planar complex.

3.1.2 Preparation of cis-1,2-bis-(diphenylphosphino)ethene complexes of Platinum and Palladium

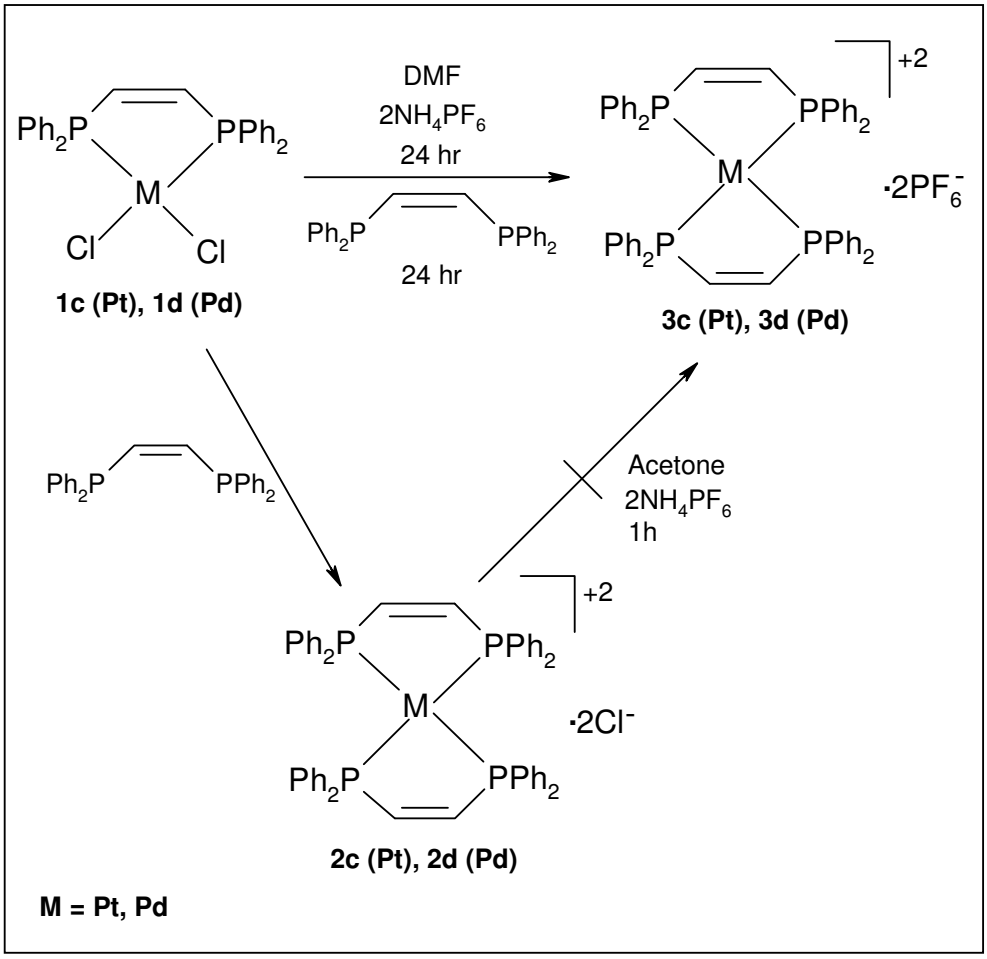

Scheme 3.2: Synthetic procedure for the preparation of Pd and Pt complexes with *cis* -bis(diphenylphosphine)ethene ligands.

Compounds **1c** and **1d** were prepared according to the literature procedures of Hope and Chow (Hope *et al.,* 1986 and Chow *et al.,* 1974), respectively. While the preparation of the palladium compound (**1d**) was straightforward, the platinum analogue (**1c**) was less soluble and had to be dissolved in boiling DMF. If this step is omitted, the products have an oligomeric $[Pt(Ph_2PCHCHPPh_2)X_2]_n$ composition which are much less soluble in organic solvents (Hope *et al.,* 1986). The amount of the oligomeric product obtained strongly depends on the stirring time (Oberhauser *et al.,* 1995). Independent of the stoichiometry used for $[PtCl_4]^{2-}$:*cis*-dppen = 1:1 or 1:2, a species of the type $[Pt(cis\text{-}dppen)_2]^{2+}$ is formed. Compounds **2c** and **2d** were prepared according to Oberhauser *et al.,* 1995.

Preparation of *cis*-dppen compounds using a similar route to that of the dppe complexes (*Scheme 3.1*) led to extremely poor yields in the case of **3c** [Pt(*cis*-dppen)$_2$][PF$_6$]$_2$. In the synthesis of the palladium complex, $^{31}P\{^1H\}$ NMR spectrum displayed a mixture of minor peaks of **1d** [PdCl$_2$(*cis*-dppen)] at 74.4 ppm and **3d** [Pd(*cis*-dppen)$_2$][PF$_6$]$_2$ at 64.6 ppm; and unidentified major peak at 18.0 ppm. The structural and reactivity differences between [MCl$_2$(dppe)] and [MCl$_2$(*cis*-dppen)] (M = Pd, Pt) complexes have been widely addressed in the literature (Devic *et al.,* 2004). The authors assigned the special properties of the *cis*-dppen ligand when compared with the saturated dppe counterpart to an enhancement of the M-to-P π bonding interaction, due to the unsaturated nature of the aliphatic backbone in the dppen.

An alternative synthetic route for the synthesis of both the palladium and platinum complexes was devised by modification of a literature procedure (*Scheme 3.2*) (Oberhauser *et al.,* 1995). In the syntheses of related complexes, the authors emphasised that the removal of the chloride from [MCl$_2$(*cis*-dppen)] (M = Pd, Pt) was important for the completion of the reactions. This was achieved by either substitution of the coordinated chlorides by other ligands and simultaneous replacement of the resulting anionic chlorides with BPh_4^- or by precipitating AgCl with a silver salt leading to a cationic intermediate. In our case, the platinum compound [Pt(dppen)$_2$][PF$_6$]$_2$ was still obtained in poor yields (19%) while the palladium compound [Pd(dppen)$_2$][PF$_6$]$_2$ was ultimately obtained in moderate yield (51%).

Other research groups have reported partial loss of chloro ligands or complete failure to abstract coordinated Cl with thallium triflate despite prolonged treatment with an excess of the salt (Devic *et al.,* 2004). Reaction of PdCl$_2$(dppen) with an excess of thallium triflate in CH_2Cl_2 afforded a complex salt, formulated as [PdCl(dppen)]$_2$(OTf)$_2$, indicating a partial dechlorination.

Table 3.2: $^{31}P\{^{1}H\}$ NMR data of Pt and Pd complexes with 1,2-bis-(diphenylphosphino)ethene

	[a]$^{31}P\{^{1}H\}$ NMR	
	δ,ppm	**$^{1}J(^{195}Pt\text{-}^{31}P)$, Hz**
dppen	-23.3 (s)	-
[b]**$PtCl_2$(dppen)**	50.1(t)	3623
$[Pt(dppen)_2]Cl_2$	59.6 (t)	2355
$[Pt(dppen)_2][PF_6]_2$ (3b)	60.2 (t)	2350
	-143.3 (spt)	711
[b]**$[Pt(dppen)_2][BPh_4]_2$**	60.9 (s)	2334
$PdCl_2$(dppen)	74.4, [b]71.3 (s)	-
$[Pd(dppen_2]Cl_2$	64.4 (s)	-
$[Pd(dppen)_2][PF_6]_2$ (6b)	64.3 (s)	-
	-143.3 (spt)	711 Hz
[b]**$[Pd(dppen)_2][BPh_4]_2$**	66.2 (s)	-

[a]Measured in DMSO (δ, ppm). Spectra were run at 298 K.

[b]Literature values (Hope *et al.,* 1986, Oberhauser *et al.,* 1995). The solvents used by the authors were DMF (for Pd-complexes) and CH_2Cl_2 or DMSO (for Pt-complexes).

s = singlet, t = triplet, spt = septet

$^{31}P\{^{1}H\}$ NMR data presented above (*Table 3.2*) shows a similar trend to that observed in dppe complexes (platinum complexes show a downfield shift in the formation of the *bis*-chelated complex from *mono*-chelated species while palladium complexes display the opposite behaviour). The rigidity of *cis*-dppen has been thought to be responsible for anomalous ^{31}P NMR chemical shifts in a series of comparable compounds (Oberhauser *et al.,* 1995). From this it is clear, that there are a number of effects which distinguish *cis*-dppen from its saturated analog dppe.

Similarly to reported data (Oberhauser *et al.,* 1995), ^{1}J(Pt,P) values of the *mono*- and *bis*-chelated platinum *cis*-dppen complexes (3623 Hz and 2350 Hz, respectively) are very close to the corresponding complexes containing dppe (3600 and 2321 Hz). It seems likely that these ^{1}J(Pt,P) parameters are completely dominated by the difference of the *trans* influences of chloride and a phosphine,

respectively (Oberhauser *et al.,* 1995). Additionally, the variation of these coupling constants, although the range is very small, tends to confirm that the strength of the Pt-Cl bonds within this series increases from $[PtCl_2(dppe)]$ to $[PtCl_2(dppen)]$, as a consequence of a stronger σ-bonding effect (Devic *et al.,* 2004).

It is worth noting that the solution ^{31}P NMR spectrum of the $[Au(dppen)_2]^+$ ($CDCl_3$) consists of a single resonance at δ 23.2, similar to that found for the chloride salt, together with a multiplet of the PF_6^- anion [$\delta(PF_6)$ -143.6, J(P-F) = 714 Hz] (Berners-Price *et al.,* 1992).

3.2 Synthesis of metal pyridylphosphine complexes

The ligands shown below (*Fig.3.1*) were synthesised according to the literature procedures (Bowen *et al.,* 1998) and complexed to either palladium or platinum.

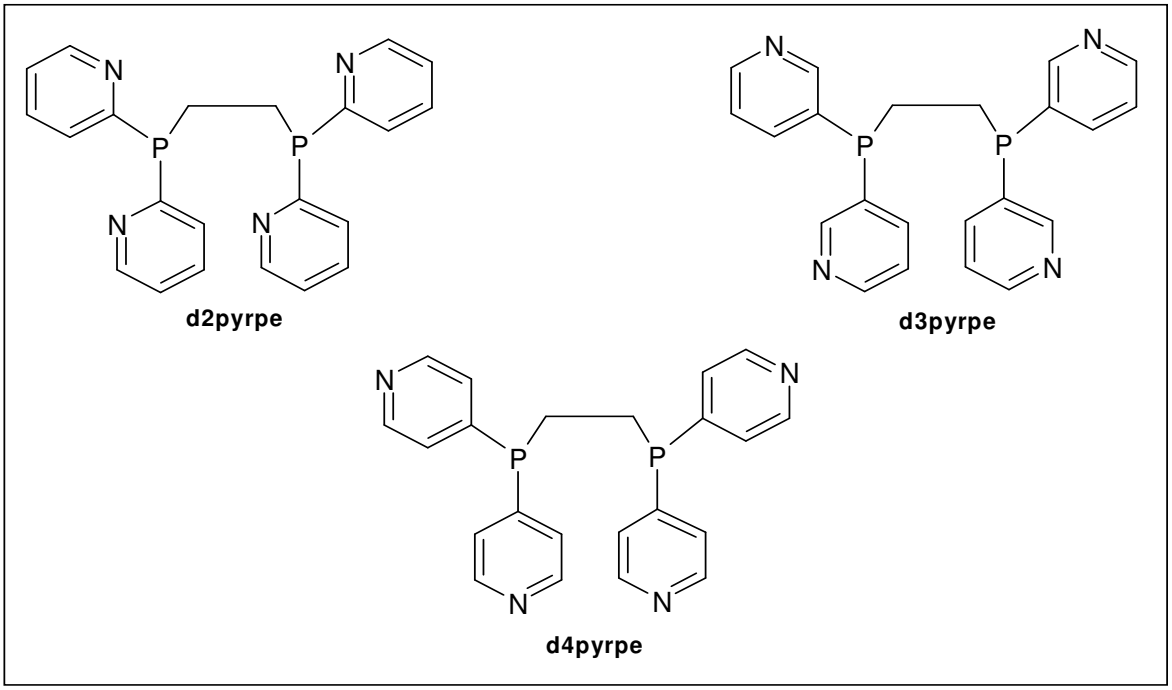

Fig. 3.1: 1,2-bis-(dipyridylphosphino)ethane ligands that have been used to prepare the palladium and platinum complexes discussed in this project. d2pyrpe, d3pyrpe d4pyrpe are 1,2-bis-(di-2-pyridylphosphino)ethane, 1,2-bis-(di-3-pyridylphosphino)ethane and 1,2-bis-(di-4-pyridylphosphino)ethane, respectively.

Synthetic routes differed among the three ligands (2-, 3- and 4-pyridyl) as well as between the two metals (M = Pt, Pd). In the preparation of the complexes,

mixtures of compounds were obtained and identified by ^{31}P NMR on the basis of the known patterns in chemical shifts as well as coupling constants.

3.2.1 Preparation of 1,2-bis-(di-2-pyridylphosphino)ethane platinum(II) complexes

Synthesis of these complexes is summarised below (Scheme 3.3).

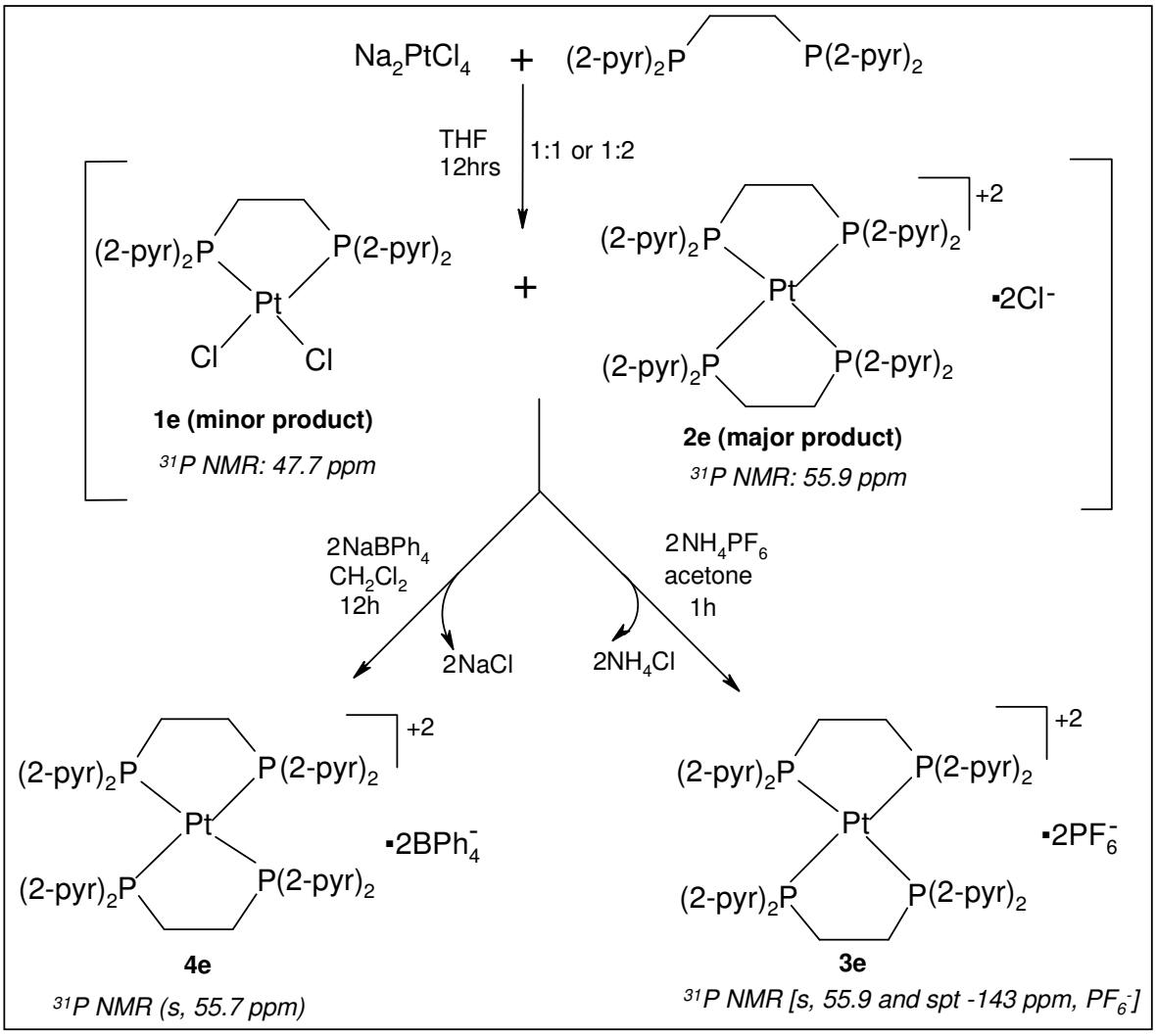

Scheme 3.3: Synthesis of 1,2-bis(di-2-pyridylphosphino)ethane platinum(II) complexes. $^{31}P\{^{1}H\}$ NMR chemical shifts (ppm) are indicated in italics.

Reaction of $Na_2[PtCl_4]$ and 1,2-bis-(di-2-pyridylphosphino)ethane (d2pyrpe) yielded a yellow mixture (insoluble in THF) of the *mono*-chelated (**1e**) and *bis*-chelated (**2e**) compounds irrespective of stoichiometry. Attempts to separate the mixture by various methods proved to be unsuccessful and only decomposition

products were obtained. It is worth noting that synthesis of the two compounds **1e** and **2e** has been attempted previously and reported in the literature (Jones *et al.,* 1999) whereby [$PtCl_2$(cod)] was used as a starting material. X-ray quality crystals of compound **1e** co-crystallised with a solvent molecule in the lattice (CH_2Cl_2) were recorded, but satisfactory elemental analysis of compound **2e** could not be obtained.

The $^{31}P\{^1H\}$ NMR spectrum (DMSO) of the mixture exhibited two phosphorus signals. One at δ = 47.7 ppm, [lit: δ = 47.1 ppm in $CDCl_3$ (Jones *et al.,* 1999)] and δ = 55.1 ppm indicating the presence of two species. These singlets were characterised by corresponding pairs of ^{195}Pt satellites (*sat*) [$^1J_{PPt}$ = 3480 (lit. 3481 Hz)], and 2470 Hz, respectively. Complex **1e** with $^1J_{PPt}$ = 3480 Hz is consistent with equivalent, mutually *cis* P atoms in a square planar arrangement; complexes of the type *cis*-Pt(halide)$_2$(pyridylphosphine)$_2$ invariably have *J*(PtP) values in the range ~3500-3900 Hz (Xie and James, 1991).

The problems encountered in the synthesis of **2e**, i.e instability and difficulty in purification, posed problems for its proposed application. Possibilities of decomposition taking place before reaching the target site in the investigation for potential anti-tumour activity were imminent. Circumvention of these problems was achieved by replacement of the counterion (Cl^-) with BPh_4^- or PF_6^-. **3e** was prepared according to a literature procedure (Jones *et al.,* 1999) and obtained in good yield (65%) while **4e** was prepared via metathesis of the crude mixture (**1e** and **2e**) with $NaBPh_4$. Colourless crystals of **4e** suitable for study by X-ray diffraction were obtained from dichloromethane/ether at -20 °C.

3.2.2 Preparation of 1,2-bis-(di-2-pyridylphosphino)ethane palladium(II) complexes

As previously observed in the preparation of the Pt compound, a mixture of the *mono*-[$PdCl_2$(d2pyrpe)] (**1f**) and *bis*-chelated compound [Pd(d2pyrpe)$_2$]Cl_2 (**2f**) was obtained irrespective of stoichiometry used, d2pyrpe:(Na_2[$PdCl_4$]). The $^{31}P\{^1H\}$ NMR spectrum of the mixture showed two singlets (70.4 and 64.0 ppm in DMSO)

and (69.9 and 62.5 ppm in $CDCl_3$) for the respective compounds. In order to distinguish the representative peaks in ^1H and ^{31}P NMR spectra, $[PdCl_2(d2pyrpe)]$ was prepared from either $PdCl_2$ or $[PdCl_2(NCCH_3)_2]$. A brown solid was obtained from the reaction of $PdCl_2$ with d2pyrpe (1:1). Interestingly, a portion of this compound was soluble in DMSO while the other fraction dissolved in $CDCl_3$. The $^{31}P\{^1H\}$ spectrum of the former sample showed the presence of only $[PdCl_2(d2pyrpe)]$ (s, δ = 70.4 ppm) while the latter sample exhibited a singlet (δ = 62.5 ppm) that signified the presence of the *bis*-chelated compound, $[Pd(d2pyrpe)_2]Cl_2$. Attempts to purify the mixture from DMF/ether were not successful.

In the other reaction, $PdCl_2$ was refluxed in acetonitrile to form the yellow intermediate, $[PdCl_2(NCCH_3)_2]$, (Mohlala *et al.,* 2005) which was subsequently reacted with the ligand, d2pyrpe (1 eq.). The orange product was insoluble in numerous solvents (acetonitrile, acetone, methanol, ether, dichloromethane) and only soluble in DMF. It is worth noting that only $[PdCl_2(d2pyrpe)]$, was formed whether 1:1 or 1:2 ratio of $[PdCl_2(NCCH_3)_2]$:dpyrpe was utilised. The observed singlet in $^{31}P\{^1H\}$ NMR spectra at 70.4 ppm in DMSO (69.9 ppm in $CDCl_3$) as well as MS-FAB spectrometry (M^+-Cl = 543), assisted in distinguishing between the *mono*- and *bis*-chelated compounds in the previously obtained mixtures. Reaction of this *mono*-chelated compound with a second equivalent of d2pyrpe, did not lead to the formation $[Pd(d2pyrpe)_2]Cl_2$.

As observed earlier in the preparation of *cis*-dppen complexes $[MCl_2(cis\text{-dppen})]$ (M = Pd, Pt), the removal of the chloro ligands from $[PdCl_2(d2pyrpe)]$ seemed to be crucial for the completion of the reactions. Further attempts to obtain the desired compound were pursued by substituting the chloro ligands with $CF_3SO_3^-$ by using silver triflate (AgOTf; OTf = $CF_3SO_3^-$). Trifluoromethanesulphonate is a readily available (counter) anion in the presence of stronger coordinating ligands (Kim *et al.,* 2002). It has been known as a weak base and hence a good leaving group, and is useful in generating new species that cannot be approached by direct synthetic methods. Numerous palladium or platinum complexes such as $[M(P\text{-}P)(OTf)_2]$, have been used within the past decade as building blocks for the

formation of supramolecular assemblies, upon triflate displacement and subsequent complexation with bridging pyridine ligands (Devic *et al.,* 2004).

Replacement of the chloro ligands with the weakly coordinating triflate anions (with concomitant precipitation of AgCl) was attempted by reacting [$PdCl_2$(d2pyrpe)] with AgO_3SCF_3. However, an intractable compound was obtained as it also precipitated out of the reaction solvent (CH_2Cl_2). There was an insignificant change in $^{31}P\{^1H\}$ NMR parameter (δ 71.1 vs 70.4 ppm). Addition of a second equivalent of d2pyrpe to the deep yellow mixture led to the formation of brick red/dark orange mixture that had traces of a yellow residue. Replacement of the triflate ions with a second equivalent of d2pyrpe was expected to lead to a cationic intermediate with triflate counter ions (Oberhauser *et al.,* 1995).

Insolubility of these mixtures in deuterated solvents resulted in poorly resolved NMR spectra and these synthetic routes were not pursued further. Solubility problems have been encountered by others in the preparation of Pd complexes containing triflate (Zhuravel and Glueck, 1999). It is worth noting that many side reactions leading to formation of decomposition products (and consequently lower yields of intended compound) occured when following these long synthetic routes that involved many handling and isolation steps.

[Pd(d2pyrpe)$_2$][PF_6]$_2$ (**3f**) was finally prepared in the same manner (S*cheme 3.3*) as the Pt analogue by using the precursor ($Na_2[PdCl_4]$) and an impure sample of [Pd(d2pyrpe)$_2$]Cl_2. Colourless crystals of **3f** suitable for single X-ray diffraction studies were obtained from DMF/ether. ^1H and/or $^{31}P\{^1H\}$ NMR data of the identifiable products in the preparation of both platinum and palladium complexes are presented below (*Table 3.3*).

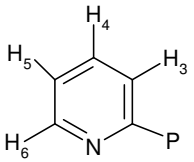

Labelling of protons for 2-pyridylphosphine ligands (Baird *et al.,* 1995).

Table 3.3: ^{1}H and $^{31}P\{^{1}H\}$ NMR data of 1,2-bis-(di-2-pyridylphosphino)ethane and its Pt and Pd complexes

		Pyridyls ^{1}H data (δ)					^{31}P data	
Compound	**Solvent**	**H_3**	**H_4**	**H_5**	**H_6**	**CH_2[a]**	**δ**	**$^{1}J_{PtP}$ or $^{1}J_{PF}$ (Hz)**
[b]**d2pyrpe**	$CDCl_3$	7.43	7.53	7.12	8.63	2.53 (8.28)	-6.0	-
[c]**1e and 2e**	DMSO	[d]7.78	[d]7.78	7.45	8.42	2.84	47.7 & 55.1	3480 & 2470
[e]**$[Pt(d2pyrpe)_2][BPh_4]_2$**	DMSO	6.88	7.00	6.64	7.61	2.00 (19.38)	55.7	2460
$[Pt(d2pyrpe)_2][PF_6]_2$	DMSO	6.93	7.00	6.67	7.64	2.06 (19.38)	[f]55.9 & -143	[f]2459 & 711
[g]**1f and 2f**	DMSO	8.00 & [d]7.74	8.12 & [d]7.74	7.61 & 7.43	8.77 & 8.42	2.89	70.4 & 64.0	-
$[PdCl_2(d2pyrpe)]$	DMSO	7.99	8.11	7.61	8.76	2.93 (21.35)	70.4	-
$[PdCl_2(d2pyrpe)]$	$CDCl_3$	7.74	8.42	7.35	8.64	3.06 (20.67)	69.9	-
$[Pd(d2pyrpe)_2]Cl_2$	$CDCl_3$	[d]7.53	7.93	[d]7.53	8.33	3.01	62.5 ([h]64.0)	-
$[Pd(d2pyrpe)_2][PF_6]_2$	DMSO	7.67	7.74	7.46	8.42	2.85	64.0 & -143	711 (spt, $[PF_6]^-$)

Spectra were run at 298 K. All the pyridyl protons appeared as multiplets and phosphorus occurred as singlets (except for PF_6^-). The ligand data was in agreement with that reported in the literature (Baird *et al.,* 1995, Bowen *et al.,* 1998).[a]Broad singlet or quasi-triplet (J = [$^{2}J(^{31}P\text{-}^{1}H)$ + $^{3}J(^{31}P\text{-}^{1}H)$] (Hz) in parentheses where resolved (Berners-Price *et al.,* 1999b) and broad doublet (only in Pd complexes). [b]Proton numbering scheme is based on lit. (Berners-Price *et al.,* 1999b) and their values are in close agreement (solvent was CD_3OD). [c]**1e** and **2e** are $[PtCl_2(d2pyrpe)]$ and $[Pt(d2pyrpe)_2]Cl_2$, respectively. [d]Overlap of the signals. [e]Phenyl protons (multiplets) of BPh_4^- at δ = 5.97 (8H), 6.10 (16H) and 6.35 (16H). [f]Singlet and septet (spt, $^{1}J_{PF}$), respectively, Lit. values = δ 54.4 (2477 Hz) and -144 (712 Hz) in CD_3OD (Jones *et al.,* 1999). [g]**1f** and **2f** are $[PdCl_2(d2pyrpe)]$ and $[Pd(d2pyrpe)_2]Cl_2$, respectively which were obtained as a mixture. [h]Chemical shift in DMSO.

The proton data showed above (*Table 3.3*) shows pyridyl protons occurring as multiplets in the expected aromatic region. The ^{1}H NMR chemical shift differences between the free ligand (δ 7.43-8.63) and the coordinated complexes (δ 6.64-8.77) were not significant. ^{1}H NMR signal for the H_6 protons always gives the most downfield signal (Baird *et al.,* 1995). More generally, the relative positions of H_3-H_5 for 2-pyridyl protons are found to vary with the solvent, and the nature of the complex.

The ethane protons (bridging CH_2) were also found in the expected regions (δ 2.00-3.06, depending on the solvent used) but coupling constants differed between the free ligand (8.28 Hz) and the complexes (19.38-21.35 Hz). The ligand (δ = 2.53) appeared as a quasi-triplet (8.28 Hz), lit. (δ 2.44 and 8.7 Hz in CD_3OD) (Berners-Price *et al.,* 1998). The ^{1}H NMR data is similar to that observed in Ag(1) complexes which is consistent with the formation of simple monomeric species. For bidentate phosphines with $(CH_2)_2$ backbones (e.g. dppe), the CH_2 protons constitute the AA' part of an $A_2XX'A_2'$ spin system as a result of unequal ^{31}P-^{1}H spin-spin coupling to the two P atoms and give rise to a quasi triplet in which the separation of the outer two peaks corresponds to $|^{2}J(^{31}P\text{-}^{1}H) + {}^{3}J(^{31}P\text{-}^{1}H)|$ (Berners-Price *et al.,* 1998).

The major difference is that while the Pt complexes $[Pt(d2pyrpe)_2][BPh_4]_2$ and $[Pt(d2pyrpe)_2][PF_6]_2$ gave rise to quasi triplets (19.38 Hz), the *bis*-chelated Pd complexes, $[Pd(d2pyrpe)_2]Cl_2$ and $[Pd(d2pyrpe)_2][PF_6]_2$ displayed broad singlets (*Table 3.3*). In contrast, Pd *mono*-chelated species, $[PdCl_2(d2pyrpe)]$ exhibited a quasi-doublet (20.67 and 21.35 Hz in DMSO and $CDCl_3$, respectively). This difference in the splitting is ascribed to spin-spin coupling ($^{1}J_{PtP}$) which results in unequal ^{31}P-^{1}H spin-spin coupling (J P-CH_2) while Pd does not induce any coupling. In *bis*-chelated gold(I) diphosphine complexes, the broadening of the $(CH_2)_2$ resonance gave an unresolved multiplet (Berners-Price *et al.,* 1998).

The singlet ^{31}P NMR chemical shifts for all the complexes fall in the downfield region, consistent with the reported, relative to deshielding of P nuclei in five-membered chelate rings (Jones *et al.,* 1999). As previously observed in dppe and dppen complexes, formation of the Pt *bis*-chelated complexes from the mono-

chelated species resulted in a ^{31}P downfield chemical shift (δ 47.7 to 55.9) while the reverse (shift to highfield region) occurred in the palladium complexes (δ 70.4 to 64.0). The magnitude of ^{1}J(Pt, P) for the *mono*- and *bis*-chelated species were in the ranges previously observed in dppe and dppen complexes (3480 and ~2500 Hz, respectively).

3.2.3. Preparation of 1,2-bis-(di-3-pyridylphosphino)ethane platinum(II) complexes

Attempts to prepare $[Pt(d3pyrpe)_2][PF_6]_2$ using Scheme 3.3 were not successful. Unlike the 2-pyridyl complex, equal amounts of $Na_2[PtCl_4]$ and d3pyrpe stirred (in THF) at room temperature for 12 hours yielded only the mono-chelated complex $[PtCl_2(d3pyrpe)]$, **1g**. The $^{31}P\{^{1}H\}$ NMR spectrum of this compound revealed a singlet at 37.8 ppm [$^{1}J_{PPt}$ = 3582 Hz]. Reaction of **1g** with a second equivalent of the ligand failed to give the expected *bis*-chelated compound even at elevated temperature (50°C). This idea was derived from a similar procedure that was successfully used in the preparation of $[Ni(d2pyrpe)_2]$ from $[Ni(cod)_2]$ and d2pyrpe (1:2 ratio, respectively) (Baird *et al.,* 1995). The above complex required heat (50°C) for its formation, but once formed, the chelate was significantly more stable in air and in solution than the tetrakis(monodentate ligand) species, $[Ni(Ppyr_3)_4]$.

Preparation of d3pyrpe complexes of Pt is shown below (*Scheme 3.4*). Unfortunately, this method was time consuming, labour intensive and it also led to extremely low yields. Isolation of $[Pt(OTf)_2(d3pyrpe)]$ prepared from $[PtCl_2(d3pyrpe)]$ was attempted and the $^{31}P\{^{1}H\}$ NMR spectrum showed no difference in the chemical shift and coupling constant $^{1}J_{(PtP)}$ (δ 37.8 and 3582 Hz). Isolation was henceforth ommitted and the solution containing the intermediate $[Pt(d3pyrpe)_2][OTf]_2$ was prepared *in situ* by adding excess d3pyrpe. Both of these compounds were unstable in air, extremely insoluble in numerous solvents and purification processes were unsuccessful. Satisfactory ^{1}H NMR spectra were not be obtained while the $^{31}P\{^{1}H\}$ NMR spectrum revealed a singlet [δ 40.0 ppm, $^{1}J_{PtP}$ = 2382 Hz] for the proposed *bis*-chelated complex, $[Pt(d3pyrpe)_2][OTf]_2$.

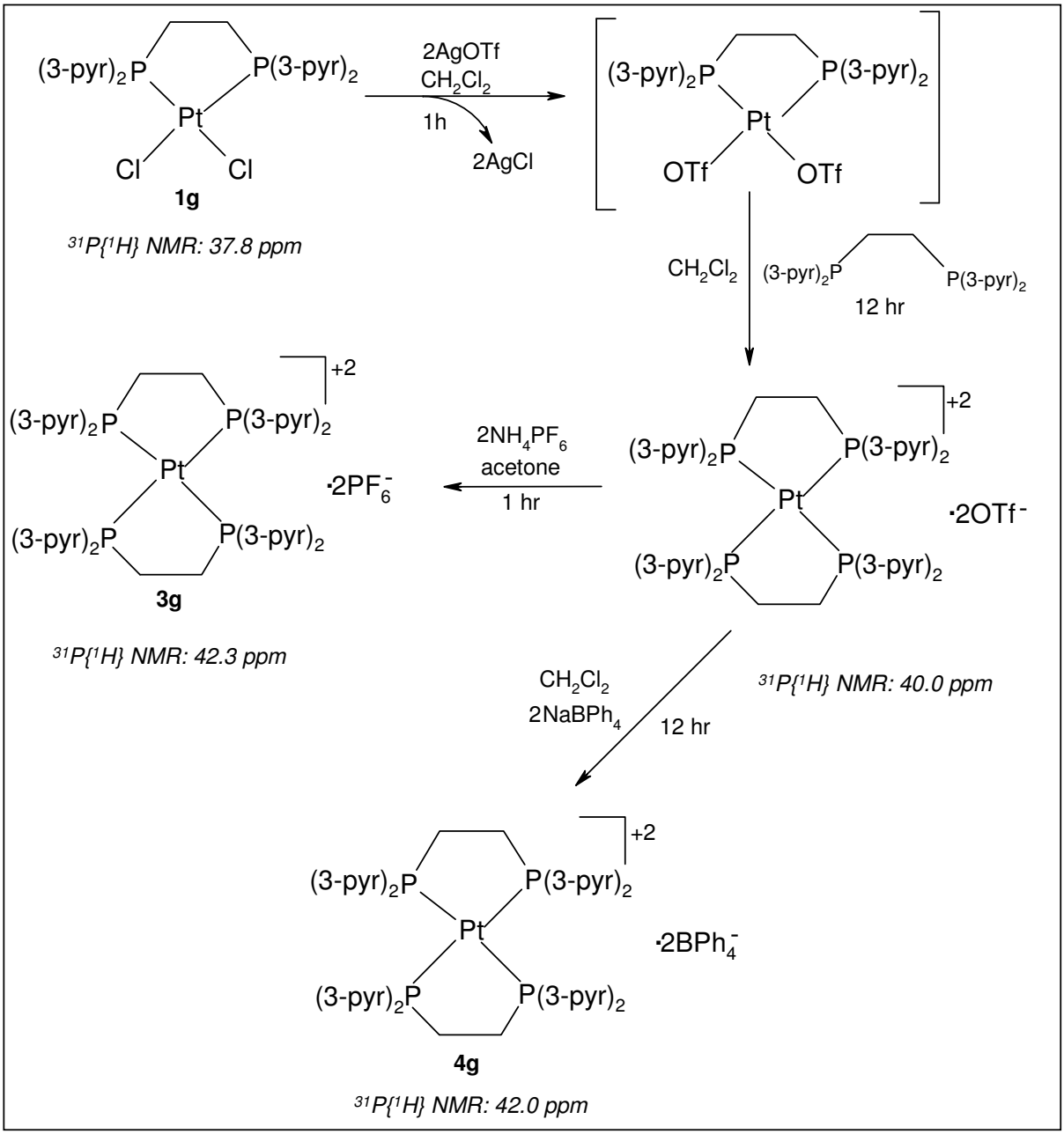

Scheme 3.4: Initial synthetic route for the preparation of Pt 3-pyridyl complexes.

Preparation of **4g** was carried out in a similar manner as the 2-pyridyl analogue and a pure product was obtained from CH_2Cl_2/ether.

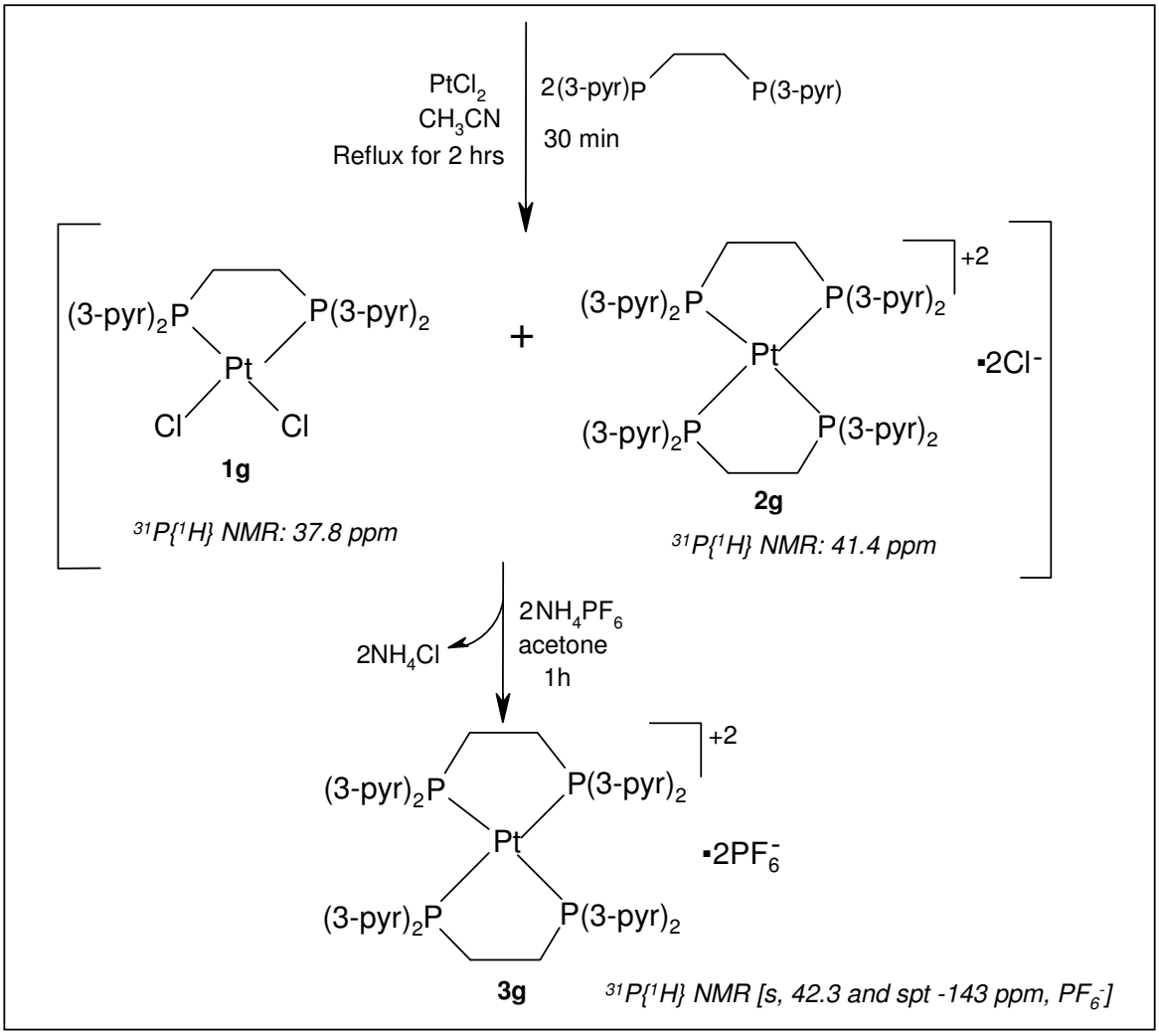

Scheme 3.5: Synthesis of 1,2-bis(di-3-pyridylphosphino)ethane platinum(II) complexes.

Illustrated above (*Scheme 3.5*) is a less laborious procedure that utilised fewer steps in the synthesis of **3g**. This method modified from the literature (Jones *et al.,* 2005) involved refluxing $PtCl_2$ in acetonitrile followed by the addition of ligand (2 eq.) to the hot grey solution. ^{1}H and $^{31}P\{^{1}H\}$ NMR spectrum of the yellow solid showed the formation of both $[PtCl_2(d3pyrpe)]$ and $[Pt(d3pyrpe)_2]Cl_2$ with $^{31}P\{^{1}H\}$ NMR chemical shifts and coupling constants $^{1}J_{(PtP)}$ of (δ 37.8, 3583 Hz) and (δ 41.4 and 2352 Hz), respectively. Separation of the two complexes was not possible as decomposition took place and hence conversion to the PF_6^- salt was carried out immediately. In addition to $[Pt(d3pyrpe)_2][PF_6]_2$, both ^{1}H and $^{31}P\{^{1}H\}$ NMR spectra showed the presence of small amounts of $[PtCl_2(d3pyrpe)]$ as well as decomposition products. The mixture was triturated with various solvents (CH_2Cl_2, THF) but there was no change in the spectra.

3.2.4 Preparation of 1,2-bis-(di-3-pyridylphosphino)ethane palladium (II) complexes.

Reaction of $Na_2[PdCl_4]$ and d3pyrpe resulted in the formation of $[PdCl_2(d3pyrpe)]$ (**1h**) irrespective of stoichiometry used (1 or 2) although there was unreacted ligand left over even after 12 h. The presence of the complex was confirmed by $^{31}P\{^1H\}$ NMR spectra (δ-value of 56.0 ppm in $CDCl_3$ and 61.0 ppm in DMSO). The same complex was also formed from $PdCl_2$ or $[PdCl_2(NCCH_3)_2]$ although the former reagent produced a mixture which contained small traces of $[Pd(d3pyrpe)_2]Cl_2$ (**2h**), $^{31}P\{^1H\}$ NMR (DMSO): 48.0 ppm. As previously observed in the synthesis of the Pt analogue, preparation of $[Pd(d3pyrpe)_2]Cl_2$ by direct addition of d3pyrpe to $[PdCl_2(d3pyrpe)]$ led to excessive decomposition. Abstraction of the coordinated chlorides with silver triflate was attempted (*Scheme 3.4*) and as before, solubility problems resulted in failure to isolate pure complexes. The triflate intermediates were insoluble in a number of solvents (CH_2Cl_2, THF, acetone) and hence could not be separated from AgCl. Satisfactory ^1H NMR spectra were not obtained but $^{31}P\{^1H\}$ NMR spectrum showed two singlets (δ 61.1 & 50.1 in DMSO), the latter (highfield) peak was assigned to a *bis*-chelated compound.

Preparation of the PF_6^- compound was attempted by reaction of the above mixture with NH_4PF_6 (2 eq.). $^{31}P\{^1H\}$ NMR spectrum of the product showed no changes and notably, no phosphorus resonance attributable to PF_6^-. As seen earlier in the synthesis of $[Pd(dppen)_2][PF_6]_2$ (**3d**), removal of the chloride from $[PdCl_2(dppen)]$ was important for the completion of the reactions. Similar attempts to achieve this by first reacting $[PdCl_2(d3pyrpe)$ with NH_4PF_6 (2 eq.) followed by addition of d3pyrpe produced the previously obtained mixture. This mixture was purified from DMF/ether over several days and crystal structure showed co-crystallisation of the *mono*-and *bis*-chelated diphosphine complexes (discussed in section 3.3). This confirmed that abstraction of the chlorides was not successful and that the expected intermediates may not have been obtained.

It has been shown that the reaction of $Pd(OAc)_2$ with dppe in methanol yielded the *bis*-chelated complex $[Pd(dppe)_2](OAc)_2$ as a kinetic product, which slowly

converted to the thermodynamic *mono*-chelate [Pd(OAc)$_2$(dppe)] (Bianchini *et al.,* 2003). This was concluded from investigations of alternating copolymerisation of carbon monoxide and ethene in MeOH by using Pd(OAc)$_2$ (as catalyst precursor) modified with chelating diphosphines (e.g dppe).

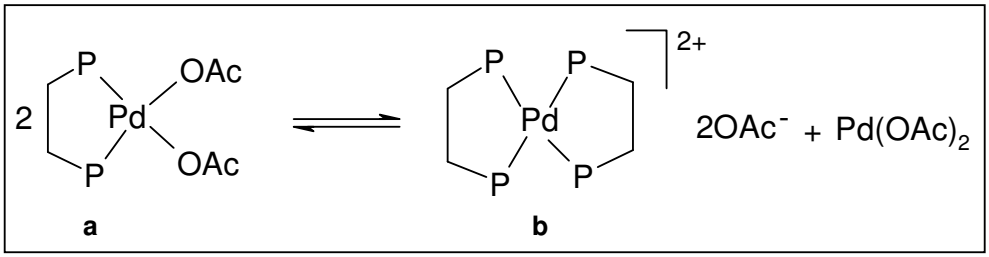

Scheme 3.7

Their interpretation of experimental evidence was that the *mono*-substituted *bis*phosphine complex in MeOH (ε = 32.6) undergoes a fast auto-ionisation process to give the bischelate and free acetate ions (*Scheme 3.7*). The mechanism of formation of **a** was also proposed in CH_2Cl_2 but the rate was too fast to allow for kinetic studies (Bianchini *et al.,* 2003). The faster kinetics in CH_2Cl_2 may be due to the fact that Pd(OAc)$_2$ exists mainly as a linear dimer in dilute solutions of halogenated solvents such as those used in this study.

In late 2002, a publication (Marson *et al.,* 2002) showed unambiguously that the *bis*-chelated complex (**b**) was the kinetic product of the stoichiometric reaction between Pd(OAc)$_2$ and dppe in methanol (Scheme 3.8).

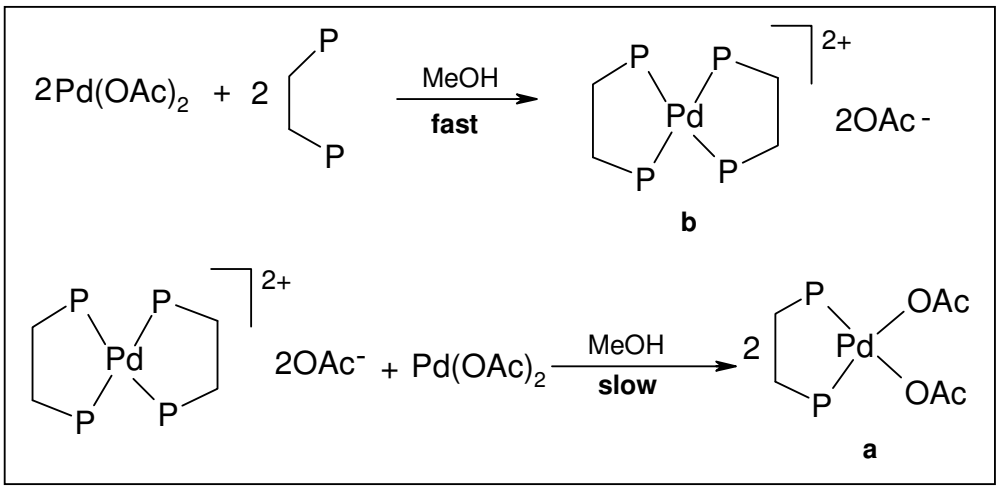

Scheme 3.8

On standing in this solvent at room temperature, it slowly converted into the thermodynamic product (*mono*-chelated phosphine, **a**). Furthermore, they showed that **a** and **b** (in contrast to Bianchini's conclusion) were not involved in autoionisation equilibrium (*Scheme 3.7*), otherwise the conversion of **b** into **a** would not have proceeded to completeness.

From the experiments executed in our laboratories and results obtained by Marson and co-workers, it is clear that the chloro ligands were only partially removed during the reaction with silver triflate. Furthermore, equilibrium existed between the neutral complex with one bisphosphine ligand and the cationic complex ion with two bisphosphine ligands; and the charge was balanced by chloride ions (*Scheme 3.9*). The mixture was confirmed by the ^{31}P NMR spectrum.

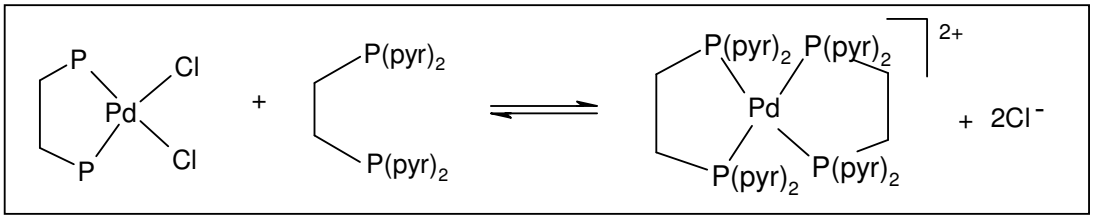

Scheme 3.9

Phosphine binding is reversible and so initial errors in binding mode can be corrected and the thermodynamic chelate product can be formed in the end (Crabtree, 2005).

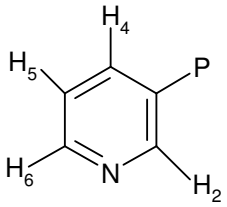

Labelling of protons for 3-pyridylphosphine ligands.

Table 3.4: ^{1}H and ^{31}P{^{1}H} NMR data of 1,2-bis-(di-3-pyridylphosphino)ethane and its Pt and Pd complexes

		Pyridyls ^{1}H data (δ)					^{31}P data	
Compound	**Solvent**	**H_2**	**H_4**	**H_5**	**H_6**	**CH_2**[a]	**δ**	**$^{1}J_{PtP}$ or $^{1}J_{PF}$ (Hz)**
[b]**d3pyrpe**	DMSO	8.54	7.74	7.35	8.54	2.25 (10.06)	-20.8	-
[$PtCl_2$(d3pyrpe)]	DMSO	9.03	8.27(19.83)	7.60	8.78	2.90 (20.1)	37.8	3583
[c]**1g and 2g**	DMSO	9.03 & 8.69	8.27 & 7.85	7.61 & 7.41	8.79 & 8.69	2.89	37.8 & 41.4	3583 & 2352
[d]**[Pt(d3pyrpe)$_2$][BPh_4]$_2$**	DMSO	7.89	6.97	6.60	7.89	[e]2.65	42.0	2332
[f]**[Pt(d3pyrpe)$_2$][PF_6]$_2$**	DMSO	7.80	7.42	[g]7.08 (102.18)	7.54	2.95	[h]42.3 & -143	2332 & 711
[$PdCl_2$(d3pyrpe)]	DMSO	9.03	8.31	7.59	8.81	3.04 (24.3)	61.0	
[$PdCl_2$(d3pyrpe)]	$CDCl_3$	[i]8.82 (18.6)	8.47	[j]7.47 (12.2)	[i]8.82 (18.6)	2.70 (23.5)	56.0	
[k]**1h & [l]2h**	DMSO	9.05 & 8.62	8.30	7.60 & 7.34	8.80	3.06 & 2.99	61.0 & 49.8	

Spectra were run at 298 K. All the pyridyl protons appeared as multiplets and phosphorus occurred as singlets (except for PF_6^-). The ligand data was in agreement with that reported in the literature (Bowen *et al.,* 1998). [a]Broad singlet or quasi-triplet (J = [$^{2}J(^{31}P\text{-}^{1}H) + {}^{3}J(^{31}P\text{-}^{1}H)$] (Hz) in parentheses where resolved (Berners-Price *et al.,* 1999b) and broad doublet (only in Pd complexes). [b]Proton numbering scheme is based on lit. (Berners-Price *et al.,* 1999b) and their values are in close agreement (solvent is $CDCl_3$). [c]**1g** and **2g** are [$PtCl_2$(d3pyrpe)] and [Pt(d3pyrpe)$_2$]Cl_2, respectively. [d]Phenyl protons (multiplets) of BPh_4^- at δ = 5.97 (8H), 6.10 (16H) and 6.35 (16H). [e]Tentative assignment due to overlap with solvent peak. [f]Tentative assignment due to the presence of [$PtCl_2$(d3pyrpe)] that caused overlaps. [g]Sharp triplet with a resolved large coupling constant (also present in **1h** and **2h**). [h]Singlet and septet (spt, $^{1}J_{PF}$), respectively. [i]quasi-triplet. [j]quasi-doublet. [k]**1h** and **2h** are [$PdCl_2$(d3pyrpe)] and [Pd(d3pyrpe)$_2$]Cl_2, respectively which were obtained as a mixture. [l]Tentative assignment due to overlap of peaks and the ratio that exists in the mixture 5d:6d = 2:1.

NMR data for the 3-pyridyl complexes exhibited a similar trend to that found in the 2-pyridyl analogues. The chemical shift position of the ethane protons of the ligand did not differ greatly to those found in the complexes. However, coupling constants (J_{PH}) of the ligand were half the magnitude (~ 10 Hz) of those found in the complexes (~ 20 Hz). As observed in the d2pyrpe complexes, Pt complexes of d3pyrpe showed a ^{31}P resonance at highfield, i.e., δ 37.6 for [$PtCl_2$(d3pyrpe)] while Pd analogues resonated downfield, i.e., δ 61.0 for [$PdCl_2$(d3pyrpe)]. It has been noted that for the same coordination number, molecular geometry, oxidation state, and phosphine, one generally observes a highfield shift of the ^{31}P resonance as one descends in a given group (Garrou, 1981).

In general, NMR data of the *mono*-chelated Cl^- complexes showed that although the chemical shift of the 3-pyridyl compound appeared in highfield region as compared to the 2-pyridyl analogue (37.6 vs. 47.7 ppm), their Pt-P coupling constants were in the same range (3583 vs 3480 Hz), respectively. The electronegativity of substituents on phosphorus and the angles between them are the two most important variables determining ^{31}P NMR chemical shifts (Tolman, 1977). In chelating diphosphines, the coordination chemical shift Δ, (Δ = $_{\delta}$complex - $_{\delta}$free ligand) depends on the ring size. Large downfield shifts are general for five membered chelate rings. Metal-phosphorus coupling constants depend on both electronic and steric factors, and in chelates, they depend on structural constraints.

3.2.5 Preparation of 1,2-bis-(di-4-pyridylphosphino)ethane platinum(II) complexes

Reaction of d4pyrpe and $Na_2[PtCl_4]$ (1:1 or 1:2, respectively) produced a compound with a ^{31}P singlet at 39.6 ppm with no indication of Pt-P coupling ($^1J_{PtP}$)] as well as the peak at 28.9 ppm (decomposition products). $Na_2[PtCl_4]$ was replaced with $PtCl_2$ (similar to the preparation of the 3-pyridyl analogue-*Scheme 3.5*) and the formation of $[Pt(d4pyrpe)_2]Cl_2$ was confirmed by $^{31}P\{^1H\}$ NMR (δ at 42.9 ppm and Pt-P coupling of 2501 Hz). Despite obtaining a compound with significantly fewer decomposition products, plenty of unreacted ligand (δ at -15.4 ppm) remained in the mixture even with longer reaction time; this was in contrast to what was observed in the preparation of the 3-pyridyl compound. $[Pt(d4pyrpe)_2][PF_6]_2$ was not obtained in sufficient quantities to obtain a satisfactory ^1H NMR spectrum. However, a singlet at 45.2 ppm (with no Pt-P coupling) was observed in $^{31}P\{^1H\}$ NMR (P-F coupling was observed). Attempts to optimise the yields were not pursued further as the compound was obtained in very low yields as a pale yellow fine powder at all times, similar to $[Pt(dppen)_2][PF_6]_2$.

3.2.6 Preparation of 1,2-bis-(di-4-pyridylphosphino)ethane palladium (II) complex.

Reaction of d4pyrpe and $Na_2[PdCl_4]$ (1:1) produced a compound that was poorly soluble in NMR solvents although a ^{31}P chemical shift of 60.0 ppm ($CDCl_3$) was observed. This was presumed to be $[Pd(d4pyrpe)_2]Cl_2$ although purification attempts led to its decomposition. Preparation of $[Pd(d4pyrpe)_2][PF_6]_2$ was attempted by reacting $[PdCl_2(NCCH_3)_2]$ with NH_4PF_6 (2 eq.) followed by addition of 1,2-bis-(di-4-pyridylphosphino)ethane (d4pyrpe) (*Scheme 3.8*). As seen in the preparation of the Pt analogue, $^{31}P\{^1H\}$ NMR spectra showed presence of large amounts of unreacted ligand even after 12hrs and plenty of decomposition products (δ 28.9).

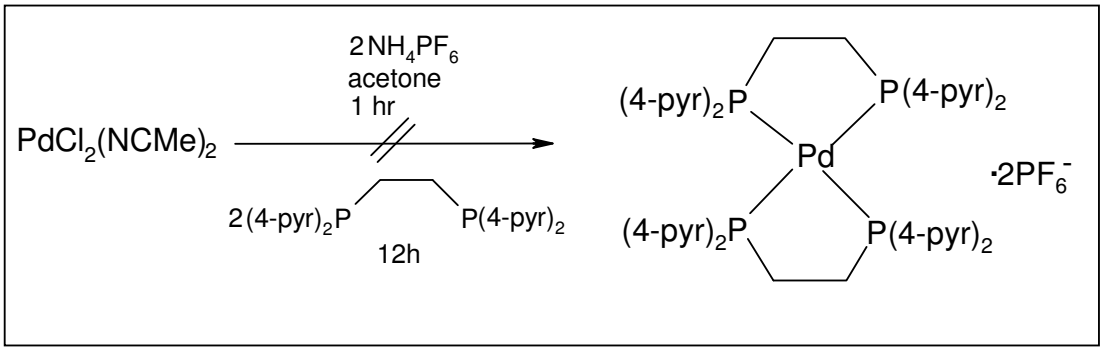

Scheme 3.10: Synthetic route for the attempted preparation of $[Pd(d4pyrpe)_2][PF_6]_2$

$^{31}P\{^1H\}$ NMR analysis of the crude compound showed the presence of a singlet (δ 65.9) and the characteristic septet of $[PF_6]^-$. However, after purification with DMF/ether, the pale yellow solid with a ^{31}P chemical shift at 66.3 ppm did not contain the septet, signifying that the product had not been obtained initially. The $^{31}P\{^1H\}$ NMR data implies only P-coordination to the metal centre as indicated by the downfield shifts (Durran *et al.,* 2006). ^1H NMR spectrum showed presence of quasi-doublet of the bridging CH_2 (δ 3.01, PH coupling = 24.9 Hz), aromatic protons (δ, m, 7.87 and 8.80).

Reactions of d4pyrpe with both Pt and Pd yielded complex mixtures of products which were identified by ^{31}P NMR on the basis of known trends in chemical shifts. Due to problems of solubility, decomposition, extremely low yields, failure to abstract the chloride etc., preparation of the desired compounds was not pursued further. One research group showed that 2-pyridyl complexes (2-metallated pyridines) reacted with organic halides about one order of magnitude faster than their 4-pyridyl analogues (Canovese *et al.,* 1996). They also showed that replacement of palladium with platinum in structurally related complexes brought about a three fold increase in reactivity and also one to two unity increase in the pK_a values, indicating a better electron donating ability of the platinum centre.

3.3 General discussion on the behaviour of the 2, 3 and 4-pyridylphosphine ligands

^{31}P NMR spectroscopy is a valuable probe to study electronic and structural features of complexes with phosphine ligands. $^{31}P\{^{1}H\}$ NMR spectroscopy studies carried out on Ag complexes of 1,2-bis-(di-*n*-pyridylphosphino)ethane for *n* = 2, 3 or 4 showed that d3pyrpe and d4pyrpe complexes existed in solution as monomeric *bis*-chelated $[Ag(d3pyrpe)_2]^+$ and $[Ag(d4pyrpe)_2]^+$, whereas the d2pyrpe complex formed equilibrium mixtures of the monomeric $[Ag(d2pyrpe)_2]^+$, dimeric $[\{Ag(d2pyrpe)_2\}_2]^{2+}$ and trimeric $[\{Ag(d2pyrpe)_2\}_3]^{3+}$ (Berners-Price *et al.,* 1998). A similar trend was observed in Au complexes (Berners-Price *et al.,* 1999b). The d2pyrpe ligands coordinated in both bridging and chelated modes with the relative percentages of the species present are dependent on the temperature and solvent, making the ^{31}P NMR solution spectra for the 2-pyridyl considerably more complex.

The authors concluded from their results that the position of the pyridine nitrogen in the ring had a significant effect on this chemistry (Berners-Price *et al.,* 1998). The 2-pyridyl complex had limited solubility in water while the increased hydrophilic character of the monomeric 3-pyridyl and 4-pyridyl complexes was as a consequence of the more exposed N atoms. In our preparations, the different reactivity of the three ligands (2-, 3- and 4-pyridyl) towards the metals (Pd and Pt) confirmed the theory stated above. It is notable that reports of the preparation, reactions and catalytic properties of pyridylphosphines and their metal complexes have been confined, almost exclusively, to those with 2-pyridyl substituents (Bowen *et al.,* 1998).

3.4 Structural analysis of compounds 3b, 4e 3f, 1h and 2h

In this section, the structures of each of the 4 compounds are discussed. The structures were determined in order to make a comparison with similar Pt and Pd complexes from the literature.

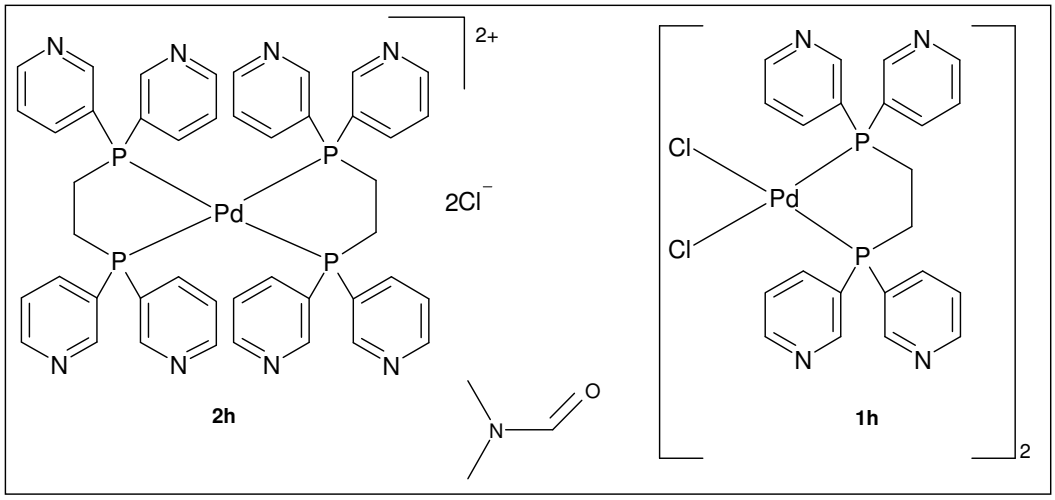

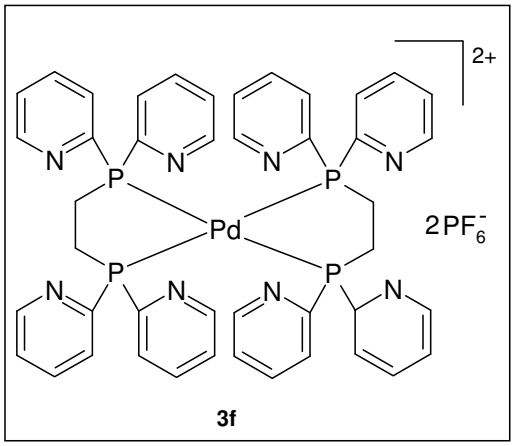

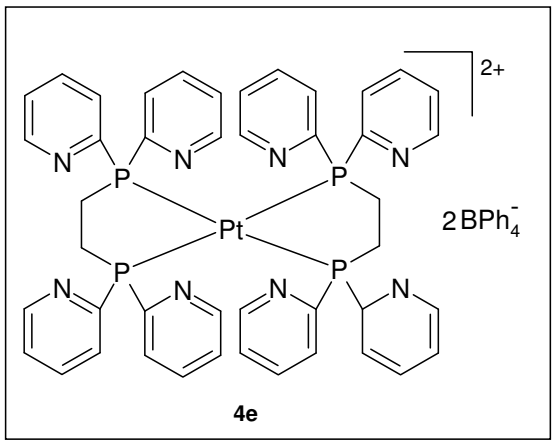

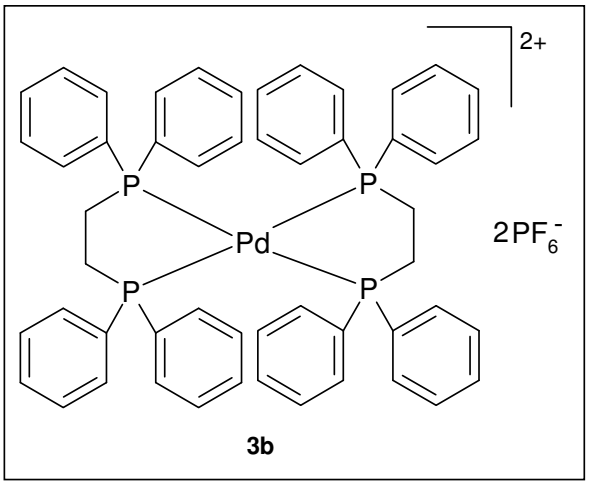

3.4.1 Crystal structures of (1h, 2h), 3f, 4e and 3b

Table 3.5 summarises crystal data for compounds **1h**, **2h**, **3f**, **4e** and **3b**. Comprehensive crystallographic data is available on CD-ROM on request.

Table 3.5: X-ray data collection and structure refinements

	1h and 2h	**3f**	**4e**	**3b**
Formula	2($C_{22}H_{20}Cl_2N_4P_2Pd$)+ $C_{44}H_{40}Cl_2N_8P_4Pd$ + C_3H_7NO	$C_{44}H_{40}F_{12}N_8P_6Pd$	$C_{92}H_{80}B_2N_8P_4Pt$	$C_{52}H_{48}F_{12}P_6Pd$
FW	1159.40 + 982.08 + 73.09	1201.66	1638.23	1193.12
T (K)	293(2)	293(2)	173(2)	293(2)
λ, Å	0.7107	0.7107	0.7107	0.7107
Crystal size/mm^3	0.28 x 0.12 x 0.10	0.44 x 0.24 x 0.18	0.28 x 0.14 x 0.14	0.36 x 0.28 x 0.20
Crystal system	Monoclinic	Orthorhombic	Triclinic	Monoclinic
Space group	*P*2$_1$/*n*	*Pnna*	*P*-1	*P* 2$_1$/*n*
a, Å	9.2654(7)	23.436(2)	15.0836(3)	11.0285(9)
b, Å	24.3917(19)	14.488(1)	16.5635(3)	16.4251(14)
c, Å	21.7761(16)	14.683(1)	18.2187(4)	14.0426(12)
α, β, γ (°)	90, 97.8240(10), 90	90, 90, 90	77.412(1), 72.435(1), 65.290(1)	90, 96.2830(10), 90
V, Å^{-3}	4875.6(6)	4985.5(8)	3919.94(14)	2528.5(4)
Z	2	4	2	2
ρ Mg/m^3	1.508	1.600	1.388	1.567
2θ, range, deg				2.23 to 26.46
Index ranges	-11<=h<=4 -30<=k<=30 -21<=l<=25	-28<=h<=26 -6<=k<=18 -18<=l<=17	-19<=h<=19 -21<=k<=21 -24<=l<=24	-13<=h<=13 -17<=k<=19 -17<=l<=7
R indices (all data)	R1 = 0.0524 wR2 = 0.1190	R1 = 0.0448 wR2 = 0.1111	R1 = 0.0374 wR2 = 0.0631	R1 = 0.0466 wR2 = 0.1056

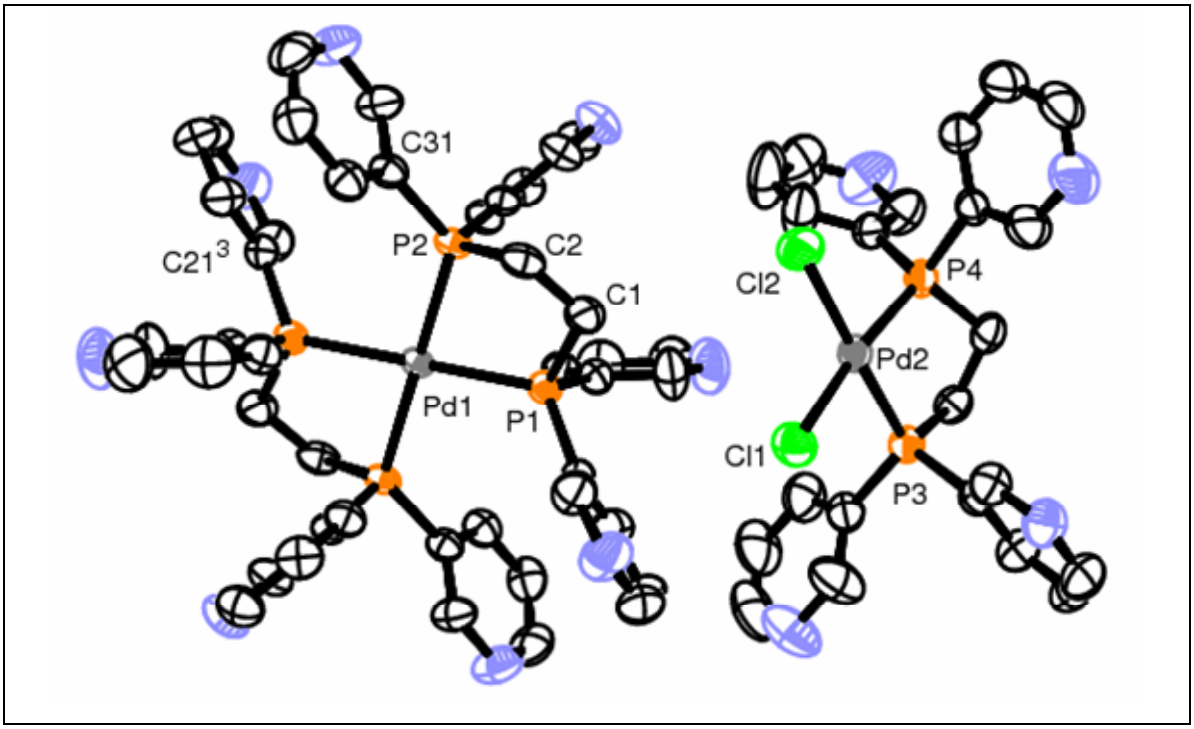

Figure 3.4: *ORTEP* representation of bis-(1,2-bis-(bis(3-pyridyl)phosphino)ethane-P-P'-palladium(II) dichloride (**6d**) and Bis[dichloro(1,2-bis(bis(3-pyridyl)phosphino)ethane-P-P')-palladium(II)] (**5d**). The hydrogen atoms, the solvate and the Cl counter ions are left out for clarity.

Compounds **1h** and **2h** co-crystallise in the monoclinic space group $P2_1/n$, Z = 2 with half a molecule of **1h**, one molecule of **2h**, a Cl counter ion and one ion of N,N-dimethylformamide solvate. The atom numbering scheme used in the corresponding tables and discussion are illustrated in Figure 3.4 and the unit cell is shown in Figure 3.5.

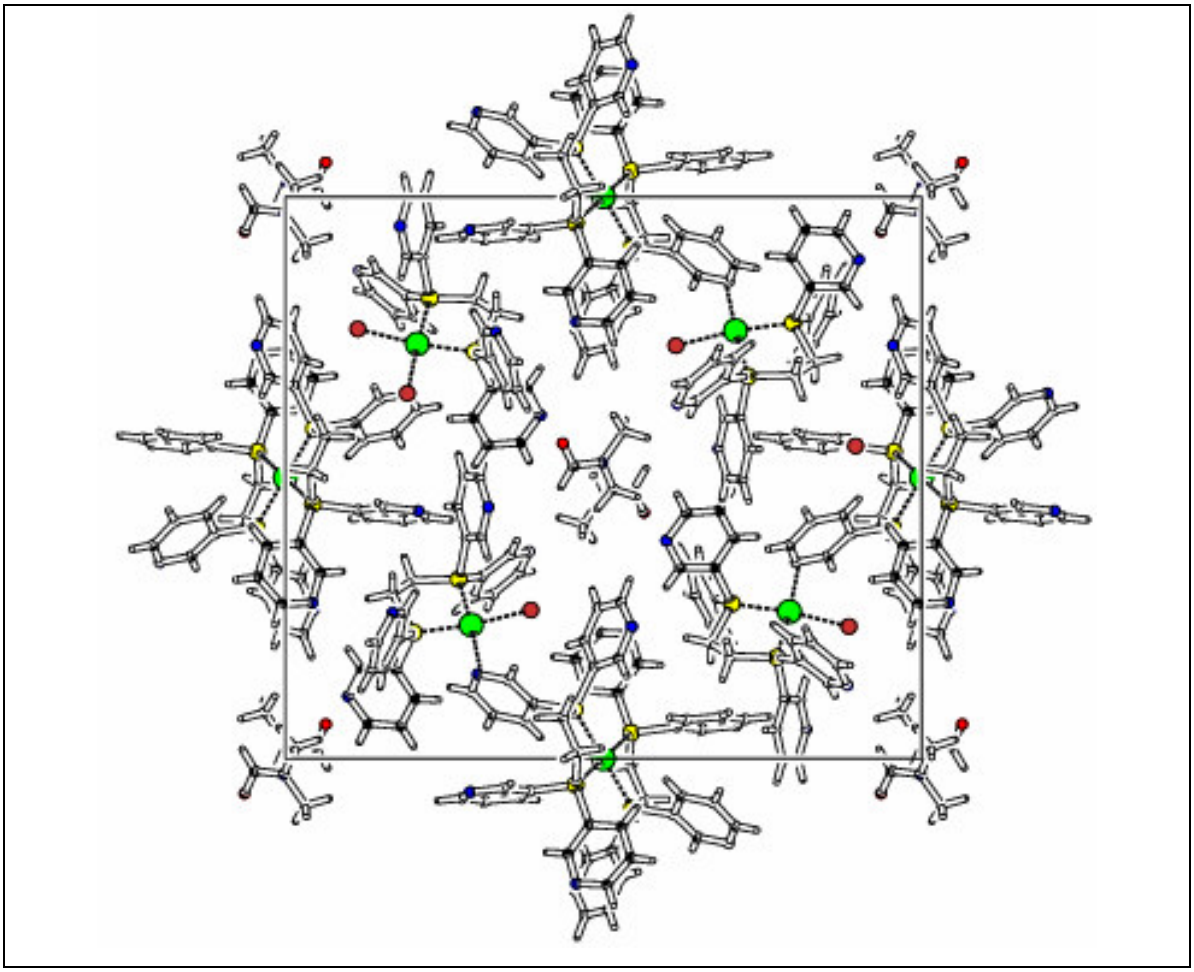

Fig 3.5: A view of the unit cell of **1h** and **2h** as viewed down the crystallographic *a* axis showing the dimethylformamide molecule surrounded by **1h** and **2h**.

In **1h** and **2h**, the crystals are arranged such that the plane containing the atoms Pd1, P1, P1', P2 and P2' in **1h** and that containing Pd2, P3, P4, Cl1 and Cl2 are at an angle of 56.67(3)°; such that the two are linked by weak C-H…Cl intermolecular interactions forming parallel layers of both molecules that run in the crystallographic *a* direction. The Cl counter ions then link **1h** and **2h** and all three molecules surround the dimethylformamide solvate. This solvate also forms C-H…O hydrogen bonded dimers that run parallel to *a* axis and is connected to the **2h** through another C-H…O interaction (see packing diagram in Figure 3.5).

Figure 3.6 shows the molecular structure of compound **3f** together with the atom numbering scheme as used in this discussion.

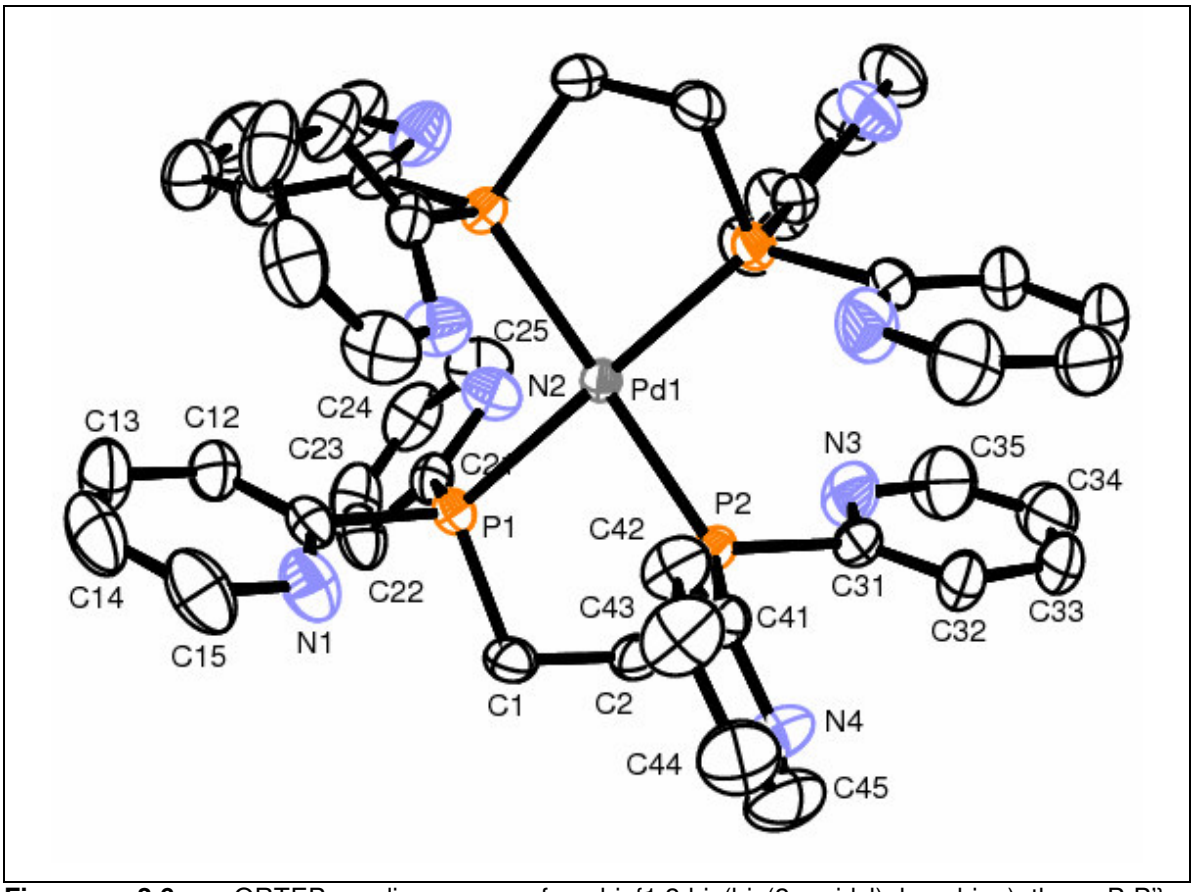

Figure 3.6: ORTEP diagram of bis{1,2-bis(bis(2-pyridyl)phosphino)ethane-P-P'}-palladium(II).bis(hexafluorophosphate) **3f**. Hydrogen atoms and the two ions of PF_6 have been omitted for purposes of clarity. Ellipsoid probability is at 50%.

Compound **3f** crystallises in the non-centrosymetric space group *Pnna* with half a molecule of the palladium complex and two ions of PF_6 in the asymmetric unit. The two PF_6 molecules are disordered. One has only the equilateral fluoride atoms disordered in a general position while the second has both axial and equilateral fluoride atoms disordered also in a general position but resulting in distorted octahedral geometry. Connection of molecules in the crystal is mainly through C-H…F intermolecular interactions.

Packing in the crystal is such that the solvate molecules are sitting in the voids between the palladium complex molecules with the less disordered ions of PF_6 being on the same axis as Pd atoms while the more disordered PF_6 molecule is positioned between the Pd complexes (*Fig. 3.7*). In compound **3f**, the conformations of the ligands are such that the pyridyl rings get positioned more above and below the coordination plane. Two pyridyl nitrogens, one on each side of the coordination plane are just over 3Å from the Pd (Liles, 2006).

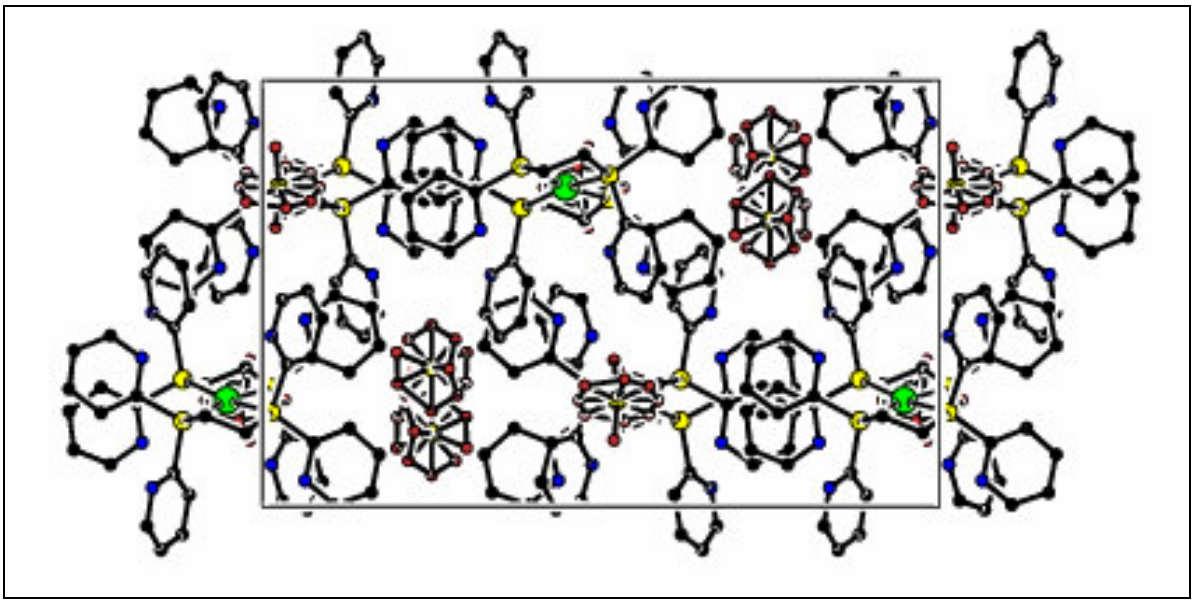

Figure 3.7: Packing diagram of compound **3f** showing the solvate molecules of PF_6 as viewed down the crystallographic *b* axis.

The molecular structure of **4e** is given in Figure 3.8 along with atom numbering scheme as used in this discussion.

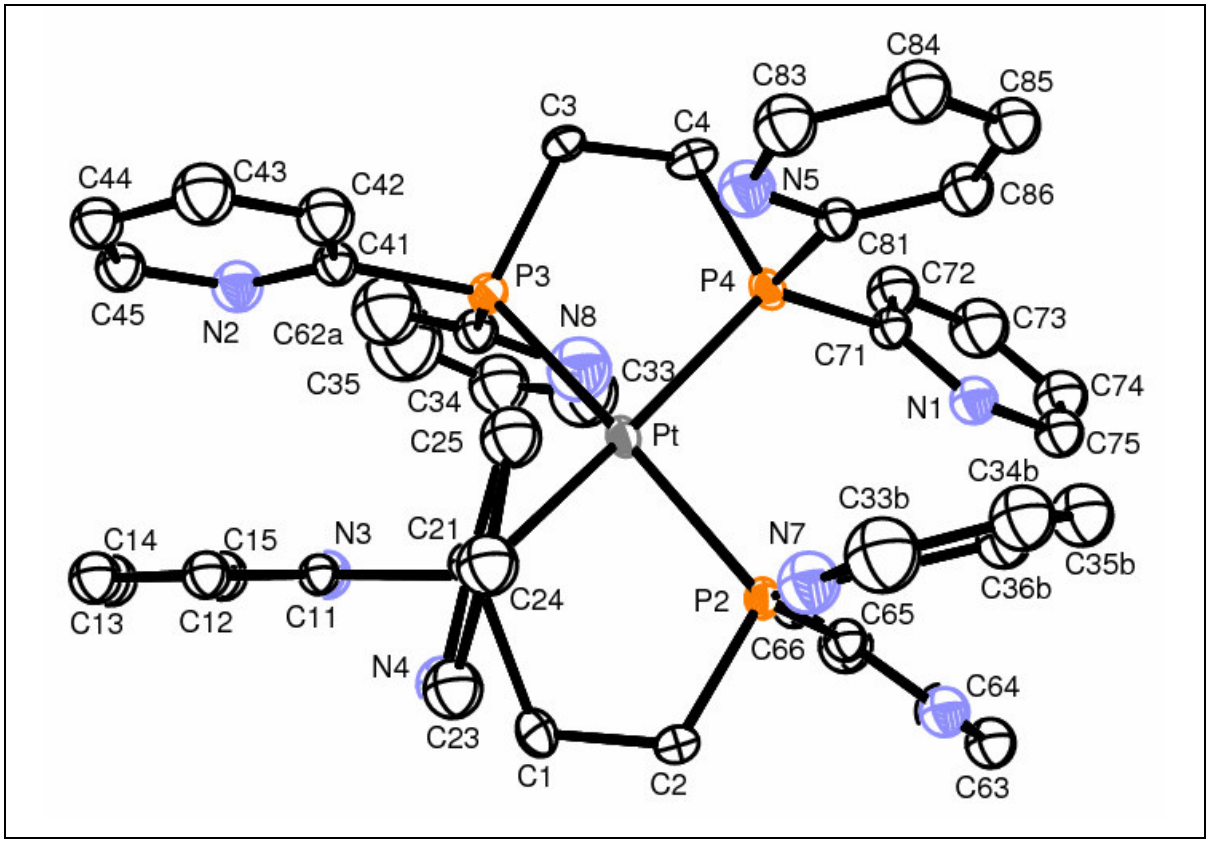

Figure 3.8: ORTEP diagram of bis{1,2-bis(bis(2-pyridyl)phosphino)ethane-P-P'}-platinum(II).bis(tetraphenylborate) **4e**. All hydrogen atoms and the two tetraphenylborate ions have been omitted for clarity purposes. Ellipsoid probabilities are given at 50%.

Compound **4e** crystallises in the centrosymmetric space group $P\bar{1}$ with one molecule of the platinum complex and two ions of tetraphenylborate. The pyridyl rings containing N7 and N8 are disordered in general positions. The orientation of the pyridyl groups seem to be affected by weak intra-molecular interactions, for example C62a-N2.

Figure 3.9 below shows the molecular structure of compound **3b** together with the atom numbering scheme as used in this discussion.

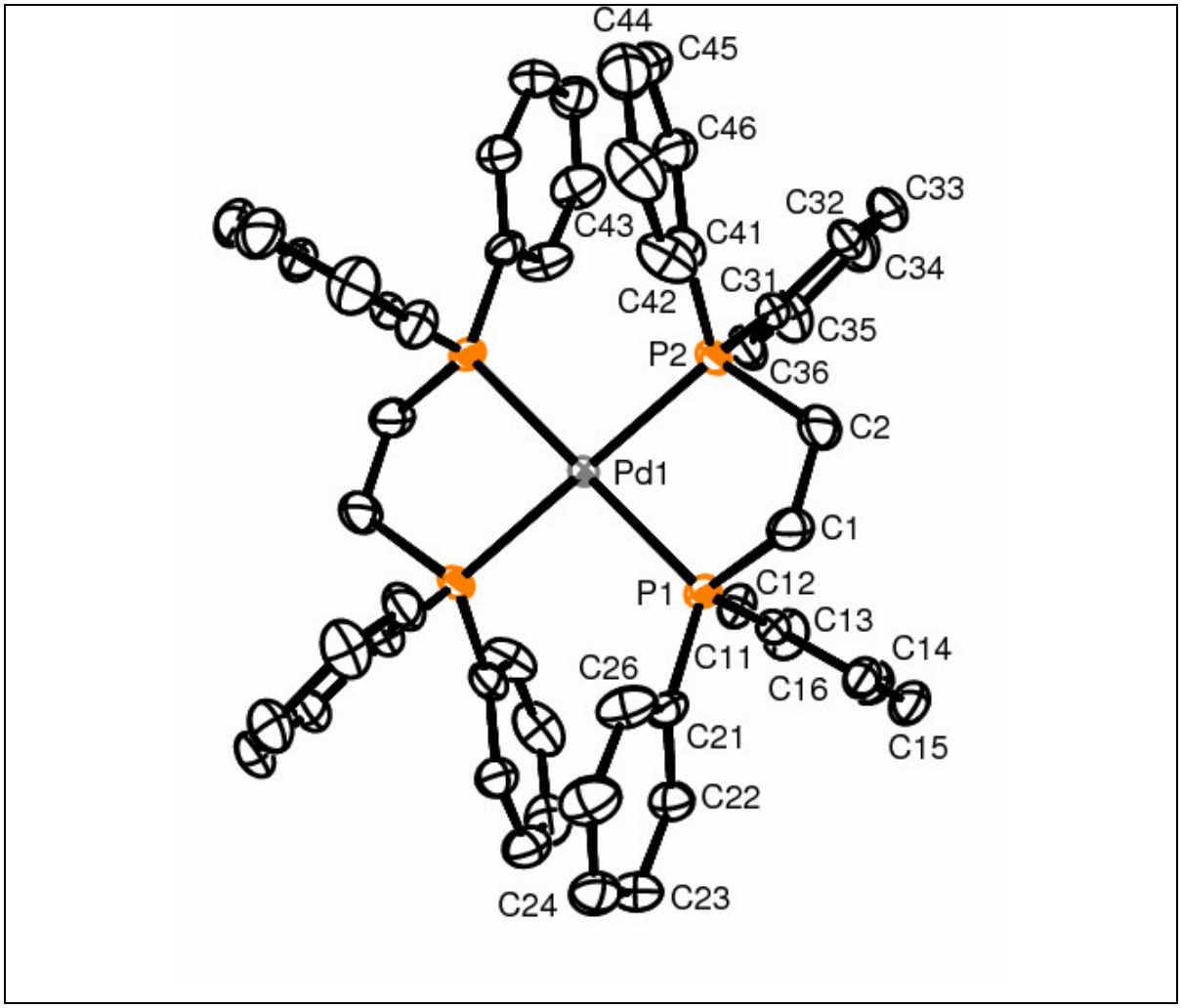

Figure 3.9: ORTEP diagram for bis{1,2-bis(diphenylphosphino)ethane-P-P'}-palladium(II).bis(hexafluorophosphate) **3b**. Hydrogen atoms and the two ions of PF_6^- have been left out for the purposes of clarity. Ellipsoid probability is at 30%.

Compound **3b** crystallises in the centrosymmetric space group $P2_1/n$ with half a molecule of the palladium complex and one ion of phosphorus hexafluoride in the asymmetric unit. The other half of the palladium complex is generated by a glide plane. The phosphorus hexafluoride ion is disordered in the general position.

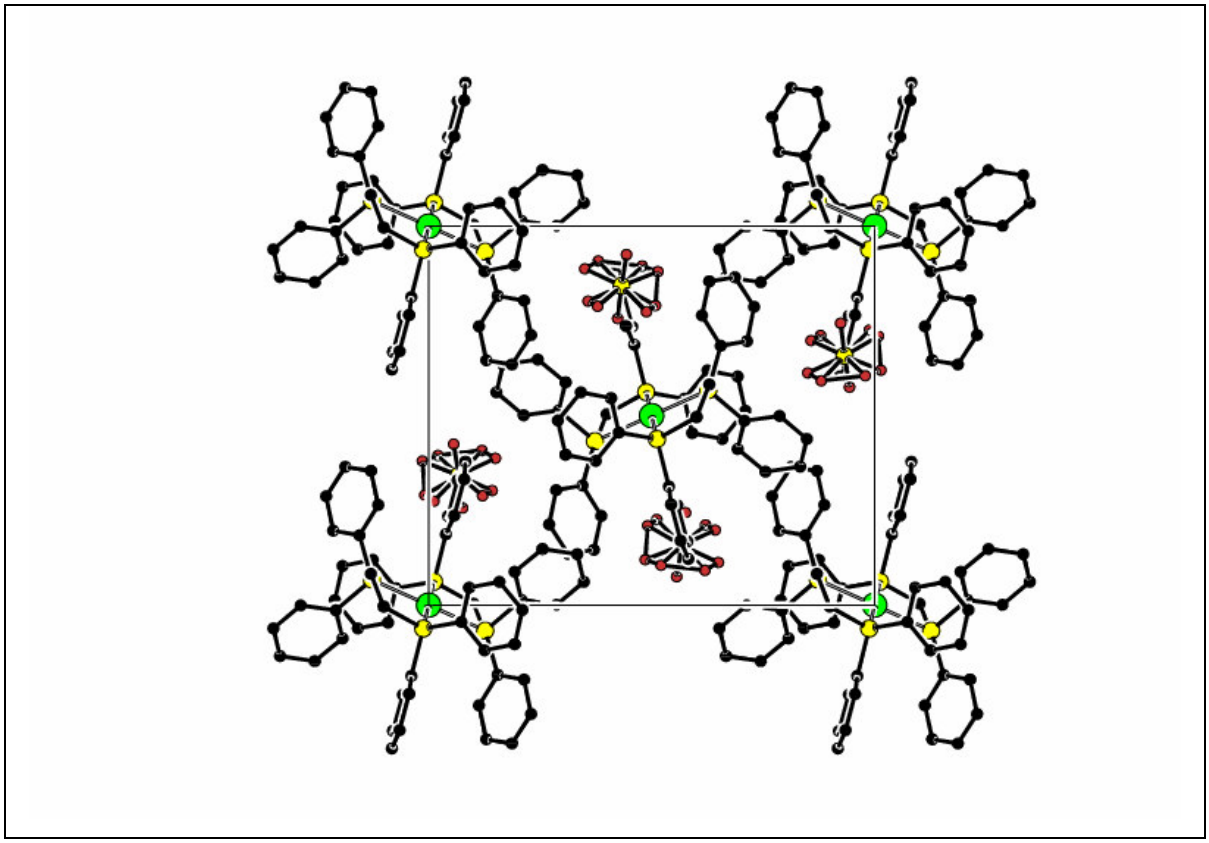

Figure 3.10: Packing diagram for compound **3b**. Hydrogen atoms are left out for clarity.

In the unit cell, the palladium atoms are sitting in special positions (*Fig. 3.10*). The crystal is stabilised through C-H…F interactions between the phenyl rings of the palladium complex and the fluorine atoms of the PF_6 anion.

3.4.2 Molecular structures of (1h, 2h), 3f, 4e and 3b

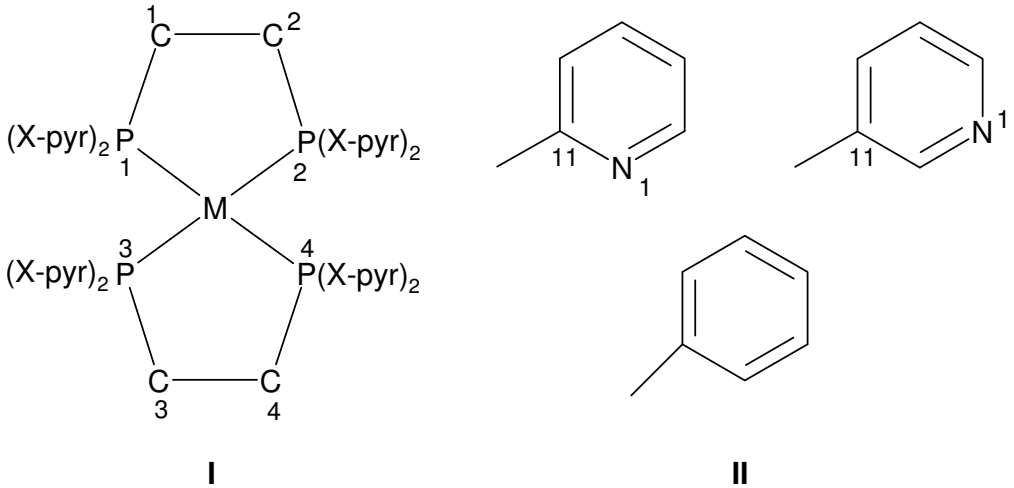

I **II**

Scheme 3.11

The structural diagram and general atom-numbering scheme for the four metal complexes is given above (*Scheme 3.11*). Each of the four compounds is distinctly different with respect to the metal and the position of the nitrogen atom on the pyridyl ring. X = position of nitrogen atom on the pyridyl ring (2 or 3), M = Metal (Pt or Pd). For each of the metal pyridyl complexes (**1h** and **2h**, **3f** and **4e**), there are eight pyridyl rings (**II**) each attached to the phosphorus atoms through C11 (as shown in the scheme) or C21, C31, C41, C51, C61, C71 and C81. All compounds were crystallised from a variety of solvents in accordance with their solubilities.

Important bond distances and angles of **1h** and **2h**, **3f**, **4e** and **3b** are tabulated below (*Table 3.7*).

Table 3.7: Selected bond distances (Å) and angles (deg) for **1h** and **2h**, **3f**, **4e** and **3b** with estimated standard deviations in parentheses

	1h	**2h**	**3f**	**4e**	**3b**
M-P1	-	2.3434(9)	2.3331(6)	2.2825(6)	2.3412(8)
M-P2	-	2.3283(8)	2.2999(6)	2.3161(6)	2.3562(8)
M-P3	2.231(1)	-	-	2.3038(6)	Same M-P1
M-P4	2.232(1)	-	-	2.3215(6)	Same M-P2
P1-C1	-	1.845(4)	1.829(3)	1.815(2)	1.829(1)
P2-C2	-	1.816(3)	1.828(3)	1.845(2)	1.854(4)
P3-C3	1.826(4)	-	-	1.829(2)	-
P4-C4	1.825(4)	-	-	1.829(3)	-
P1-C11	-	1.803(4)	1.822(3)	1.820(2)	1.809(3)
P1-C21	-	1.813(4)	1.820(3)	1.827(2)	1.804(3)
P2-C31	-	1.806(4)	1.822(3)	1.827(7)	1.804(4)
P2-C41	-	1.809(3)	1.821(3)	1.819(2)	1.809(4)
C1-C2	-	1.526(5)	1.516(4)	1.523(3)	1.461(5)
C3-C4	1.538(6)	-	1.516(4)	1.519(4)	1.461(5)
P-F (*ave*)	-	-	1.517	-	1.561
P1-M-P2		81.59(3)	83.10(2)	83.13(2)	82.94(3)
P3-M-P4	86.47(4)	-	-	83.74(2)	82.94(3)
P1#1-M-P2	-	98.41(3)	98.02(3)	97.26(2)	97.06(3)
P1-M-P1#1		180.00(4)	171.62(2)	170.87(2)	180.0
P1-M-P2#1			97.01(3)	97.22(2)	97.06(3)
Cl1-Pd-Cl1	94.22(2)	-	-	-	-
P3-Pd2-Cl1/Cl2	88.98(4) /90.41(4)	-	-	-	-
C1-P1-M	-	108.80(1)	109.37(9)	107.05(8)	105.92(1)
C2-P2-M	-	103.87(1)	107.82(9)	109.50(8)	108.07(1)
C3-P3-M	108.52(1)	-	-	-	-
C4-P4-M	107.71(1)	-	-	-	-
M-P1-C11		111.01(1)	123.49(9)	120.99(8)	110.63(1)
M-P1-C21		122.08(1)	104.04(9)	108.03(7)	121.24(1)
M-P2-C31		125.04(1)	118.91(1)	114.0(2)	114.66(1)
M-P2-C41		108.32(1)	112.18(9)	112.70(9)	117.16(1)
C11-P1-C21	-	104.72(1)	108.43(1)	109.80(1)	106.91(1)
C31-P2-C41	-	105.83(1)	108.61(1)	113.2(3)	106.92(1)

The molecular geometry of the four compounds (**1h** and **2h**, **3f**, **4e** and **3b**) is similar in that all show a distorted square planar arrangement of the phosphorus atoms around the central metal atom. The deviation from the mean square plane through the five atoms ranges from 81.59 to 83.13° and is as a consequence of the endocyclic P1-M-P2 angle being constrained between 81-84° (Oberhauser *et al.,* 1995). These angles seem to be similar for all the compounds and compare well with those of dppe containing Pd(II) and Pt(II) complexes from the literature with 81.65(8)° in $[Pd(dppe)_2]Cl_2$ (Oberhauser *et al.,* 1997b), 82.66(4)° in $[Pd(dppe)_2][PO_2(OPh)_2]_2$ (Stockland *et al.,* 2004), 82.09(5) in $[Pt(dppe)_2]I_2.2CDCl_3$ (Ferguson *et al.,* 1993) and 81.88(3)° in $[Pd(dppe)_2][CB_{11}H_{11}Cl]_2.3CH_2Cl_2$ (Lassahn *et al.,* 2003). The latter group also found that the phenyl rings of the opposing dppe ligands in $[Pd(dppe)_2]^{2+}$ cations were too far apart for a meaningful π-π interaction, which was different from the situation in the $[Ni(dppe)_2]^{2+}$.

The corresponding exocyclic angles between the phosphorus atoms not chelating are therefore open slightly more than 90°. The bridging carbon atoms lie on either sides of the coordination plane of metal atoms with torsion angles about the C-C bond being -40.66 (**4e** Pt 8.11), -40.26 (**3b** Pd 0.01), 49.62 (**3f** Pd 8.38), -37.70 (**1h** Pd 0.01) and 48.50 (**2h** Pd 0.01). There is a marked deviation from sp^3-hybridisation around the phosphorus atom for all the four complexes since most of the angles are not very close to 109.5°. The M-P-C(aryl) angles differ significantly and range from 108.32(1)-125.04(1) in **2h**, 108.03(7)-120.99(8) in **4e**, 104.04(9)-123.49(9) in **3f** and 110.63(1)-121.24(1)° in **3b**. This represents the electronically most favoured sites resulting from the crowded square planar geometry of the complex and the puckered chelate ring.

Changing the *mono*-chelate system as in **1h** to a *bis*-chelate system like in **2h, 3f, 4e** and **3b** leads to a structural change in which the C-C bond distance between the bridging carbons is slightly shortened by about 0.01 Å. However, the C-C "backbone" distances found in **1h**, **2h**, **3f** and **4e** [1.538 (6), 1.526 (5), 1.516 (4) and 1.523(3) Å] are comparable to those found in the free (d2pyrpe) and coordinated ligand, $[PtCl_2(d2pyrpe)_2]$, 1.527 and 1.531 Å, respectively (which are essentially identical) (Jones *et al.,* 1999). There is a significant variation in P-CH_2 bond lengths in three of the four structures with 1.816(3) and 1.845(4) in **2h**;

1.815(2) and 1.845(2) in **4e**; and 1.829(4) and 1.854(4) Å in **3b**. The same effect is not observed in **1h** [P-CH_2 bond lengths of 1.825(4) and 1.826(4)] and **3f** [P-CH_2 bond lengths of 1.828(3) and 1.829(3)].

3b has average P-C(CH_2) and C-C bond lengths of 1.842(4) and 1.461(5) Å while distances of 1.829(3) and 1.521(7) Å are found in free dppe, respectively (Zhuravel and Glueck, 1999). The difference observed between free dppe and **3b** may indicate that the chelating dppe is sterically constrained. This difference in-turn affects the C1-C2 bond length in **3b** [1.461(5) Å]. As expected, the average P-C(sp^3) bond lengths of 1.8305(3) in **2h** and 1.8415 (4) Å in **3b** Å are longer than the corresponding P-C(sp^2) bond lengths of 1.8078(4) and 1.8065(3) Å, respectively. However, significant differences between P-C(sp^3) bond lengths and P-C(sp^2) are not observed in **1h,** 1.8255(4) vs 1.8123(4); 1.8285(3) vs 1.8233(3) in **4e**; and 1.8300(2) vs 1.8213(3) Å in **3f**. The free ligand (d2pyrpe) of the two latter complexes exhibits significantly longer P-C(CH_2) and P-C(sp^2) bond lengths of 1.842 and 1.848 Å, respectively (Jones *et al.,* 1999).

Another observation is that the P-$C_{(sp^2)}$ bond lengths of **1h** [1.8123(4)], **2h** [1.8078(4)] and **3b** [1.8065(3)Å] are noticeably shorter than those found in the complexes coordinated to 2-pyridyl ligands [**4e** = 1.8233(3) and **3f** = 1.8213(3) Å]. The latter complexes have similar values to those observed in [$PtCl_2$(d2pyrpe)] (1.820 Å) (Jones *et al.,* 1999). In contrast to **3b**, longer average P-C(Ph) bond lengths (1.827 Å) are reported for dppe complexes (Jones *et al.,* 1999).

Most of the remaining bond distances and angles are comparable to those of corresponding complexes from the literature supporting the notion that replacing palladium with platinum causes a very small and barely significant change in M-P distances (Engelhardt *et al.,* 1984). An example is the analogous platinum complex of $[Pd(dppe)_2]^{2+}$, bis[1,2-bis-(diphenylphosphino)ethane]platinum(II) iodide which has Pt-P distance of 2.3310(13) Å (Ferguson *et al.,* 1993) which is not dissimilar to that found in **3b** [Pd-P = 2.3412(8) Å]. In general, the M-P distances for **2h**, **4e**, **3f** and **3b** (2.2825 – 2.3434 Å) are within the range for square-planar d^8 complexes of palladium and platinum, for compounds with two phosphines *trans* to each other (Engelhardt *et al.,* 1984). While the *trans*-effect of

replacing phosphorus by chlorine in the coordination sphere (as in **1h** and **2h**) is very pronounced, causing a contraction in the metal-phosphorus bond of 0.1 Å (average length of 2.232(1) vs 2.3359(8) Å, respectively), the effect of this upon the two different metal atom systems does not differ significantly in respect of M-P bond lengths (Engelhardt *et al.,* 1984).

This phenomenon is also observed in **4e** where the average Pt-P bond length (2.316 Å) is significantly longer than that determined for $[PtCl_2(d2pyrpe)]\cdot CH_2Cl_2$ (2.210 Å) while the P-Pt-P angle is significantly smaller (83.44 vs 86.17°) (Jones *et al.,* 1999). This can be attributed to a competitive π-interaction of two *trans* P-atoms in square planar geometry and a greater congestion of atoms caused by the pyridyl substituents of two chelating rings compared to one. A value of 86° for P-Pt-P angles is consistent with values found in structures of other Pt-bidentate phosphine complexes with five membered chelate rings (Miedaner *et al.,* 1993). The two chelate rings in **4e** differ with one having shorter Pt-P distances compared to the other chelate ring [2.2993(6) vs 2.3127(6) Å]. This is also reflected in the bite angles of the chelate rings [C11-P1-C21 = 109.80(1) and C31-P2-C41 = 113.2(3)°].

Table 3.7 below shows analytical data, melting points and % yields of all the pure compounds.

Table 3.7: Analytical data and melting points of the complexes that were obtained as pure compounds

Compound & Formula	[a]Elemental analysis			m.p (°C)	% yield
	C	N	H		
$[Pt(dppe)_2][PF_6]_2$ ($C_{52}H_{48}P_6F_{12}Pt$)	48.72		3.77	190-192	58
(FW: 1281.8)	(48.01)	(0.28)	(3.49)		
$[Pd(dppe)_2][PF_6]_2$ ($C_{52}H_{48}P_6F_{12}Pd$)	52.35	(0.12)	4.06	214-216 (dec.)	48
(FW: 1193.12)	(52.09)		(4.05)		
$[Pd(dppen)_2][PF_6]_2$ ($C_{52}H_{44}P_6F_{12}Pd$)	52.52		3.73	210-212 (dec.)	51
(FW:1189.16)	(53.37)	(1.57)	(4.48)		
$[Pt(d2pyrpe)_2][PF_6]_2$ ($C_{44}H_{40}N_8P_6F_{12}Pt$)	40.98	8.69	3.13	170-172 (dec.)	65
(FW:1289.76)	(39.32)	(8.45)	(2.54)		
$[Pd(d2pyrpe)_2][PF_6]_2$ ($C_{44}H_{40}N_8P_6F_{12}Pd$)	44.00	9.33	3.36	208-210 (dec.)	37
(FW: 1201.66)	(44.26)	(9.32)	(3.31)		
[b]$[Pt(d3pyrpe)_2][PF_6]_2$ ($C_{44}H_{40}N_8P_6F_{12}Pt$)	40.98	8.69	3.13	176-178 (dec.)	45
(FW: FW:1289.76)	(42.46)	(10.46)	(4.24)		
$[Pt(d2pyrpe)_2][BPh_4]_2$ ($C_{92}H_{80}N_8P_4B_2Pt$)	67.45	6.84	4.92	>230	50
(FW: 1638.23)	(67.69)	(6.83)	(4.96)		
[c]$[Pt(d3pyrpe)_2][BPh_4]_2$ ($C_{92}H_{80}N_8P_4B_2Pt$)	67.45	6.84	4.92	140-145 (dec.)	40
(FW: 1638.23)	(62.54)	(6.27)	(5.35)		

[a]Calculated and found (in parentheses) data in %. All the compounds except the last two were recrystallised from DMF/ether. All the phenyl complexes and $[Pt(d3pyrpe)_2][PF_6]_2$ had DMF coordinated to them leading to great differences between the expected and obtained values (%). [b]$[Pt(d3pyrpe)_2][PF_6]_2$·4DMF ($C_{56}H_{68}N_{12}O_4P_6F_{12}Pt$)- calc. C, 42.51; N, 10.62; H, 4.33 % and [c]$[Pt(d3pyrpe)_2][BPh_4]_2.2CH_2Cl_2$ ($C_{94}H_{84}N_8P_4B_2Cl_4Pt$, 1808.17) - calc. C, 62.44; N, 6.20; H, 4.68 % which correspond closely to the obtained values shown in the table.

The colour of all the PF_6 complexes that were successfully synthesised ranged from yellow to white, were air-stable, and soluble in polar solvents such as acetonitrile, dimethylsulphoxide and dimethylformamide. They were partially soluble in chlorinated solvents such as CH_2Cl_2 and $CHCl_3$ and insoluble in ether, hexane, water and tetrahydrofuran. This low solubility has been shown in similar complexes containing PF_6^- as the counterion (Tanase *et al.,* 1993). It is also worth noting that complexes that required long synthetic routes as well as those that were obtained in poor yields were not investigated for biological activity. This was due to the fact that short and simple synthetic routes that produce higher yields are ideal in the production of pharmaceutical products. Additionally, some of them could not be characterised conclusively due to poor yields coupled by solubility problems.

Finally, six complexes were used in biological assays that are described in the Pharmacology Sections (Chapter 5-10). [1]These are $[Pt(dppe)_2][PF_6]_2$ (**Pg 1**), $[Pd(dppe)_2][PF_6]_2$ (**Pg 3**), $[Pd(cis\text{-}dppen)_2][PF_6]_2$ (**Pg 4a**), $[Pt(d2pyrpe)_2][PF_6]_2$ (**Pg 5**), $[Pt(d3pyrpe)_2][PF_6]_2$ (**Pg 6**), $[Pd(d2pyrpe)_2][PF_6]_2$ (**Pg 8**), and $[Au(dppe)_2]Cl$ (used as a standard in all investigations). The compounds used in biological assays were purified by washing with diethyl ether (as described in Chapter 4) and not purified from DMF. This is due to the fact that DMF coordinated to the complexes (as seen in X-ray structure) and also demonstrated from elemental analyses.

[1] The naming scheme depicted for the test compounds is different from the ones shown in the synthetic routes.

Chapter IV

Experimental details

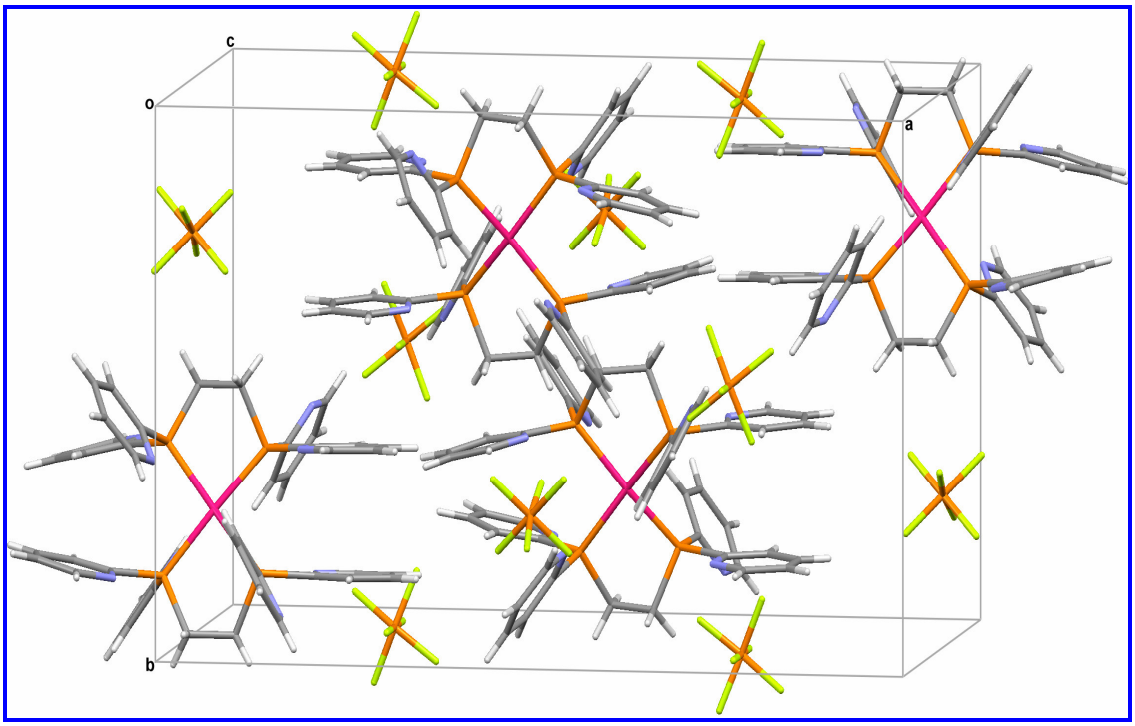

4.1 General

All manipulations (unless stated otherwise) were carried out under an argon atmosphere, using standard Schlenk techniques. Solvents were distilled from sodium/benzophenone ketyl and degassed.

4.1.1 NMR spectroscopy

NMR spectra were recorded in DMSO and $CDCl_3$ at 298 K using the following Bruker instruments; *AVANCE* 300 and ARX 300 (^{1}H, 300.1 MHz; ^{13}C, 75.5 MHz; ^{31}P, 121.5 MHz) and referenced internally to residual solvent resonances (data in δ) in the case of ^{1}H and ^{13}C NMR spectra. The ^{31}P NMR spectra were referenced externally to 85% H_3PO_4. All NMR spectra other than ^{1}H were proton decoupled. First order analysis was used to assign the spectra. Recording of ^{13}C NMR spectra proved to be problematic due to solubility problems (as discussed in 3.1.1) and hence only the complexes with distinguishable chemical shifts are reported below.

4.1.2 Melting points

Melting points were recorded in unsealed capillaries and are uncorrected.

4.1.3 Elemental analysis

Elemental analysis (empirical formulae shown) was determined by the Institute for Soil, Climate and Water, Pretoria.

4.1.4 MS-FAB

Fast atomic bombardment mass spectra were recorded with a VG70SEQ by micromass.

4.1.5 X-ray crystallography

Intensity data, for the crystal structure **4e** was collected on a Bruker SMART 1K CCD area detector diffractometer with graphite monochromated Mo K_α radiation (50kV, 30mA) at 173 K. The collection method involved ω-scans of width 0.3°. Data reduction was carried out using the program *SAINT* (Bruker, 1999a) and the absorption corrections were made using the program *SADABS* (Sheldrick, 1996). The crystal structure was solved by direct methods using *SHELXTL* (Bruker, 1999b). Hydrogen atoms were located in the difference map then positioned geometrically and allowed to ride on their respective parent atoms. Diagram and publication material were generated using *SHELXTL* (Bruker. 1999b) *and PLATON* (Spek, 2003).

Intensity data, for the crystal structures (**3f, 1h and 2h, 3b**) were collected on a Bruker SMART 1K CCD area detector diffractometer with graphite monochromated Mo K_α radiation (50kV, 30mA) at 298 K.

4.2 Synthesis of phenyl phosphine complexes

4.2.1 Synthesis of [Au(dppe)$_2$]Cl

This compound was prepared by modification of a literature procedure (Berners-Price and Sadler, 1986). 1,2-bis-(diphenylphosphine)ethane (0.56 g, 1.406 mmol) in THF (10 ml) was added dropwise to a stirring solution of $ClAuSMe_2$ (0.185 g, 0.713 mmol) at 0°C. The mixture was stirred for 15 mins then allowed to warm to room temperature to give a white solid. The solvent was removed *in vacuo.* Yield: 87% (0.62 g). $^{31}P\{^1H\}$ NMR, (DMSO, δ, ppm): 21.7; lit. 21.9 (Berners-Price and Sadler, 1987b). MS-FAB, m/z 993 (M^+-H).

4.2.2 Synthesis of [PtCl$_2$(dppe)] (1a)

The compound was synthesised according to a literature procedure (Westland, 1965) (*Eq. 4.1*). A fine white compound was obtained. Yield: 300 mg (35 %). $^{31}P\{^1H\}$ NMR (DMSO, δ, ppm): 43.4 (J_{PtP} = 3547 Hz).

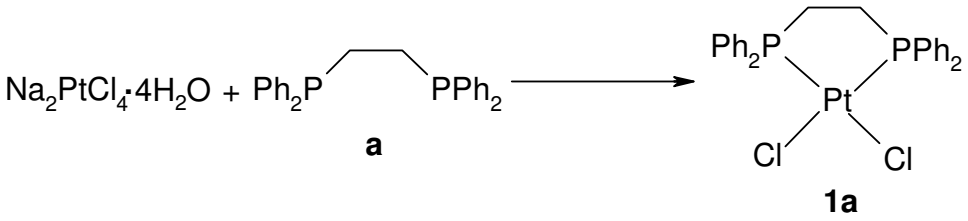

Eq. 4.1

4.2.3 Synthesis of [Pt(dppe)$_2$]Cl$_2$ (2a)

Compound **1a** was treated with 1,2-bis-(diphenylphosphine)ethane (dppe) to yield **2a** according to equation 4.2 (Westland, 1965). It was isolated in good yield (320 mg, 83 %). $^{31}P\{^{1}H\}$ NMR (DMSO, δ, ppm): 48.9, (J_{PtP} = 2331 Hz).

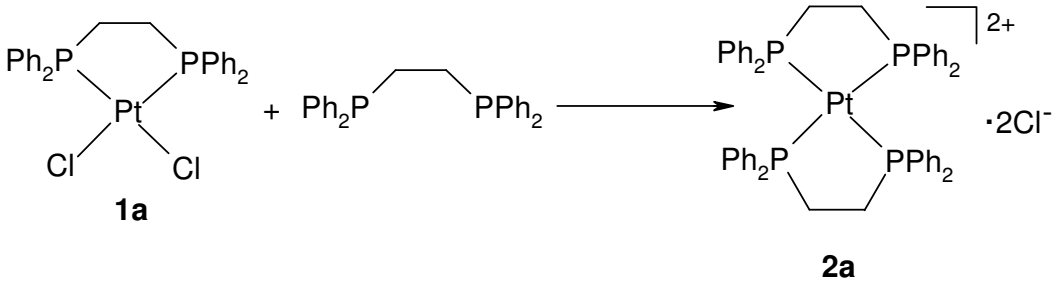

Eq. 4.2

4.2.4 Synthesis of [Pt(dppe)$_2$][PF$_6$]$_2$ (3a)

3a was prepared according to a literature procedure (Jones *et al.,* 1999). NH_4PF_6 (0.03 g, 0.184 mmol) was added to a stirred solution of [Pt(dppe)$_2$]Cl$_2$ (0.10 g, 0.094 mmol) in acetone (25 ml). The white mixture was stirred for 45 min and the resultant mixture filtered through celite 545, which was subsequently washed with acetone (3 x 5 ml). The combined colourless filtrate was reduced to ~3ml to yield a white precipitate and ether (15 ml) was added to facilitate more precipitation. The white compound was isolated by filtration, washed with ether (3 x 5ml) and dried *in vacuo*.

Yield: 70 mg (58 %). $^{31}P\{^{1}H\}$ NMR (DMSO, δ, ppm): 49.3 ($^{1}J_{PtP}$ = 2323 Hz), -143 (spt, $^{1}J_{PF}$ = 712 Hz, PF_6^-). ^{13}C NMR (DMSO): δ 29.4 (s, bridging CH_2), 125.3 (*Ipso*-C), 129.4 (s, *m*-Ph), 133.3 (s, *p*-Ph), 134.0 (s, *o*-Ph). MS-FAB; m/z 991 (M^+-2PF_6). Anal. Calcd for $C_{52}H_{48}P_6F_{12}Pt$ (1281.8): C, 48.72; H, 3.77; found: C, 48.01; H, 3.49; N (DMF), 0.28 %.

4.2.5 Synthesis of [PdCl$_2$(dppe)] (1b)

This pale yellow compound was synthesised according to a literature procedure (Westland, 1965) (*Eq. 4.3*). Yield 480 mg (61 %). $^{31}P\{^{1}H\}$ NMR (DMSO, δ, ppm): 67.5 (s).

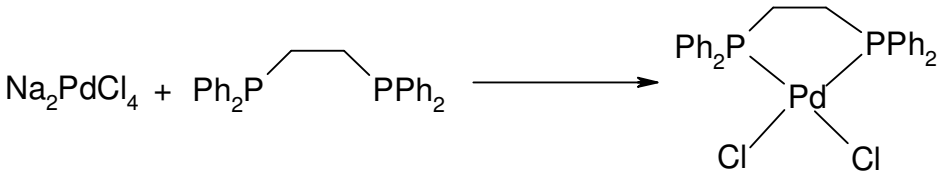

Eq. 4.3

1b

4.2.6 Synthesis of [Pd(dppe)$_2$]Cl$_2$ (2b)

1b was treated with 1,2-bis-(diphenylphosphine)ethane (dppe) to yield **2b** according to equation 4.4. Yield: 1.19 g (37 %). $^{31}P\{^{1}H\}$ NMR (DMSO, δ, ppm): 57.4 (s).

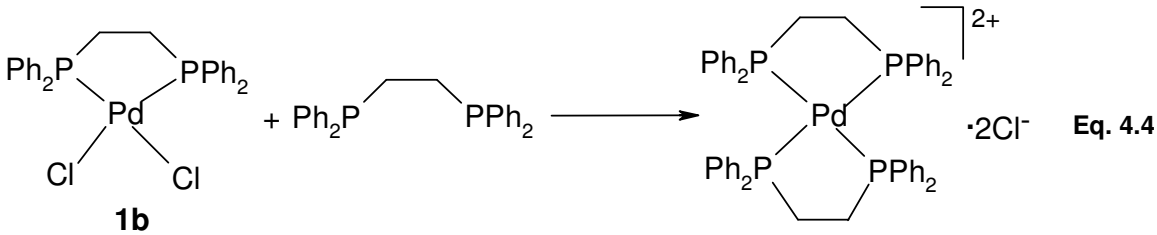

Eq. 4.4

1b **2b**

4.2.7 Synthesis of [Pd(dppe)$_2$][PF$_6$]$_2$ (3b)

3b was prepared following the same procedure used for **3a**. A mixture of NH_4PF_6 (0.29 g, 1.779 mmol) and **2b** (0.88 g, 0.903 mmol) in acetone were stirred for 1 hr. A white compound was obtained after work up as described above (4.2.4).

Yield: 520 mg (48 %). $^{31}P\{^{1}H\}$ NMR (DMSO, δ, ppm): 58.1 (s), -143.3 (spt, $^{1}J_{PF}$ = 711 Hz, PF_6^-). MS-FAB; m/z 902 (M^+-2PF_6). Anal. Calcd for $C_{52}H_{48}P_6F_{12}Pd$ (1193.2): C, 52.35; H, 4.06; found: C, 52.09; H, 4.05; N (DMF), 0.12 %.

4.2.8 Synthesis of $[Pt(dppen)_2][PF_6]_2$ (3c)

This compound was prepared in the same manner as **3a**. Reaction of $[Pt(dppen)_2]Cl_2$ (0.10 g, 0.094 mmol) and NH_4PF_6 (0.03 g, 0.189 mmol) in acetone (25 ml) yielded a white compound. Yield: 30 mg (25 %). $^{31}P\{^1H\}$ NMR (DMSO, δ, ppm): 60.2 ($^1J_{PtP}$ = 2350 Hz), -143 (spt, $^1J_{PF}$ = 711 Hz, PF_6). MS-FAB; m/z 989 (M^+-2PF_6), (FW = 1277).

Alternative route, NH_4PF_6 (0.18 g, 1.310 mmol) was added to a stirring solution of $[PtCl_2(dppen)]$ (**1c)** (0.30 g, 0.547 mmol) in DMF for 24h. The precipitated NH_4Cl was filtered and *cis*-dppen (0.021 g, 0.053 mmol) was added to the remaining pale yellow solution. Yield: 13 mg (19 %).

4.2.9 Synthesis of $[Pd(dppen)_2][PF_6]_2$ (3d)

A modified procedure (Oberhauser *et al.,* 1995) was used to prepare this compound. $[PdCl_2(dppen)]$ (0.15 g, 0.326 mmol) and NH_4PF_6 (0.11 g, 0.653 mmol) were suspended in DMF. The orange mixture was stirred for 24 h at room temperature. The formed NH_4Cl was filtered off. *cis*-dppen (0.12 g, 0.295 mmol) was added to the remaining yellow solution and stirred for a further 24 h at room temperature. The solution was concentrated *in vacuo* followed by addition of ether to induce precipitation. The white solid was washed with ether (3 x 5 ml) and dried *in vacuo*.

Yield 180 mg (51 %). $^{31}P\{^1H\}$ NMR (DMSO, δ, ppm): 64.3 (s), -143 (spt, $^1J_{PF}$ = 711 Hz, PF_6^-). MS-FAB; m/z 899 (M^+-2PF_6). Anal. Calcd for $C_{52}H_{44}P_6F_{12}Pd$ (1189.1): C, 52.52; H, 3.73; found: C, 53.37; H, 4.48; N (DMF), 1.57 %.

4.3 Preparation of pyridyl phosphine ligands

4.3.1 Preparation of 1,2-bis-(di-2-pyridylphosphino)ethane (d2pyrpe)

A literature procedure was followed in the preparation of this ligand (Bowen *et al.,* 1998). The general procedure is shown in equation 4.5.

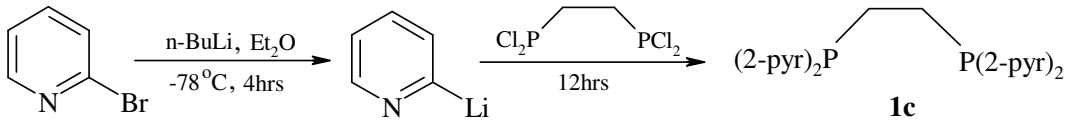

1c **Eq. 4.5**

D3pyrpe and d4pyrpe were prepared by the procedure shown above (Eq. 4.5).

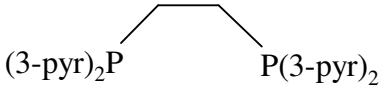

d3pyrpe

d4pyrpe

4.4 Preparation of 2-pyridyl phosphine complexes

4.4.1 Preparation of [Pt(d2pyrpe)$_2$]Cl$_2$ (2e)

1,2-bis-(di-2-pyridylphosphino)ethane (d2pyrpe) (0.31 g, 0.778 mmol) was added to a stirred solution of Na_2PtCl_4 (0.30 g, 0.784 mmol) in THF. The red solution of Na_2PtCl_4 slowly turned from red to pink and a white precipitate formed immediately. The mixture was stirred vigorously for 12hrs. The yellow solution was filtered and off- white residue was dried *in vacuo*.

Yield (crude): 610 mg (73 %). $^{31}P\{^1H\}$ NMR (DMSO, δ, ppm): 55.1 ($^1J_{PtP}$ = 2370 Hz), and [2]47.7 ($^1J_{PtP}$ = 3480 Hz)

4.4.2 Preparation of [Pt(d2pyrpe)$_2$][PF$_6$]$_2$ (3e)

This compound was prepared in a similar manner as the previous PF_6 complexes. NH_4PF_6 (0.55 g, 0.337 mmol) was reacted with [Pt(d2pyrpe)$_2$] Cl_2 (0.18 g, ~0.168 mmol) in acetone to yield a white solid.

Yield: 150 mg (65 %). $^{31}P\{^1H\}$ NMR (DMSO, δ, ppm): 55.9 ($^1J_{PtP}$ = 2459 Hz), -143 (spt, $^1J_{PF}$ = 711 Hz, PF_6^-). Lit: (Jones *et al.,* 1999), $^{31}P\{^1H\}$ NMR (81.015 MHz, CD_3OD): δ 54.42 ($^1J_{PtP}$ = 2477 Hz), -144 (spt, $^1J_{PF}$ = 712 Hz, PF_6^-). ^{13}C NMR (DMSO): δ 27.2 (s, bridging CH_2), 126.8 (s, *p*-pyr), 130.8 (s, *o*-pyr), 137.3 (s, *m*-

[2] This chemical shift indicates the presence of the mono-chelated compound, [$PtCl_2$(d2pyrpe)].

pyr), 150.8 (s, CN). *Ipso*-C of pyridyl moiety was not observed. MS-FAB; m/z 999 (M^+-2PF_6). Anal. Calcd for $C_{44}H_{40}N_8P_6F_{12}Pt$ (1289.8): C, 40.98; N, 8.69; H, 3.13; found: C, 39.32; N, 8.45; H, 2.54 %.

4.4.3 Preparation of the [Pt(d2pyrpe)$_2$][BPh$_4$]$_2$ (4e)

$NaBPh_4$ (0.19 g, 0.560 mmol) was added to a stirred solution of impure [Pt(d2pyrpe)$_2$]Cl_2 (0.30 g, ~0.280 mmol) in CH_2Cl_2. The mixture was stirred for 12 hrs at room temperature. The formed NaCl was filtered off and the clear yellow solution was removed i*n vacuo* to yield a yellow solid. Colourless crystals of **4e** were obtained (at -5°C) by dissolving the crude compound in excess dichloromethane and layering with ether.

Yield: 250 mg, (50 %). $^{31}P\{^1H\}$ NMR (DMSO, δ, ppm): 55.7 ($^1J_{PtP}$ = 2460 Hz). ^{13}C NMR (DMSO): δ 26.8 (s, bridging CH_2), 121.5 (s, BPh), 125.3 (s, BPh), 126.4 (s, BPh), 130.4 (s, *p*-pyr), 135.5 (s, *o*-pyr), 136.9 (s, *m*-pyr), 150.4 (s, CN), 163.7 [q, *ipso*, $^1J(^{13}C\text{-}^{11}B)$ 49.3 Hz]. *Ipso*-C of pyridyl moiety was not observed. MS-FAB, m/z 999 (M^+-2BPh_4). Anal. Calcd for $C_{92}H_{80}N_8P_4B_2Pt$ (1638.3): C, 67.45; N, 6.84; H, 4.92; found: C, 67.69; N, 6.83; H, 4.96 %.

4.4.4 Preparation of [Pd(d2pyrpe)$_2$]Cl$_2$ (2f)

This compound was prepared in a similar manner to the platinum analogue (**2e**). 1,2-bis-(di-2-pyridylphosphino)ethane (d2pyrpe) (0.54 g, 1.342 mmol) was added to a stirred solution of Na_2PdCl_4 (0.20 g, 0.680 mmol) in THF. A pale yellow solid was formed after 1 hr of stirring. After stirring vigorously for 12hrs, the yellow solution was filtered and off white residue was dried *in vacuo*.

Yield (crude): 430 mg (60 %). $^{31}P\{^1H\}$ NMR (DMSO, δ, ppm): 64.0 and [3]70.4.

[3] This chemical shift indicates the presence of the *mono*-chelated compound, [$PdCl_2$(d2pyrpe)].

4.4.5 Preparation of [Pd(d2pyrpe)$_2$][PF$_6$]$_2$ (3f)

This compound was prepared as previously described for complexes containing PF_6. NH_4PF_6 (0.07 g, 0.429 mmol) was reacted with a crude sample $[Pd(d2pyrpe)_2]Cl_2$ (0.22 g, ~0.224 mmol) in acetone to yield a white solid.

Yield: 100 mg (37%). $^{31}P\{^1H\}$ NMR (DMSO, δ, ppm): 64.0 (s), -143.3 (spt, $^1J_{PF}$ = 711 Hz, PF_6^-). ^{13}C NMR (DMSO): δ 25.8 (s, bridging CH_2), 126.5 (m, *p*-Ph), 132.1 (d, *o*-Ph), 137.2 (m, *m*-Ph), 151.0 (m, CN). *Ipso*-C not observed. MS-FAB, m/z 910 (M^+-2PF_6). Anal. Calcd for $C_{44}H_{40}N_8P_6F_{12}Pd$ (1201.1): C, 44.00; N, 9.33; H, 3.36; found: C, 44.26; N, 9.32; H, 3.31 %.

4.5 Preparation of 3-pyridyl phosphine complexes

4.5.1 Preparation of [PtCl$_2$(d3pyrpe)$_2$] (1g)

1,2-bis-(di-3-pyridylphosphino)ethane (d3pyrpe) (0.24 g, 0.602 mmol) was added to a stirred solution of Na_2PtCl_4 (0.25 g, 0.653 mmol) in THF. A yellow precipitate formed immediately. After stirring for 12 hours at room temperature, filtration was carried out and the yellow residue was dried *in vacuo*.

Yield (crude): 320 mg (82%). $^{31}P\{^1H\}$ NMR (DMSO, δ, ppm): 37.8 ($^1J_{PtP}$ = 3583 Hz).

4.5.2 Preparation of [Pt(d3pyrpe)$_2$]Cl$_2$ (2g)

This compound was prepared by modification of a literature method (Jones *et al.,* 2005). $PtCl_2$ (0.10 g, 0.38 mmol) in CH_3CN (15 ml) was refluxed for 2h to give a yellow solution. The ligand, d3pyrpe (0.30 g, 0.746 mmol) was added to the hot solution to give a yellow precipitate.

Yield: 450 mg (56 %). $^{31}P\{^1H\}$ NMR (DMSO, δ, ppm): 41.4 ($^1J_{PtP}$ = 2352 Hz).

4.5.3 Preparation of [Pt(d3pyrpe)$_2$][PF$_6$]$_2$ (3g)

Preparation of this compound was similar to the one described for **3e**. NH_4PF_6 (0.12 g, 0.736 mmol) was added to a stirred solution of [Pt(d3pyrpe)$_2$]Cl_2 (0.40 g, ~0.374 mmol) in acetone. The white compound contained traces of the unreacted ligand and hence it was triturated with THF to yield a pale yellow solid.

Yield: 130 mg (45 %). $^{31}P\{^1H\}$ NMR (DMSO, δ, ppm): δ 42.3 ($^1J_{PtP}$ = 2332 Hz), -143 (spt, $^1J_{PF}$ = 711 Hz, PF_6^-). Anal. Calcd for [Pt(d3pyrpe)$_2$][PF$_6$]$_2$·4DMF ($C_{56}H_{68}N_{12}O_4P_6F_{12}Pt$); C, 42.51; N, 10.62; H, 4.33; found: C, 42.46; N, 10.46; H, 4.24 %.

4.5.4 Preparation of [Pt(d3pyrpe)$_2$][BPh$_4$]$_2$ (4g)

AgO_3SCF_3 (0.23 g, 0.898 mmol) was added to a stirred solution of [$PtCl_2$(d3pyrpe)] (0.30 g, 0.449 mmol) in CH_2Cl_2 (15 ml). The ligand was sparingly soluble in DCM and a pale yellow precipitate was formed after 30 mins of stirring. After 1 h of stirring, the formed AgCl was filtered off. Additional d3pyrpe (0.10 g, 0.251 mmol) was added to the remaining solution. The pale yellow solution changed to light brown in colour on addition of the ligand and this mixture was stirred for 12 hrs at room temperature. $NaBPh_4$ (0.11 g, 0.309 mmol) was added to the clear yellow solution of impure [Pt(d3pyrpe)$_2$][CF_3SO_3]$_2$ (0.20 g, ~0.154 mmol) in CH_2Cl_2. After stirring for 20 minutes, the clear yellow solution became turbid. The mixture was stirred for 12 hrs to yield a clear deep yellow solution and yellow oil. The solvent was removed *in vacuo* to give a mustard coloured compound. This compound was purified from CH_2Cl_2 at -5°C.

Yield: 100 mg (40 %). $^{31}P\{^1H\}$ NMR (DMSO, δ, ppm): 42.0 ($^1J_{PtP}$ = 2332 Hz). ^{13}C NMR (DMSO): δ 30.1 (s, bridging CH_2), 121.4 (s, BPh), 124.3 (s, BPh), 125.2 (s, BPh), 135.5 (s, *p*-pyr), 140.6 (s, *o*-pyr), 153.1 (s, *m*-pyr), 153.8 (s, CN), 163.3 [q, *ipso*, $^1J(^{13}C\text{-}^{11}B)$ 49.4 Hz]. *Ipso*-C of pyridyl moiety was not observed. MS-FAB: m/z 999 (M^+-2BPh_4). Anal. Calcd for [Pt(d3pyrpe)$_2$][BPh_4]$_2$.2CH_2Cl_2 ($C_{94}H_{84}N_8P_4B_2Cl_4Pt$, 1808.17): C, 62.44; N, 6.20; H, 4.68; found: C, 62.54; N, 6.27; H, 5.35 %.